KU Leuven
Groep Biomedische Wetenschappen
Faculteit Geneeskunde
Departement Beeldvorming & Pathologie
OMFS-IMPATH Onderzoeksgroep
Centrum orale beeldvorming

The use of 2D and 3D imaging modalities and its influence on diagnosis and treatment planning in orthodontics

Pisha PITTAYAPAT

Promotor: Prof. Dr. Reinhilde Jacobs
Copromotoren: Prof. Dr. Guy Willems; Prof. Dr. Raphaël Olszewski

Proefschrift voorgedragen tot het behalen van de graad van
Doctor in de Biomedische Wetenschappen

September 2014

KU Leuven
Biomedical Sciences Group
Faculty of Medicine
Department of Imaging & Pathology
OMFS-IMPATH Research group
Oral Imaging Center

The use of 2D and 3D imaging modalities and its influence on diagnosis and treatment planning in orthodontics

Pisha PITTAYAPAT

Jury:
Promoter: Prof. Dr. Reinhilde Jacobs
Co-promoter: Prof. Dr. Guy Willems
Co-promoter: Prof. Dr. Raphaël Olszewski
Chair: Prof. Dr. Philippe Demaerel
Secretary: Prof. Dr. An Verdonck
Jury members: Prof. Dr. An Verdonck
Prof. Dr. Dirk Vandermeulen
Prof. Dr. Guy De Pauw
Assoc. Prof. Dr. Soontra Panmekiate

Dissertation presented in partial fulfilment of the requirements for the degree of Doctor in Biomedical Sciences.

September 2014

Acknowledgements

After a truly long journey, the day has finally arrived, the day when I am finishing my PhD. Looking back to the past years, I must admit that I cannot remember the exact date that I decided to continue my study abroad, but it was about 9 years ago. I was then a young lecturer of the Department of Radiology, Faculty of Dentistry at Chulalongkorn University who, like any other colleagues in my profession, wished to acquire more knowledge and skills in my field of study. The South-East Asian Tsunami in 2004 was a turning point in my career. My involvement in the victim identification process did give me an incentive to study more in Forensic Odontology and this has driven me here to Leuven, Belgium since 2007. Taking this very first opportunity, I would like to express my sincere gratitude to Nenbutsushu Buddhist Sect of Japan and Chulalongkorn University for their financial support which enabled me to achieve my Master's Degree. My decision to continue the doctoral study at the Oral Imaging Center, OMFS-IMPATH research group was a real great step forward which has led me to the end of my long journey today. At this point, I must say that my great expectation to complete my PhD Project would never have been realized without the enormous supports from everybody around me and, to be more exact, from around the world, to whom I herewith would like to express my heartfelt thanks.

First and foremost, I would like to thank Prof. Rik Torfs, Rector of the KU Leuven, Prof. Jan Goffin, Dean of the Faculty of Medicine, Prof. John Creemers, Director of the Doctoral School of Biomedical Sciences, Prof. Philippe Demaerel, Chair of the Department of Imaging & Pathology, Prof. Dominique Declerck, Chair of the Department of Oral Health Sciences, Prof. Constantinus Politis, Chair of the Oral and Maxillofacial Surgery, and Prof. Raymond Oyen, Head of the Radiology of the KU Leuven, who have granted me an opportunity to undertake this doctoral project.

Prof. Reinhilde Jacobs (KU Leuven), who has been more than my main promoter, but she has also been my advisor and my guide. I have known her since I was doing the Master in Forensic Odontology as she was my co-promoter back then.

With her endless help and untiring support and above all her valuable knowledge as well as her useful advice, this PhD thesis of mine has finally been completed. I have gained a lot of experiences, not only about the PhD alone but also in all other aspects, from working closely with her throughout the passing years. I especially want to say to you 'Thank you very much.'. I am so grateful for all that you have given to me.

Secondly, I would like to thank my co-promoter, Prof. Guy Willems (KU Leuven) who has always been understanding and very patient with me during my Master year and also along the PhD project. Being new at the KU Leuven, I have since the beginning learned a lot from Prof. Guy Willems and so feel very grateful to him for his guidance. On this occasion, I would also like to thank Prof. Raphaël Olszewski (Université Catholique de Louvain), my co-promoter, who too is very patient with me and has helped leading me through the three-dimensional world.

Besides my promoters, I would like to express my deep gratitude towards all members of the thesis committee: Prof. An Verdonck, Prof. Dirk Vandermeulen, Prof. Guy De Pauw, and Assoc. Prof. Soontra Panmekiate - Head of the Department of Radiology, Faculty of Dentistry, Chulalongkorn University. Assoc. Prof. Panmekiate, my deep appreciation goes to you for taking time to travel a long way to act as an international jury member on this occasion.

This doctoral project was supported by a doctoral scholarship in the framework of the Interfaculty Council for Development Co-operation (IRO) (October 2010-September 2013). I would like to thank Mr. Edmundo Guzman and Ms. Yalina Zaldivar Hernández for the help and coordination regarding the doctoral scholarship.

There are also three important persons I wish to thank. The statistical part of this thesis would never have been clearly analysed and presented without the help of Wim Coucke, Guillaume A. Odri, and George Kalema. Thank you very much for your collaboration and for the valuable discussions that we have had together.

I must never forget my best friends, who are all classmates from the Faculty of Dentistry, Chulalongkorn University: Jum, Ik, Pae, Bitong, Ploy, Joyce and Tiya.

Since some of us including myself have been spending so much of our time abroad, we find getting together is not always easy. The news and the greetings from them every now and then, no matter how far they are, always helps lifting up my spirit. I wish to thank you all for your love and support which, on many occasions, have given me strength to fight through the hard times.

I especially want to acknowledge the Department of Radiology, Faculty of Dentistry, Chulalongkorn University, as well as my colleagues for granting me an opportunity to study abroad and for the kind support always extended to me. I would also like to thank Assoc. Prof. Wichitsak for your consistent kindness, Pasupen for your friendly support, Oranart for your help and for the great friendship and also Tingting for the design of this thesis cover. I do owe you all for the success I have today.

Big thanks go to all my Thai friends living not only in Leuven but also in some other parts of Europe: Pong, Pendithee, Praonrat, Adis, Noppawan, Chong, Napat and many more for your regular help and support. We have had a great time together in this lovely city and will surely keep in touch when I am back to Thailand.

I would never have enjoyed doing my work in the hospital as much as I really did without my colleagues and friends at the OMFS-IMPATH research group: Prof. Michael Bornstein, Yan, Ruben, Maryam, Maria, Livia, Olivia, Bart, Roland, Carine, Jeroen, Mostafa, Ahmed, Bassant, Tatiana, Andres, Laura, Min, Karla, Karla Rovaris, Thaís, Christiano, Paulo, Soraya, João, Ivete, Elke, Dominique, Peter Vermaelen and also Ali and Karoline from the Orthodontics. I do appreciate you all for your helping, supporting and sharing the joyful moments together.

Finally, I would like to dedicate this thesis to every member of my family: my mother, father, brother, my cousin and also my grandparents. This thesis would not have been possible without you. I know that it has been a long tough time and I do hope you will all be proud of me and of my success today.

Pisha

Table of Contents

Acknowledgements .... **I**
Table of Contents .... **V**
List of Abbreviations .... **VII**
Preface .... **IX**

Chapter 1: General introduction and aims 1

PART I: LITERATURE REVIEW
Chapter 2: 3D Cephalometric analysis in orthodontics: a systematic review . 25

PART II: PANORAMIC IMAGING
Chapter 3: An in vitro comparison of subjective image quality of panoramic views acquired via 2D or 3D imaging 65
Chapter 4: Agreement between cone-beam CT images and panoramic radiographs for initial orthodontic evaluation 83

PART III: CEPHALOMETRIC IMAGING
Chapter 5: Accuracy of linear measurements using 3 imaging modalities: two lateral cephalograms and one 3D model from CBCT data 105
Chapter 6: Reproducibility of sella turcica landmark in 3 dimensions using a sella turcica specific reference system 125
Chapter 7: A new mandible-specific landmark reference system for three-dimensional cephalometry 143
Chapter 8: Three-dimensional Frankfort horizontal plane revisited and evaluation of new horizontal planes 161
Chapter 9: General discussion and conclusions 181

Summary/Samenvatting **207**
Curriculum vitae **215**

List of Abbreviations

2D	Two-dimensional
3D	Three-dimensional
ALARA	As Low As Reasonably Achievable
ANOVA	Analysis of Variance
Ave	Average
CBCT	Cone Beam Computed Tomography
CCD	Charge-Coupled Device
CDSR	Cochrane Database of Systematic Reviews
CENTRAL	Cochrane Central Register of Controlled Trials
Ceph	Cephalometric
CI	Confidence Interval
CMOS	Complementary Metal–Oxide–Semiconductor
CT	Computed Tomography
DARE	Cochrane Database of Abstracts of Reviews of Effects
DEO	Difference for Every Observer
DICOM	Digital Imaging and Communications in Medicine
EMBASE	Excerpta Medica database
FH	Frankfort Horizontal
FOV	Field of View
ICC	Intraclass Correlation Coefficient
kV	kilovoltage
kVp	Peak kilovoltage
lat ceph	Lateral cephalogram
mA	milliampere
mAs	product of mA x s
M	Mean
ME	Method Error
MEDLINE	Medical Literature Analysis and Retrieval System Online
MeSH	Medical Subject Headings
Min	Minimum

Max	Maximum
MSCT	Multi-Slice Computed Tomography
NS	No statistically significant difference
O	Observer
ODM	average Observer Difference of the Mean
OMF	Oral and MaxilloFacial
PRISMA	Preferred Reporting Items for Systematic Reviews and Meta-Analyses
PSP	PhotoStimulable Phosphor plates
PUBMED	Publisher Medline
Q	Question
QUADAS	Quality of Diagnostic Accuracy Studies
SD	Standard Deviation of the mean
SE	Standard Error
SEM	Standard Error of the Mean
SDD	Smallest Detectable Difference
Sig diff	Statistically significant difference
TIFF	Tagged Image File Format

Preface

This doctoral thesis is based on the following research papers:

Chapter 2:

Pittayapat P, Limchaichana-Bolstad N, Willems G, Jacobs R. Three-dimensional cephalometric analysis in orthodontics: a systematic review. *Orthod Craniofac Res.* 2014;17:69-91.

Chapter 3:

Pittayapat P, Galiti D, Huang Y, Dreesen K, Schreurs M, Souza PC, Rubira-Bullen IR, Westphalen FH, Pauwels R, Kalema G, Willems G, Jacobs R. An in vitro comparison of subjective image quality of panoramic views acquired via 2D or 3D imaging. *Clin Oral Investig*. 2013;17:293-300.

Chapter 4:

Pittayapat P, Willems G, Alqerban A, Coucke W, Ribeiro-Rotta RF, Couto Souza P, Westphalen FH, Jacobs R. Agreement between cone beam computed tomography images and panoramic radiographs for initial orthodontic evaluation. *Oral Surg Oral Med Oral Pathol Oral Radiol.* 2014;117:111-9.

Chapter 5:

Pittayapat P, Bornstein MM, Imada T, Coucke W, Lambrichts I, Jacobs R. Accuracy of linear measurements using 3 imaging modalities: two lateral cephalograms and one 3D model from CBCT data. *Eur J Orthod.* 2014. (in press)

Chapter 6:

Pittayapat P, Jacobs R, Odri G, Vasconcelos KdeF, Willems G, Olszewski R. Reproducibility of sella turcica landmark in 3 dimensions using a sella turcica specific reference system. *Submitted.*

Chapter 7:

Pittayapat P, Jacobs R, Odri G, Kwon MS, Lambrichts I, Willems G, Politis C, Olszewski R. A new mandible-specific landmark reference system for three-dimensional cephalometry. *Submitted.*

Chapter 8:

Pittayapat P, Jacobs R, Odri G, Zogheib T, Lambrichts I, Willems G, Politis C, Olszewski R. Three-dimensional Frankfort horizontal plane revisited and evaluation of new horizontal planes. *Submitted.*

Chapter 1

General introduction and aims

Imaging is one of the most important diagnostic tools in dentistry apart from patient's history and a thorough clinical examination. Several types of imaging are used in a dental practice, and each has a specific indication. From the most basic radiographs, a periapical radiograph and a bitewing radiograph, that are used in daily dental practice, to more technologically sophisticated imaging such as panoramic radiography and cone-beam computed tomography, all of which help the clinicians in diagnosing any pathologies. Radiography is essential for caries detection, periodontal evaluation, endodontic treatment, implant surgery, pre-surgical treatment planning and post-surgical evaluation of craniofacial pathology and also for orthodontics (1). A correct orthodontic diagnosis that leads to an optimal treatment plan for a patient needs to be based on accurate images of the craniofacial region. In this introduction, two-dimensional and three-dimensional radiographic imaging modalities used in orthodontics are explained in detail.

1.1 Two-dimensional imaging

Two-dimensional radiography has been vastly used in medical and dental fields. Its principle lies in the image projection theory that a 3D object is projected by an X-ray beam onto an image receptor, then a shadow of that 3D object appears on the image receptor in two dimensions (1). Structures aligned obliquely to the image receptor may result in distorted shadows. A distance between the X-ray source to the object and a distance between the object to the image receptor are crucial factors that influence the image magnification. Interpretation of these 2D conventional radiographs requires good knowledge on anatomical structures projected on an X-ray film and also good training and experience to differentiate between normal and abnormal shadows. Quality assurance of these radiograps is also essential to keep the standard of the diagnostic capacity optimal (1).

In orthodontics, since many decades, panoramic radiography and lateral cephalometric radiography are radiographic techniques required for orthodontic treatment planning and follow-up.

Panoramic radiography

Panoramic radiography has been used as a diagnostic tool in dentistry for more than half a century (2-4). It acquires the image by rotating both X-ray source and an image receptor (5). Traditionally, the image receptor is an X-ray film but since the development of digital technology, image receptors can be photostimulable phosphor (PSP) plates, complementary metal–oxide–semiconductor (CMOS) receptors or charge-coupled device (CCD) receptors (1, 6).

Panoramic radiography has been widely used as a tool to obtain an overview look of a patient's oral condition or as a screening tool. Beside its importance for orthodontic treatment, it is also essential in oral surgery (1). Although the technique has been known for several limitations such as geometric distortion and superimposition of anatomical structures (7-10), it is widely used in dental practice.

In orthodontics, a panoramic radiograph is used as a tool to assess a broad view of the patient's oral condition, showing any possible pathologic lesions, impacted teeth or supernumerary teeth (1, 11) (Fig. 1.1). It also enables the initial evaluation of the temporomandibular joint (11). Based on the panoramic radiograph, the orthodontist decides whether additional radiographs such as periapical radiographs, bitewing radiographs or 3D images are required in order to formulate a full treatment plan for each individual.

Figure 1.1
A panoramic radiograph of an orthodontic patient, showing the unerupted upper right canine and formation of wisdom teeth.

Cephalometric radiography

Cephalometric analysis was first introduced in 1930s by Hofrath (12) in Germany and Broadbent (13) in the United States. A lateral cephalogram or a lateral cephalometric radiograph is used to evaluate the craniofacial complex, dentofacial proportions, malocclusion and changes related to growth, all of which are crucial for orthodontic treatment (11) (Fig. 1.2).

The difference of this technique compared to a lateral skull radiograph is the positioning device: an ear rod and a cephalostat are used to fix the patient's position during image acquisition. The radiograph can be repeated in the same position over time which allows a good treatment follow-up (1). Several cephalometric analyses have been invented for this purpose by quantifying and measuring the craniofacial structures (14). The measured values can be compared to the norm values, which were obtained from a population with normal occlusion (15).

In addition to a lateral cephalogram, a postero-anterior cephalometric radiograph or a frontal cephalogram may be added for specific cases involving asymmetry and orthognathic surgery (16). The method of using together both the lateral and frontal view was sometimes called 'three-dimensional cephalometry' in the past (17-20), before computed tomography (CT) was introduced to orthodontics.

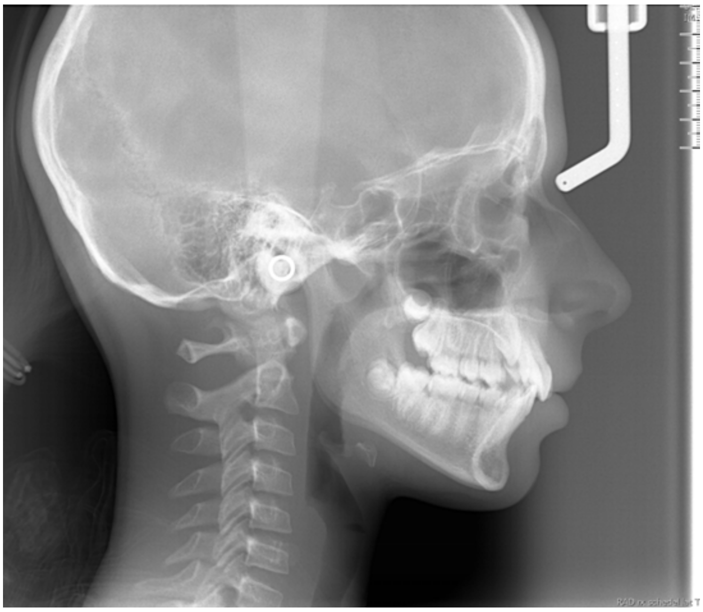

Figure 1.2
A lateral cephalogram of an orthodontic patient with inserted ear rods and a nasal rest pointing at Nasion (N). The image not only shows bony structure but also soft tissue outline.

A conventional lateral cephalogram is a 2-dimensional shadow of 3-dimensional structures thus superimposition and geometric distortion of anatomical structures is expected (21-23). In normal cases, these factors may not interfere with the treatment planning but in borderline cases or patients with severe skeletal malformation, they may affect how the orthodontists and surgeons analyse the data and make the specific treatment planning.

1.2 Three-dimensional imaging

Withstanding 2D limitations, 3D imaging modalities have become more important in dentistry during the last few decades. There has been an upward trend in utilizing 3D information as an aid in dentomaxillofacial diagnosis. Initially, this information was mainly obtained from computed tomography (CT) or multi-slice CT (MSCT). At a later stage, cone-beam computed tomography (CBCT) has become more popular.

Multi-slice computed tomography

In 1980s-1990s, CT images have been introduced to dental treatment. First, it was aiming toward implant surgery to overcome the geometric distortion in panoramic radiography. The distortion indeed affected measurements for implant planning (24-26).

The technology of the CT scan has been improved continuously since its first launch (27). Most scanners nowadays can make rapid scans due to the increased number of detectors; therefore, the recent CT devices are usually referred to as multi-slice computed tomography (MSCT). With its geometry, anatomical structures are scanned and displayed in real size (1:1), thus measurements on the CT images can be compared directly to the real structures.

The images are usually shown in 3 views in the multiplanar reformation (MPR) mode: axial, coronal and sagittal view. 3D cross-sectional images, made by reconstructing the 3D images, allow clinicians to view mandibular canals in relation to their adjacent structures. Surgeons can thus plan the size, the direction and the location to place an implant correctly without interfering with the neurovasucular bundles inside the canal. This helps to decrease post-operative complications (25, 26, 28).

CT images were used as a tool to help analyse patient's cranofacial structures and make a 3D orthodontic treatment plan. However, because of its relatively high radiation dose and costs, the use has been rather limited (1, 29, 30).

Cone-beam computed tomography

Since the introduction of cone-beam computed tomography (CBCT) in 1998 (31), its technology has been continuously developed to enable volumetric craniofacial imaging at reasonable costs and doses (32). It features the ability to capture craniofacial structures with high resolution and details (Fig. 1.3); therefore, the technique becomes very useful for many fields in dentistry such as implant dentistry, oral surgery, endodontics, and orthodontics (33). Depending on the selection of the CBCT devices and parameters, the market offers a wide range of selection. Careful consideration must be taken when choosing the devices for a specific task (34-37).

The CBCT offers numerous diagnostic potentials for orthodontic treatment, as long as radiation doses, image quality, diagnostic yield and treatment outcome can be properly balanced (38, 39). Justification is very crucial when it comes to exposing children with radiation. There are several published guidelines and recommendations available (34-36, 40). The guidelines offer an evidence-based strategy for patient selection and dose optimization (34-36, 40). The CBCT use in orthodontics is elaborated in the next part of the introduction "**1.3 3D imaging for orthodontic application**".

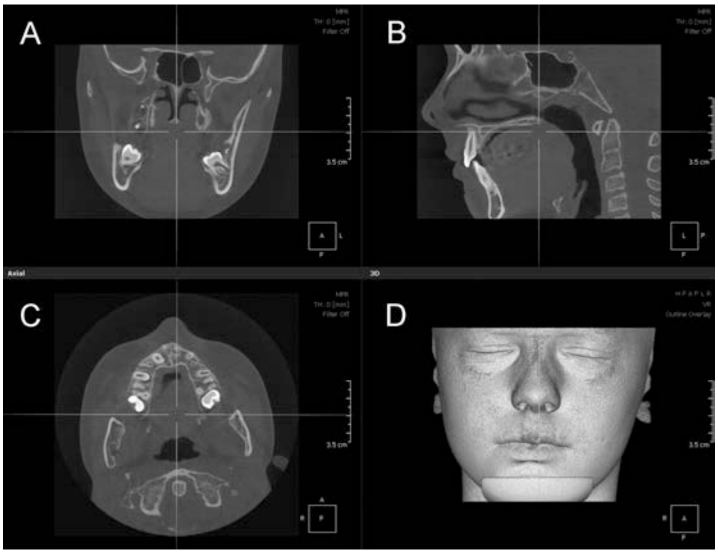

Figure 1.3 MPR view of a patient's CBCT scan, showing 3 views: A- coronal view, B - sagittal view, C - axial view, with one 3D volume rendering model (D).

Other 3D imaging modalities

Other useful 3D imaging modalities are magnetic resonance imaging (MRI), laser scanning system and stereophotogrammetry, all of which are techniques not using ionizing radiation. They are useful and can be applied for orthodontic treatment. MRI is generally used to evaluate TMJ condition in patients with TMJ pathology (41). One study used MRI to evaluate the Frankfort horizontal plane in 3D (42). Laser scanning system and stereophotogrammetry, also commercialised as 3dMD® (3dMD Ltd, Atlanta, USA) are used for evaluating the soft tissue landmarks and soft tissue changes of the patients (43-48).

1.3 3D imaging for orthodontic application

At first, CBCT was used mostly for maxillofacial surgery and implant surgery but later it was applied for orthodontic use (33, 49). CBCT offers high resolution images with fine details. Image quality can differ enormously among devices in the market and also depends on parameter settings (50-53).

Scientific evidence has proven that 3D imaging especially CBCT, has good impact in orthodontic treatment (54). CBCT can be applied in several aspects of orthodontic treatment such as cases with canine impaction, root resorption, an analysis of the airway, orthognathic surgery and last but not least, it can be used for 3D cephalometric analysis (38, 39, 54).

Maxillary canine impaction and root resorption

The maxillary canine is an important tooth, not only for the function but also for esthetics (11, 55). The incidence of impacted maxillary canines ranges from 1-3% (56, 57). To know the exact position of the maxillary canine is an important information for orthodontic treatment planning. Conventional 2D radiographic techniques - a shift-tube technique and an occlusal radiography - were used in the past to localize the canine position (1). However, 2D radiographs cannot represent the actual anatomical relationship between structures and therefore, 3D imaging started to play an important role in diagnosing canine impaction cases. Studies have shown that 3D imaging was advantageous in the management of impacted canines (58-60) although a few studies reported no statistically significant difference between impacted maxillary canine treatment planning using a cone-beam CT scan or a panoramic radiograph (61, 62).

When dealing with ectopic eruption of maxillary canines, another incident may occur: root resorption of maxillary lateral incisors (63). Conventionally, this pathology was assessed by using 2D periapical radiography and panoramic radiography (63), but because of the superimposition, it was difficult to diagnose only with 2D images. Several papers articles on 3D imaging and root resorption have been published (51, 59, 64-66). CBCT provided more accurate detection of root resorption and measurements in comparison to panoramic radiography.

3D cephalometry and 3D treatment planning

3D images give orthodontists and maxillofacial surgeons the opportunity to view all anatomical structures in three dimensions, much alike to reality. With the continuing development of 3D image viewing software, 3D treatment planning software, and 3D rapid prototype fabrication, CBCT images are utilized enormously in surgical planning (Fig. 1.4). First, MSCT data were used but after the invention and development of CBCT, CBCTs have been increasingly popular in the field. Several researchers and clinicians have used CBCT data for orthodontic treatment planning, orthognathic surgical planning, maxillofacial surgical planning and 3D cephalometric analysis (67-72).

In 3D cephalometry, the main principle of cephalometric analysis remains: linear measurements, angular measurements and proportional measurements are performed, depending on the analyses being used (67, 69, 70). The difference from 2D cephalometric analysis is that there is an extra dimension to everything measured. A 2D plane, which is a line by connecting 2 landmarks, is transformed into a plane that is composed of 3 landmarks as both left and right side of the human head were taken into account (67). There were many discussions on how to use traditional 2D cephalometric analysis in 3D software and how the norm values should be calculated as measurement values might change due to the added dimension (73). Furthermore, the number of publications focusing on the accuracy of the 3D imaging technique has increased during the past few years. However, only few studies were performed in a clinical situation. Therefore, the scientific evidence of the effect of 3D cephalometry on treatment planning and treatment outcome is very limited (54, 73). The scientific evidence of the effect of 3D cephalometry is evaluated in detail in **Chapter 2** of this doctoral thesis.

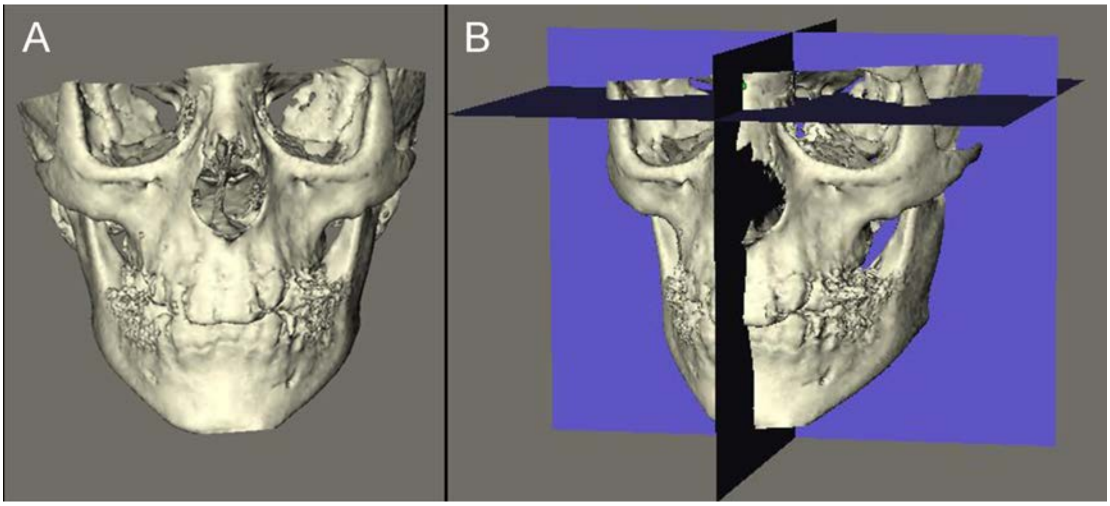

Figure 1.4 A) a 3D surface model of an orthodontic patient created in Maxilim® software. B) The same model with constructed reference planes using landmarks. The software offers 3D cephalometric analysis and surgical planning.

Reformatted panoramic images

Besides its usage in specific cases, CBCT images can provide a panoramic-like view by reformatting the CBCT volume (Fig. 1.5). This reformatted panoramic image can be useful for dentists to have an overview in a panoramic view that they have more experience in diagnosis. Unlike conventional panoramic radiographs, this view does not suffer from geometric distortion. The image is reconstructed by the curve drawn along the dental arch. Some studies have reported that this image is useful and give more accurate measurements when compared with the panoramic radiograph, which is prone to geometric distortion (74-79).

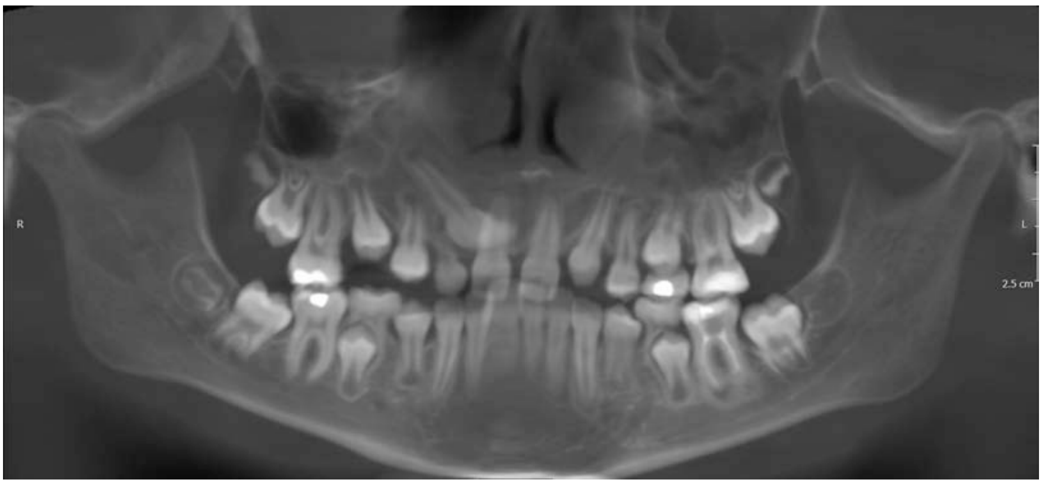

Figure 1.5 A 15-mm-thick reformatted panoramic view from 3D Accuitomo® 170 data of an orthodontic patient.

Radiation to patients

Radiation exposure to patients is one of the main concerns in using CBCT images on orthodontic patients. Most of the orthodontic patients are young children and adolescents who are more sensitive to radiation (80, 81). Justification is very crucial in the decision making process of whether conventional radiography is sufficient for each individual. *ALARA principle*, as low as reasonably achievable, must always be followed rigorously (82) and the benefits of CBCT images must outweigh their radiation risk. Several guidelines and recommendations were published related to cone-beam CT use (34-36, 40). Clinicians should follow these guidelines to avoid any possible misuse of these 3D CBCT devices.

The lack of scientific evidence on the influence on orthodontic treatment of 3D CBCT images in comparison with 2D radiographs leads to the primary aim of this doctoral project (54, 73). Whether the 3D CBCT can offer better diagnostic potential, which leads to better treatment planning and eventually better orthodontic treatment outcome when compared with 2D imaging modalities such as panoramic radiographs and lateral cephalograms, needs to be evaluated.

1.4 Aims and hypotheses

General research aims

The primary aim of this doctoral thesis was to investigate 2D and 3D imaging modalities and their application in orthodontic treatment.

As the use of 3D CBCT images has grown enormously during the past years, the secondary aim of this doctoral project was to develop a robust 3D cephalometric measurement system that can be applied to orthodontic practice which may help improve the treatment planning of orthodontic patients.

Detailed research aims

<u>PART I LITERATURE REVIEW</u>

Chapter 2: 3D Cephalometric analysis in orthodontics: a systematic review

Aim: To assess the scientific evidence for the diagnostic efficacy of 3D cephalometry.

Hypothesis: Scientific evidence of the diagnostic efficacy of 3D cephalometry is limited.

<u>PART II PANORAMIC IMAGING</u>

Chapter 3: An in vitro comparison of subjective image quality of panoramic views acquired via 2D or 3D imaging

Aim: To compare *in vitro* subjective image quality and diagnostic validity of reformatted panoramic views from CBCT with digital panoramic radiographs, regarding orthodontic treatment planning.

Hypothesis: The subjective image quality of a reformatted panoramic view from some CBCTs is similar to the subjective image quality of a digital panoramic radiograph.

Chapter 4: Agreement between cone-beam CT images and panoramic radiographs for initial orthodontic evaluation

Aims: To compare the agreement between cone-beam computed tomography (CBCT) and panoramic radiographs for initial orthodontic evaluation.

Hypothesis: The observer agreement between the CBCT and panoramic radiographic evaluation is good and CBCT can offer the same amount of information necessary for initial orthodontic evaluation.

PART III CEPHALOMETRIC IMAGING

Chapter 5: Accuracy of linear measurements using 3 imaging modalities: two lateral cephalograms and one 3D model from CBCT data

Aim: To compare the linear measurement accuracy of different cephalometric imaging modalities from 2D to 3D method.

Hypothesis: The accuracy of linear measurements on cephalograms taken by a cephalometric machine with a 3-meter source-to-mid-sagittal-plane distance (SMD) is better than the digital lateral cephalogram from a 1.5-meter SMD machine, but the accuracy of measurements on 3D models from CBCT data is the best among the three modalities.

Chapter 6: Reproducibility of sella turcica landmark in 3 dimensions using a sella turcica specific reference system

Aim: To develop 3D reference system in order to systematically improve landmark identification in 3 dimensions: a reference system for sella turcica landmark.

Hypothesis: A new 3D reference system can help increase the reproducibility of sella turcica landmark identification in 3D.

Chapter 7: A new mandible-specific landmark reference system for three-dimensional cephalometry

Aim: To develop a 3D reference system for mandibular cephalometric landmarks in order to systematically improve landmark identification in 3 dimensions.

Hypothesis: A new 3D reference system can help increase the reproducibility of mandibular cephalometric landmark identification in 3D cephalometry.

Chapter 8: Three-dimensional Frankfort horizontal plane revisited and evaluation of new horizontal planes

Aims: 1) To assess, in 3D CBCT, the precision and reproducibility of landmarks used in Frankfort horizontal plane (FH) and 2 new landmarks and 2) to evaluate the angular differences of newly introduced planes to the FH.

Hypothesis: The precision and reproducibility of landmarks used in FH and 2 new included landmarks is good and new planes are closely parallel to the traditional FH. The new planes can then be used instead of FH, when FH is not constructible.

1.5 References

1. Stuart CW, Michael JP. Oral Radiology. Principles and Interpretation. 7th ed. Canada: Elsevier Mosby; 2014.
2. Numata H. Consideration of the parabolic radiography of the dental arch. *J Shimazu Stud*. 1933;10:13.
3. Paatero Y. The use of a mobile source of light in radiography. *Acta Radiol*. 1948;29:221.
4. Paatero Y. A new tomographic method for radiographing curved outer surfaces. *Acta Radiol*. 1949;32:177.
5. Pettit GG. Panoramic radiography. *Dent Clin North Am*. 1971;15:169-82.
6. Farman AG, Farman TT. Panoramic dental radiography using a charge-coupled device receptor. *J Digit Imaging*. 1998;11:166-8.
7. Tronje G, Eliasson S, Julin P, Welander U. Image distortion in rotational panoramic radiography. II. Vertical distances. *Acta Radiol Diagn (Stockh)*. 1981;22:449-55.
8. Tronje G, Welander U, McDavid WD, Morris CR. Image distortion in rotational panoramic radiography. III. Inclined objects. *Acta Radiol Diagn (Stockh)*. 1981;22:585-92.
9. Tronje G, Welander U, McDavid WD, Morris CR. Image distortion in rotational panoramic radiography. I. General considerations. *Acta Radiol Diagn (Stockh)*. 1981;22:295-9.
10. Pfeiffer P, Bewersdorf S, Schmage P. The effect of changes in head position on enlargement of structures during panoramic radiography. *Int J Oral Maxillofac Implants*. 2012;27:55-63.
11. Proffit WR, Fields HW, Jr., Sarver DM. Contemporary Orthodontics. 4th ed. St.Lois, MO: Elsevier Mosby; 2007.
12. Hofrath H. Bedeutung der Röntgenfern und Abstands Aufnahme für die Diagnostik der Kieferanomalien. *Fortschr Orthod*. 1931;1:231-58.
13. Broadbent BH. A new x-ray technique and its application to orthodontia. *Angle Orthod*. 1931;1:45-66.
14. Jacobson A, Jacobson RL. Radiographic Cephalometry: From Basics to 3-D Imaging. 2 ed. USA: Quintessence Publishing; 2006.

15. Ricketts RM. Cephalometric analysis and synthesis. *Angle Orthod*. 1961;31:141-56.
16. Grummons D, Ricketts RM. Frontal cephalometrics: practical applications, part 2. *World J Orthod*. 2004;5:99-119.
17. Heflin BM. A three-dimensional cephalometric study of the influence of expansion of the midpalatal suture on the bones of the face. *Am J Orthod*. 1970;57:194-5.
18. Baumrind S, Peltzman P, Moffitt FH. New system for integrated three dimensional craniofacial mapping. *J Dent Res*. 1971;50:1496-7.
19. Baumrind S, Moffitt FH, Curry S. The geometry of three-dimensional measurement from paired coplanar x-ray images. *Am J Orthod*. 1983;84:313-22.
20. Haralabakis NB, Yiagtzis SC, Toutountzakis NM. Cephalometric characteristics of open bite in adults: a three-dimensional cephalometric evaluation. *Int J Adult Orthodon Orthognath Surg*. 1994;9:223-31.
21. Bjork A, Solow B. Measurement on radiographs. *J Dent Res*. 1962;41:672-83.
22. Baumrind S, Frantz RC. The reliability of head film measurements. 2. Conventional angular and linear measures. *Am J Orthod*. 1971;60:505-17.
23. Baumrind S, Frantz RC. The reliability of head film measurements. 1. Landmark identification. *Am J Orthod*. 1971;60:111-27.
24. Schwarz MS, Rothman SL, Chafetz N, Rhodes M. Computed tomography in dental implantation surgery. *Dent Clin North Am*. 1989;33:555-97.
25. Tal H, Moses O. A comparison of panoramic radiography with computed tomography in the planning of implant surgery. *Dentomaxillofac Radiol*. 1991;20:40-2.
26. Jacobs R, van Steenberghe D. Radiographic Planning and Assessment of Endosseous Oral Implants. 1st ed: Springer Verlag; 1998.
27. Beckmann EC. CT scanning the early days. *Br J Radiol*. 2006;79:5-8.
28. Lamoral Y, Quirynen M, Peene P, Vanneste F, Lemahieu SF, Baert AL*, et al.* Computed tomography in the preoperative planning of oral endo-osseous implant surgery. *Rofo*. 1990;153:505-9.

29. Scaf G, Lurie AG, Mosier KM, Kantor ML, Ramsby GR, Freedman ML. Dosimetry and cost of imaging osseointegrated implants with film-based and computed tomography. *Oral Surg Oral Med Oral Pathol Oral Radiol Endod*. 1997;83:41-8.
30. Loubele M, Bogaerts R, Van Dijck E, Pauwels R, Vanheusden S, Suetens P, *et al.* Comparison between effective radiation dose of CBCT and MSCT scanners for dentomaxillofacial applications. *Eur J Radiol*. 2009;71:461-8.
31. Mozzo P, Procacci C, Tacconi A, Martini PT, Andreis IA. A new volumetric CT machine for dental imaging based on the cone-beam technique: preliminary results. *Eur Radiol*. 1998;8:1558-64.
32. Pauwels R, Beinsberger J, Collaert B, Theodorakou C, Rogers J, Walker A, *et al.* Effective dose range for dental cone beam computed tomography scanners. *Eur J Radiol*. 2012;81:267-71.
33. Scarfe WC, Farman AG, Sukovic P. Clinical applications of cone-beam computed tomography in dental practice. *J Can Dent Assoc*. 2006;72:75-80.
34. American Dental Association Council on Scientific Affairs. The use of cone-beam computed tomography in dentistry: an advisory statement from the American Dental Association Council on Scientific Affairs. *J Am Dent Assoc*. 2012;143:899-902.
35. European Commission. Guidelines on CBCT for Dental and Maxillofacial Radiology: Evidence Based Guidelines: Radiation Protection Publication 2012. Available from: http://www.sedentexct.eu/content/guidelines-cbct-dental-and-maxillofacial-radiology.
36. American Academy of Oral Maxillofacial Radiology. Clinical recommendations regarding use of cone beam computed tomography in orthodontic treatment. Position statement by the American Academy of Oral and Maxillofacial Radiology. *Oral Surg Oral Med Oral Pathol Oral Radiol*. 2013;116:238-57.
37. Bornstein MM, Scarfe WC, Vaughn VM, Jacobs R. Cone beam computed tomography in implant dentistry: a systematic review focusing on guidelines, indications, and radiation dose risks. *Int J Oral Maxillofac Implants*. 2014;29 Suppl:55-77.

38. Kau CH, Richmond S, Palomo JM, Hans MG. Three-dimensional cone beam computerized tomography in orthodontics. *J Orthod*. 2005;32:282-93.
39. Mah JK, Huang JC, Choo H. Practical applications of cone-beam computed tomography in orthodontics. *J Am Dent Assoc*. 2010;141:7S-13S.
40. European Commission. Radiation Protection 136. European guidelines on radiation protection in dental radiology. The safe use of radiographs in dental practice. 2004. Available from: http://ec.europa.eu/energy/nuclear/radiation_protection/doc/publication/136.pdf.
41. Limchaichana N, Petersson A, Rohlin M. The efficacy of magnetic resonance imaging in the diagnosis of degenerative and inflammatory temporomandibular joint disorders: a systematic literature review. *Oral Surg Oral Med Oral Pathol Oral Radiol Endod*. 2006;102:521-36.
42. Daboul A, Schwahn C, Schaffner G, Soehnel S, Samietz S, Aljaghsi A*, et al.* Reproducibility of Frankfort horizontal plane on 3D multi-planar reconstructed MR images. *PLoS One*. 2012;7:e48281.
43. Hajeer MY, Ayoub AF, Millett DT, Bock M, Siebert JP. Three-dimensional imaging in orthognathic surgery: the clinical application of a new method. *Int J Adult Orthodon Orthognath Surg*. 2002;17:318-30.
44. Kusnoto B, Evans CA. Reliability of a 3D surface laser scanner for orthodontic applications. *Am J Orthod Dentofacial Orthop*. 2002;122:342-8.
45. Plooij JM, Swennen GR, Rangel FA, Maal TJ, Schutyser FA, Bronkhorst EM*, et al.* Evaluation of reproducibility and reliability of 3D soft tissue analysis using 3D stereophotogrammetry. *Int J Oral Maxillofac Surg*. 2009;38:267-73.
46. Toma AM, Zhurov A, Playle R, Ong E, Richmond S. Reproducibility of facial soft tissue landmarks on 3D laser-scanned facial images. *Orthod Craniofac Res*. 2009;12:33-42.
47. Brons S, van Beusichem ME, Bronkhorst EM, Draaisma J, Berge SJ, Maal TJ*, et al.* Methods to quantify soft-tissue based facial growth and treatment outcomes in children: a systematic review. *PLoS One*. 2012;7:e41898.

48. Pittayapat P, Kwon MS, Olszewski R, Coucke W, Politis C, Jacob R. Validation of a 3D facial scanning system. *manuscript in preparation*.
49. De Vos W, Casselman J, Swennen GR. Cone-beam computerized tomography (CBCT) imaging of the oral and maxillofacial region: a systematic review of the literature. *Int J Oral Maxillofac Surg*. 2009;38:609-25.
50. Liang X, Jacobs R, Hassan B, Li L, Pauwels R, Corpas L*, et al.* A comparative evaluation of Cone Beam Computed Tomography (CBCT) and Multi-Slice CT (MSCT) Part I. On subjective image quality. *Eur J Radiol*. 2010;75:265-9.
51. Alqerban A, Jacobs R, Fieuws S, Nackaerts O, Willems G. Comparison of 6 cone-beam computed tomography systems for image quality and detection of simulated canine impaction-induced external root resorption in maxillary lateral incisors. *Am J Orthod Dentofacial Orthop*. 2011;140:e129-39.
52. Schulze R, Heil U, Gross D, Bruellmann DD, Dranischnikow E, Schwanecke U*, et al.* Artefacts in CBCT: a review. *Dentomaxillofac Radiol*. 2011;40:265-73.
53. Bamba J, Araki K, Endo A, Okano T. Image quality assessment of three cone beam CT machines using the SEDENTEXCT CT phantom. *Dentomaxillofac Radiol*. 2013;42:20120445.
54. van Vlijmen OJ, Kuijpers MA, Berge SJ, Schols JG, Maal TJ, Breuning H*, et al.* Evidence supporting the use of cone-beam computed tomography in orthodontics. *J Am Dent Assoc*. 2012;143:241-52.
55. Freisfeld M, Dahl IA, Jager A, Drescher D, Schuller H. X-ray diagnosis of impacted upper canines in panoramic radiographs and computed tomographs. *J Orofac Orthop*. 1999;60:177-84.
56. Dachi SF, Howell FV. A survey of 3,874 routine full-mouth radiographs. I. A study of retained roots and teeth. *Oral Surg Oral Med Oral Pathol*. 1961;14:916-24.
57. Thilander B, Myrberg N. The prevalence of malocclusion in Swedish schoolchildren. *Scand J Dent Res*. 1973;81:12-21.

58. Walker L, Enciso R, Mah J. Three-dimensional localization of maxillary canines with cone-beam computed tomography. *Am J Orthod Dentofacial Orthop*. 2005;128:418-23.
59. Alqerban A, Jacobs R, Fieuws S, Willems G. Comparison of two cone beam computed tomographic systems versus panoramic imaging for localization of impacted maxillary canines and detection of root resorption. *Eur J Orthod*. 2011;33:93-102.
60. Botticelli S, Verna C, Cattaneo PM, Heidmann J, Melsen B. Two- versus three-dimensional imaging in subjects with unerupted maxillary canines. *Eur J Orthod*. 2011;33:344-9.
61. Alqerban A, Hedesiu M, Baciut M, Nackaerts O, Jacobs R, Fieuws S*, et al.* Pre-surgical treatment planning of maxillary canine impactions using panoramic vs cone beam CT imaging. *Dentomaxillofac Radiol*. 2013;42:20130157.
62. Alqerban A, Willems G, Bernaerts C, Vangastel J, Politis C, Jacobs R. Orthodontic treatment planning for impacted maxillary canines using conventional records versus 3D CBCT. *Eur J Orthod*. 2014. in press.
63. Sameshima GT, Asgarifar KO. Assessment of root resorption and root shape: periapical vs panoramic films. *Angle Orthod*. 2001;71:185-9.
64. Liu DG, Zhang WL, Zhang ZY, Wu YT, Ma XC. Localization of impacted maxillary canines and observation of adjacent incisor resorption with cone-beam computed tomography. *Oral Surg Oral Med Oral Pathol Oral Radiol Endod*. 2008;105:91-8.
65. Alqerban A, Jacobs R, Souza PC, Willems G. In-vitro comparison of 2 cone-beam computed tomography systems and panoramic imaging for detecting simulated canine impaction-induced external root resorption in maxillary lateral incisors. *Am J Orthod Dentofacial Orthop*. 2009;136:764 e1-11; discussion -5.
66. Dudic A, Giannopoulou C, Leuzinger M, Kiliaridis S. Detection of apical root resorption after orthodontic treatment by using panoramic radiography and cone-beam computed tomography of super-high resolution. *Am J Orthod Dentofacial Orthop*. 2009;135:434-7.

67. Swennen GR, Schutyser F, Hausamen JE. Three-Dimensional Cephalometry: A Color Atlas and Manual. 1st ed. Heidelberg, Germany: Springer Verlag; 2005.
68. Swennen GR, Schutyser F. Three-dimensional cephalometry: spiral multi-slice vs cone-beam computed tomography. *Am J Orthod Dentofacial Orthop*. 2006;130:410-6.
69. Swennen GR, Schutyser F, Barth EL, De Groeve P, De Mey A. A new method of 3-D cephalometry Part I: the anatomic Cartesian 3-D reference system. *J Craniofac Surg*. 2006;17:314-25.
70. Olszewski R, Cosnard G, Macq B, Mahy P, Reychler H. 3D CT-based cephalometric analysis: 3D cephalometric theoretical concept and software. *Neuroradiology*. 2006;48:853-62.
71. Olszewski R, Zech F, Cosnard G, Nicolas V, Macq B, Reychler H. Three-dimensional computed tomography cephalometric craniofacial analysis: experimental validation in vitro. *Int J Oral Maxillofac Surg*. 2007;36:828-33.
72. Olszewski R, Reychler H, Cosnard G, Denis JM, Vynckier S, Zech F. Accuracy of three-dimensional (3D) craniofacial cephalometric landmarks on a low-dose 3D computed tomograph. *Dentomaxillofac Radiol*. 2008;37:261-7.
73. Pittayapat P, Limchaichana-Bolstad N, Willems G, Jacobs R. Three-dimensional cephalometric analysis in orthodontics: a systematic review. *Orthod Craniofac Res*. 2014;17:69-91.
74. Pawelzik J, Cohnen M, Willers R, Becker J. A comparison of conventional panoramic radiographs with volumetric computed tomography images in the preoperative assessment of impacted mandibular third molars. *J Oral Maxillofac Surg*. 2002;60:979-84.
75. Ludlow JB, Laster WS, See M, Bailey LJ, Hershey HG. Accuracy of measurements of mandibular anatomy in cone beam computed tomography images. *Oral Surg Oral Med Oral Pathol Oral Radiol Endod*. 2007;103:534-42.
76. Mischkowski RA, Ritter L, Neugebauer J, Dreiseidler T, Keeve E, Zoller JE. Diagnostic quality of panoramic views obtained by a newly developed

digital volume tomography device for maxillofacial imaging. *Quintessence Int*. 2007;38:763-72.

77. Angelopoulos C, Thomas SL, Hechler S, Parissis N, Hlavacek M. Comparison between digital panoramic radiography and cone-beam computed tomography for the identification of the mandibular canal as part of presurgical dental implant assessment. *J Oral Maxillofac Surg*. 2008;66:2130-5.
78. Dreiseidler T, Mischkowski RA, Neugebauer J, Ritter L, Zoller JE. Comparison of cone-beam imaging with orthopantomography and computerized tomography for assessment in presurgical implant dentistry. *Int J Oral Maxillofac Implants*. 2009;24:216-25.
79. Van Elslande D, Heo G, Flores-Mir C, Carey J, Major PW. Accuracy of mesiodistal root angulation projected by cone-beam computed tomographic panoramic-like images. *Am J Orthod Dentofacial Orthop*. 2010;137:S94-9.
80. International Commission on Radiological Protection. Recommendations of the International Commission on Radiological Protection. ICRP Publication 103. Ann ICRP 37. Oxford, UK: Pergamon Press; 2007.
81. Theodorakou C, Walker A, Horner K, Pauwels R, Bogaerts R, Jacobs R, *et al.* Estimation of paediatric organ and effective doses from dental cone beam CT using anthropomorphic phantoms. *Br J Radiol*. 2012;85:153-60.
82. Farman AG. ALARA still applies. *Oral Surg Oral Med Oral Pathol Oral Radiol Endod*. 2005;100:395-7.

PART I

LITERATURE REVIEW

Chapter 2

3D Cephalometric analysis in orthodontics: a systematic review

This chapter is based on:

Pittayapat P, Limchaichana-Bolstad N, Willems G, Jacobs R. Three-dimensional cephalometric analysis in orthodontics: a systematic review. *Orthod Craniofac Res.* 2014;17:69-91.

2.1 Abstract

Context: The scientific evidence of 3D cephalometry in orthodontics has not been well established.

Objective: The aim of this systematic review was to evaluate the evidence for the diagnostic efficacy of 3D cephalometry in orthodontics, focusing on measurement accuracy and reproducibility of landmark identification.

Data sources: PubMed, EMBASE and the Cochrane library (from beginning to March 13, 2012) were searched. Search terms included: cone-beam computed tomography; tomography, spiral computed; imaging, three-dimensional; orthodontics.

Study selection: Two reviewers read the retrieved articles and selected relevant publications based on pre-established inclusion criteria. The selected publications had to elucidate the hierarchical model of the efficacy of diagnostic imaging systems by Fryback and Thornbury.

Data extraction: The data was then extracted according to two protocols, which were based on the Quality Assessment of Diagnostic Accuracy Studies (QUADAS) tool. Next, levels of evidence were categorized into 3 groups: low, moderate and high evidence.

Data synthesis: 571 publications were found by database search strategies and 50 additional studies by hand search. A total of 35 publications were included in this review.

Conclusions: Limited evidence for the diagnostic efficacy of 3D cephalometry was found. Only 6 studies met the criteria for a moderate level of evidence. Accordingly, this systematic review reveals that there is still need for methodologically standardized studies on 3D cephalometric analysis.

2.2 Introduction

Cephalometric analysis was first introduced in 1930s by Hofrath (1) in Germany and Broadbent (2) in the United States. The method uses frontal and lateral cephalometric radiographs to evaluate the craniofacial complex, dentofacial proportions, malocclusion and changes related to growth, all of which are crucial for orthodontic treatment planning and evaluation. A conventional cephalometric radiograph is a two-dimensional representation of three-dimensional structures. Although widely accepted as a standard tool for treatment planning, it still has several downsides, such as geometric distortion and superimposition of structures (3-5).

Recently, three-dimensional images have started to play an important role in oral health and diagnosis. Several years ago computed tomography (CT) was introduced into the dental field. However, its high radiation dose has led to controversy. In 1996, dental cone-beam computed tomography (CBCT) was invented, and the technology has been evolving ever since. With relatively lower radiation doses than multi-slice CT (MSCT), CBCT has become very popular in dentistry. Some researchers have also introduced the use of a clinical low-dose CT protocol for 3D cephalometric application (6-8). Both modalities allow orthodontists to visualize craniofacial structures in three dimensions and overcome the drawback of 2D cephalometric analysis.

Several studies have been conducted on cephalometric images derived from CBCTs. These derived lateral cephalometric images were proven to be accurate and comparable with direct measurements on skulls (9-12) and conventional cephalograms of patients (13). This method is the first step towards 3D cephalometry. Nevertheless, it still implies that a patient's anatomy is not evaluated in three dimensions. A combination of measurements on the axial, coronal and sagittal view was also used in several studies (14, 15). This method has been sometimes referred to as 2.5D as it does not allow full access to the patients' structures in real three dimensions (8,15). Three-dimensional cephalometric analysis requires input from 3D images of the patient, either on CBCTs or on MSCTs, and software that offers 3D cephalometric measurement tools (8, 16-19).

An increasing amount of research has been conducted to evaluate the measurement accuracy, reliability and reproducibility of 3D craniofacial landmark identification and to justify whether further elaboration of 3D cephalometry is more beneficial than the standard 2D analysis. To our knowledge, a systematic review specifically focusing on 3D cephalometry for orthodontic diagnosis and treatment planning was not yet available. The aim of this review was therefore to systematically evaluate the current evidence for the diagnostic efficacy of 3D cephalometry, focusing on measurement accuracy and reproducibility of landmark identification for orthodontic diagnosis.

2.3 Materials and methods

Methods of the analysis and inclusion criteria were specified in advance and were documented in a protocol.

Eligibility criteria

The selected publications had to elucidate the model of efficacy: diagnostic accuracy efficacy, diagnostic thinking efficacy, therapeutic efficacy, or any combination of the preceding adapted from by Fryback and Thornbury (20).

Diagnostic accuracy efficacy (20) was defined as:

- Observer performance expressed as overall agreement, Kappa Index or correlation coefficients;
- Diagnostic accuracy as percentage of correct landmark identification;
- Diagnostic accuracy as percentage of correct cephalometric linear and/or angular measurement;
- Sensitivity, specificity or predictive values;

Diagnostic thinking efficacy (20) was defined as:

- Percentage of cases in a series in which 3D cephalometry was judged ‘helpful’ to guide the orthodontic treatment;
- Difference in clinicians’ subjectively estimated diagnosis probabilities pre- to post-3D cephalometric information;

Therapeutic efficacy (20) was defined as:

- Percentage of times 3D cephalometry judged helpful in planning management of the patient in a case series;

- Percentage of times therapy-planned pre-3D cephalometry changed after the 3D cephalometric information was obtained;
- Percentage of times clinicians' prospectively stated therapeutic choices changed after 3D cephalometric information.

Information sources

A comprehensive electronic database search was performed in MEDLINE via PubMed (from beginning to March 13, 2012), EMBASE via embase.com (from beginning to March 13, 2012), and the Cochrane library website (from beginning to March 13, 2012). No restrictions were imposed regarding time period or types of study design (i.e. case-controlled, randomized controlled trial). The publications were searched electronically by using controlled index terms and relevant specific free text words. The last search was performed on March 13, 2012. Detailed search strategies for both MEDLINE and EMBASE are shown in Table 2.1. The Cochrane Central Register of Controlled Trials (CENTRAL), the Cochrane Database of Systematic Reviews (CDSR) and the Cochrane Database of Abstracts of Reviews of Effects (DARE) were searched using the search term 'cephalometry'.

Search strategy

The following Medical Subject Headings (MeSH) were used when searching the literature: Cephalometry; Cone-beam computed tomography; Tomography, Spiral Computed; Imaging, Three-Dimensional; Orthodontics.

Study selection

The lists of publications from both databases were imported into EndNote® Web 3.3 (Thomson Reuters, New York, USA). Duplicate articles were deleted, after which two reviewers independently read the resulting collection of titles and abstracts. Book chapters, review studies and animal studies were excluded. Both *in vitro* and *in vivo* studies were included. The full texts of selected publications were then retrieved. When an abstract was considered to be relevant by one of the authors, the publication was then read in full text.

Grey literature were searched but excluded if full texts were not available. When publications elucidated only observer performance, the analysis had to be based on a minimum of 2 observers.

Table 2.1 Search strategies for MEDLINE via PubMed and EMBASE via embase.com (database search was last performed on 13 March 2012)

	Number of publications
MEDLINE via PUBMED	524
("Cephalometry"[Mesh] OR cephalometr*) AND ("Cone-Beam Computed Tomography"[Mesh] OR "Tomography, Spiral Computed"[Mesh] OR "Imaging, Three-Dimensional"[Mesh:NoExp] OR "Cone Beam Computed Tomography"[All Fields] OR "Cone Beam CT"[All Fields] OR "Volumetric Computed Tomography"[All Fields] OR "Volume Computed Tomography"[All Fields] OR "Volume CT"[All Fields] OR "Volumetric CT"[All Fields] OR "Cone beam CT"[All Fields] OR "CBCT"[All Fields] OR "digital volume tomography"[All Fields] OR "DVT"[All Fields] OR "Spiral Computed Tomography"[All Fields] OR "Spiral Computer-Assisted Tomography"[All Fields] OR "Spiral Computerized Tomography"[All Fields] OR "spiral CT Scan"[All Fields] OR "spiral CT Scans"[All Fields] OR "Helical CT"[All Fields] OR "Helical CTS"[All Fields] OR "Helical Computed Tomography"[All Fields] OR "Spiral CAT Scan"[All Fields] OR "Spiral CAT Scans"[All Fields] OR 3D OR 3-D OR "three dimension"[All Fields] OR "three dimensions"[All Fields] OR "three dimensional"[All Fields]) AND ("Orthodontics"[Mesh] OR orthodontic*)	
EMBASE via embase.com	175
#1 'cephalometry'/exp #2 cephalometr* AND [embase]/lim #3 #1 OR #2 #4 'cone beam computed tomography'/exp #5 'spiral computer assisted tomography'/exp #6 'three dimensional imaging'/exp #7 'multidetector computed tomography'/exp #8 3d OR '3-d' OR 'three dimension' OR 'three dimensions' OR 'three dimensional' AND [embase]/lim #9 'cone beam computed tomography'/syn AND [embase]/lim #10 'volumetric computed tomography'/syn OR 'volume computed tomography'/syn OR 'volume ct'/syn OR 'volumetric ct'/syn OR 'cone beam ct'/syn OR 'cbct' OR 'digital volume tomography' OR 'dvt' AND [embase]/lim #11 'spiral computed tomography'/syn OR 'spiral computer-assisted tomography'/syn OR 'spiral computerized tomography' OR 'spiral ct scan' OR 'spiral ct scans' OR 'helical ct'/syn OR 'helical cts' OR 'helical computed tomography'/syn OR 'spiral cat scan' OR 'spiral cat scans' AND [embase]/lim #12 #4 OR #5 OR #6 OR #7 OR #8 OR #9 OR #10 OR #11 #13 #3 AND #12 #14 'orthodontics'/exp #15 orthodontic* AND [embase]/lim #16 #14 OR #15 #17 #13 AND #16	
Total number of publications	699
Total number of publications after excluding duplications	571

The second step was to hand search the reference lists of the publications that were found to be relevant in the first step. Titles of the articles should contain a keyword: 'cephalometry' 'cephalometric' and 'cone-beam computed tomography' 'CBCT' or 'computed tomography 'CT' or 'three-dimensional' or '3D'. Similar to the first step, when an abstract was considered to be relevant by one of the reviewers, the full texts were then retrieved.

Data extraction

Two authors independently extracted the data into protocol 1 (Table 2.2) which was formulated based on the Cochrane Handbook for Diagnostic Test Accuracy (DTA) Reviews and the Cochrane Handbook for Systematic Reviews of Interventions (21,22) and literature describing how to critically appraise studies on diagnostic methods (23,24).

Table 2.2 Protocol 1 for primary data extraction

	First author				
	Title of publication				
	Journal		Year	Volume	Page
1	Is there a well-defined hypothesis?		Yes	No	Unclear
2	Method studied				
	CBCT				
	Multi-slice CT				
	Conventional cephalogram				
	Imaging software				
3	Study design				
	In-vitro	Number of objects	Type of objects		
	In-vivo	Number of patients	Condition of patients		
4	Reference method		Yes		No
5	How is the outcome described?				
	Sensitivity	Specificity	Predictive value		
	Accuracy	ROC analysis	Likelihood ratio		
	Statistical analysis				
6	Value of diagnostic information				
	Eliminating superimposition of landmarks with other anatomical structure				
	Left-Right anatomical landmarks are both counted				
	Treatment planning are performed in 3D				
7	What is the level according to Fryback and Thornbury of this study?				
	Level 1 Technical efficacy				
	Level 2 Diagnostic accuracy efficacy				
	Level 3 Diagnostic thinking efficacy				
	Level 4 Therapeutic efficacy				
	Level 5 Patient outcome efficacy				
8	Is this publication relevant to the review?			Yes	No
	Signature			Date	

Secondly, protocol 2 (Table 2.3) was applied to the included articles to assess the quality of the publications. This protocol is based on the Quality Assessment of Diagnostic Accuracy Studies (QUADAS) tool and the Cochrane Handbook for DTA Reviews (21,25). Information was extracted from included studies concerning: type of studies, number of samples, reference method, specific method used in the study, number of observers, statistical method and results according to authors.

Levels of evidence

The quality and internal validity (level of evidence) of each publication was judged to be high, moderate, or low according to the following criteria (23,24).

A study was assessed to have a *high level of evidence* if it fulfilled all of the following criteria:

- There was an independent blind comparison between test and reference methods.
- The population was described so that the status, prevalence, and severity of the condition were clear. The spectrum of patients was similar to the spectrum of patients on whom the test method will be applied in clinical practice.
- The results of the test method being evaluated did not influence the decision to perform the reference method(s).
- Test and reference methods were well described, concerning technique and implementation.
- The judgments (observations, measurements) were well described considering diagnostic criteria applied and information and instructions to the observers.
- The reproducibility of the test method was described for 1 observer (intra-observer performance) as well as for several (minimum 2) observers (inter-observer performance).
- The results were presented in terms of relevant data needed for necessary calculations.

Table 2.3 Protocol 2 for quality assessment of publications

Paper No.			Date information extracted:	
1st author:				
Journal			Year	Volume	Page
1	Did the sample include an appropriate spectrum of objects (patients)?			
	Yes	No	Unclear	
2	Were selection criteria clearly described?			
	Yes	No	Unclear	
3	Were the methods for performing the measurement described in sufficient detail to permit replication?			
	Yes	No	Unclear	
4	Was the execution of the reference standard described in sufficient detail to permit its replication?			
	Yes	No	Unclear	
5	For the in-vitro study, did the test situation imitate a clinical situation?			
	Yes	No	Unclear	
6	Is the reference standard likely to classify the target condition correctly?			
	Yes	No	Unclear	
7	Was the reference standard independent of the index test? (i.e. the index test did not form part of the reference standard)			
	Yes	No	Unclear	
8	Were the index test results interpreted without knowledge of the results of the reference standard?			
	Yes	No	Unclear	
9	Were the reference standard results interpreted without knowledge of the results of the index test?			
	Yes	No	Unclear	
10	Were the same clinical data available when test results were interpreted as would be available when the test is used in practice?			
	Yes	No	Unclear	
11	Were uninterpretable / intermediate test results reported?			
	Yes	No	Unclear	
12	Were withdrawals from the study explained?			
	Yes	No	Unclear	
13	Was the number of observers sufficient to evaluate the influence of observer reproducibility and diagnostic efficacy?			
	Yes	No	Unclear	
14	Was observer reproducibility described?			
	Yes	No	Unclear	
15	Were appropriate results presented (accuracy, percentage of correct diagnosis, sensitivity, specificity, predictive values, measures of ROC, likelihood ratios, or other relevant measures) and were these calculated appropriately?			
	Yes	No	Unclear	
	Level of Evidence			
	High	**Moderate**	**Low**	**Exclude**
	Comments:			

A study was assessed to have a *moderate level of evidence* if any of the above criteria were not met. On the other hand, the study was assessed not to have deficits that are described below for studies with a low level of evidence.
A study was assessed to have a low level of evidence if it met any of the following criteria:

- The result of the test method influenced the decision to perform the reference method.
- The test or the reference method or both were not satisfactorily described.
- The judgments were not well described.
- The reproducibility of the test method was not described or was described for only 1 observer.
- The results could have a systematic bias.
- The results were not presented in a way that allowed efficacy calculations to be made.

The scientific evidence on diagnostic efficacy was evaluated according to the scale: strong, moderately strong, limited or insufficient (23,24) depending on the quality and the level of evidence of the publications.

- Strong research-based evidence: at least 2 publications with a high level of evidence
- Moderately strong research-based evidence: 1 publication with a high level of evidence and 2 publications with a moderate level of evidence
- Limited research-based evidence: at least 2 of the publications with a moderate level of evidence
- Insufficient research-based evidence: scientific evidence is insufficient or lacking according to the criteria defined in this study

Synthesis of results

The results were analysed descriptively. No meta-analysis was performed because of the lack of original studies.

2.4 Results

Study selection

The results of this systematic review are reported based on the PRISMA statement (26). A total of 524 publications were found from the PubMed database, 175 publications from the EMBASE database and no systematic reviews or clinical trials on 3D cephalometry were found in the Cochrane library. This resulted in 571 publications after removing of duplicates and a total of 77 publications were included in the systematic review after the first assessment (Fig. 2.1) (26).

Data extraction was then performed firstly using protocol 1 (Table 2.2). Publications that were not relevant to the model of efficacy were excluded in this step, thus a total of 77 articles were read and their quality was assessed. Quality assessment of these studies was evaluated by using protocol 2, based on the QUADAS tool (Table 2.3).

The second step of the search was done by hand searching the reference lists of included publications. Fifty additional articles met the search criteria and were added to the list of protocol 1. As a result of this assessment, 29 original articles were additionally included to the review, setting the total number of articles submitted to the protocol 2 evaluation at 106 publications (Fig. 2.1).

In this step, studies that did not have a representative sample spectrum (sample size smaller than 10) were excluded. Studies, in which the observer performance was evaluated but which had only 1 observer, were excluded. Studies that did not have a valid reference standard were regarded as low quality.

Finally, 35 original articles were included in systematic review (7,8,17,27-58). These included publications were categorized into three different levels: low, moderate and high level of evidence (23,24).

Study characteristics

To be able to report the diagnostic accuracy of these studies, articles were categorized based on the topics of studies as followed: landmark identification, linear and angular measurement, facial asymmetry, and other topics.

The most reported topic was landmark identification. No study met the criteria for high level of evidence. Six publications were qualified as moderate level of evidence (Table 2.4) and 29 publications were qualified as low level of evidence (Table 2.5-2.8). All studies were related to the diagnostic accuracy efficacy. No publication that reported on diagnostic thinking efficacy and therapeutic efficacy was found.

Figure 2.1 Flow diagram of the included studies according to the PRISMA.

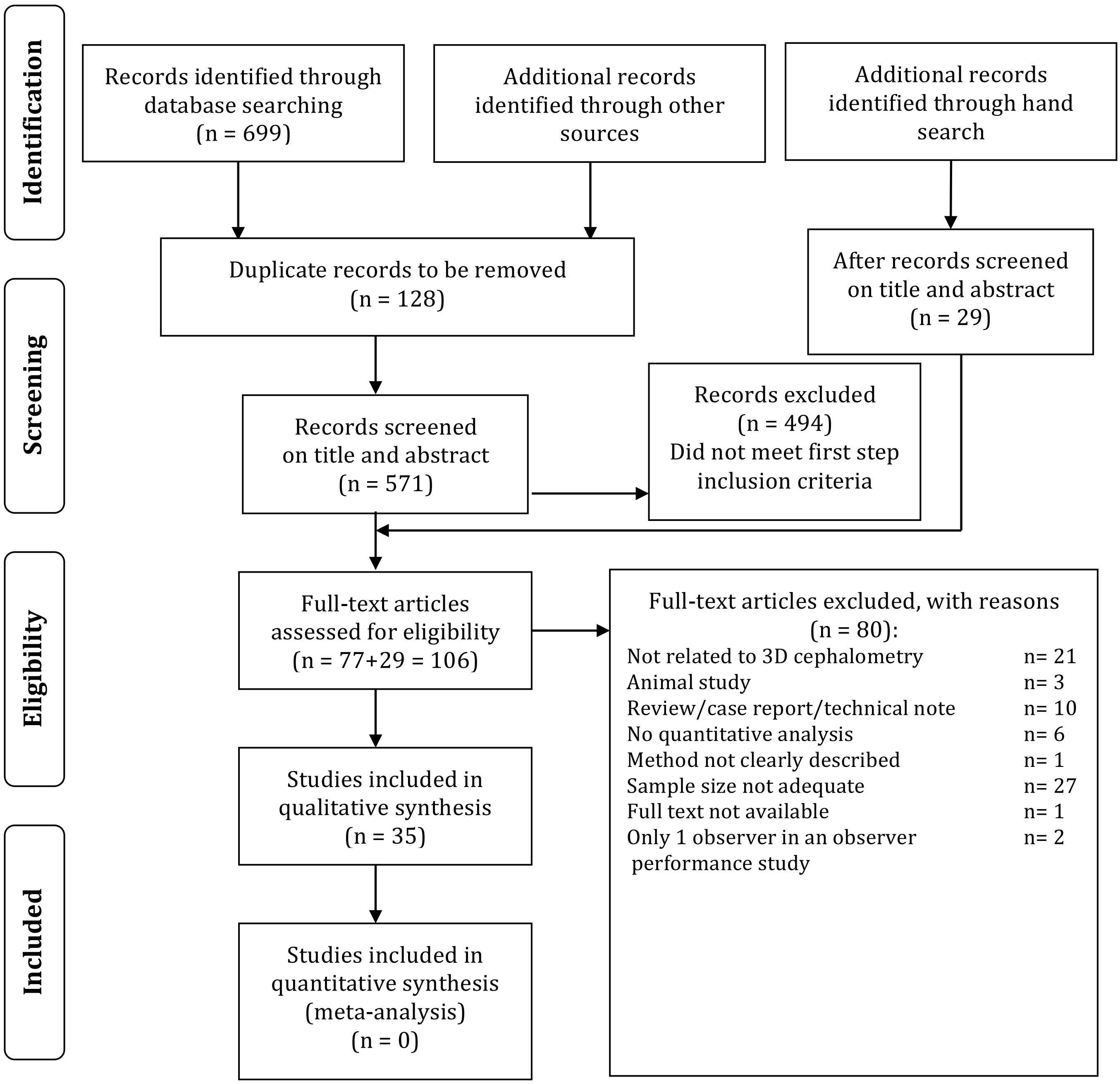

Table 4 Studies with a moderate level of evidence

Authors	Study topic	Type of study	Sample size	Reference method	M&M	Observers	Statistical method	Results according to authors
Cavalcanti *et al.* 2004	Measurement accuracy & precision	*In vitro*	13 cadaver heads	Electromagnetic 3 Space™ digitizer	- Spiral CT - Vitrea© version 2.3 software - Anthropometric anatomical points	2 observers x 2	Mean absolute error percentage, SD, CI, intra- and inter-observer reliability, ANOVA	Intra- vs inter-observer: NS Imaging vs physical: NS Standard error 0.45-1.44% % Error: physical vs 3D Bone = 0.83% Soft tissue = 1.78%
Olszewski *et al.* 2007	3D ceph craniofacial analysis	*In vitro*	26 dry skulls	3D measuring instrument to assess 3D position (x, y, z)	- Lat ceph - Spiral CT - ACRO 3D© software - Delaire's ceph analysis	2 observers x 2	Reproducibility, accuracy	Intra-observer: ICC 2D = 0.06-0.90 ICC 3D CT = 0.97-1.00 Inter-observer: ICC 2D = 0.13-0.84 ICC 3D CT = 0.94-1.00 User accuracy of 3D (absolute difference) between 0.75mm (±0.05) and 0.99mm (±0.08)
Olszewski *et al.* 2008	Landmark accuracy	*In vitro*	15 dry skulls	Calculated reference standard based on the index test	- Spiral CT - Low-dose CT protocol - ACRO 3D© software - 12 ceph landmarks	2 observers x 2	Non-parametric test, accuracy, reliability	Intra-observer mean distances: high-dose < low-dose (p = 0.37) Inter-observer mean distances: high-dose < low-dose (p = 0.03)
Lopes *et al.* 2008	Angular measurements	*In vitro*	28 dry skulls	Beyond Crysta-C9168 series 900 device for 3D coordinates	- Multi-slice CT - Craniometric anatomical points - 6 angular measurements	2 observers x 2	Precision, accuracy	Inter-observer: NS Intra-observer: NS Difference between physical and 3D measurement: -3.16% to -0.10%
Lagravère *et al.* 2011	Cranial base foramen	*In vitro*	10 dry skulls	Gutta percha placed at landmarks	- CBCT - AMIRA© software - 4 references foramen landmark	3 observers (Principal x3 Others x1)	Accuracy, intra- and inter-observer reliability (ICC)	Intra-observer ICC > 0.93 Inter-observer ICC > 0.92 Accuracy: large average mean difference (max. 3.60 mm for foramen rotundum)
Olszewski *et al.* 2012	Landmark reproducibility	*In vitro*	10 dry skulls	Calculated reference standard based on the index test	- CBCT - Maxilim© software - 24 osseous landmarks	2 observers x 2	Reproducibility	Intra-observer mean distance: CBCT < low-dose CT (p=0.000075) Inter-observer mean distance: CBCT < low-dose CT (p=0.00087)

Landmark identification

Fourteen publications regarding landmark identification are shown in Table 2.5. Two publications from Olszewski *et al*. (2008) (7) and Olszewski *et al*. (2012) (8) reached the moderate level of evidence and both of which are *in vitro* studies on dry human skulls. All studies that were done on patients lacked a gold standard and were therefore regarded as low level of evidence.

In the 2008, study of Olszewsksi *et al*., the authors compared low- and high-dose CT protocols for landmark identification in 3D cephalometry. They reported that the global intra- and inter-observer mean distances for all landmarks were smaller with a high-dose CT protocol (p = 0.37) and (p = 0.03), respectively (7). Olszewsksi *et al*. did a similar study in 2012 but this time comparing a low-dose CT protocol and a CBCT for landmark identification in 3D cephalometry. The results revealed that the CBCT showed better reproducibility. The intra- and inter-observer mean distance of the CBCT (p = 0.000075) were smaller than those from the low-dose CT (p = 0.00087) (8).

Regarding the precision of landmark identification, studies reported it in different manners. In 1995, Richtsmeier *et al*. found that the precision in locating landmarks was less than 0.5 mm for all landmarks. In addition, the accuracy of linear measurements was reported as average difference between 1-2 mm (48). In 2009, Ludlow *et al.*, reported the precision of landmark identification in another manner. It was found that overall correlation was 0.98 and 13 of 24 landmarks had statistically less variability in at least 1 direction of measurement in the multi-planar reformation (MPR) views (41). Schlicher *et al*. showed that the average consistency across all 32 landmarks amongst 9 examiners was 1.64 mm, while the average precision (SD) was 0.87 mm. Sella turcica was the most consistent (0.50 mm) and most precise (0.23 mm) (50). Hassan *et al*. defined the precision as the absolute difference between an observer's repeated measurements and the mean of all measurements per landmark. The 3D surface model together with multiplanar reformation (MPR) images improved the tracing precision in 15 landmarks but only statistically significant in 6 of 22 landmarks. The total precision of measurements ranged between 0.29 ± 0.17 mm and 2.82 ± 7.53 mm (36).

The most reported results are about the observer performance, reproducibility, and repeatability of the landmarks. Concerning the observer reliability, studies reported the results as mean measurement differences (38,44,51) or intraclass correlation coefficient values (ICC) (29,33,38,39). The ICC ranged between more than 0.70 to more than 0.90 for intra-observer and between more than 0.64 to more than 0.90 for inter-observer (29,33,38,39). Zamora *et al*. found ICC higher than 0.99 with the best results for landmark identification in the Z-direction (58). Chien *et al*. (2009) found lower ICC in 2D: inter-observer 0.35 versus intra-observer 0.57 (29) but Lagravère *et al*. (2010) reported values > 0.90 (39). In Chien's study, 2D landmark identifications were generally much less repeatable than in 3D (29).

Linear and angular measurement

Thirteen publications regarding the measurement topic were shown in Table 2.6. Two publications from Cavalcanti *et al*. (28) and Lopes *et al*. (40) reached the moderate level of evidence and both of which are *in vitro* studies. As similar to the studies in the landmark identification group, all studies that were done on patients lacked a gold standard and were consequently considered as low level of evidence.

Studies reporting on observer performance, ICC of 3D measurements ranged from 0.86-0.99 for intra-observer and from 0.76-0.99 for inter-observer reliability (31,32,34,47). Some studies used Pearson correlation coefficients and the results showed that the coefficients ranged between 0.42-0.98 (average ICC around 0.89-0.91) (54-56). Two studies reported observer performance as mean difference in measurements (27,35).

Lopes *et al*. reported on precision and accuracy of 6 angular measurements. Difference between physical and 3D measurement ranged between -3.16% to -0.10% (40). In the study of Cavalcanti *et al*., the results of the comparison between 2D-CT, 3D-CT volume rendering and physical measurements showed that the error between mean physical measurement and mean 3D-based measurements was 0.83% for bone, and 1.78% for soft tissue (28). Both studies reported no statistically significant differences in the inter- and intra-observer reliability.

Concerning studies with low level of evidence, some studies reported the accuracy of measurements. In 2008, Periago *et al*. found statistical differences between CBCT means and true dimensions for all of the midsagittal measurements except Nasion-A point and 6 of the 12 bilateral measurements (47). In a study published by Brown *et al*. in 2009, there were no differences between 3D CBCT and actual skull measurements for 6 dimensions. CBCT produced generally lower measurements than skull values (27).

Facial asymmetry

Three publications with low level of evidence were found (Table 2.7). The studies were performed *in vitro* with only 1 observer and without a standard reference. In 2009, Van Vlijmen *et al*. used 40 dry skulls to test the intra-observer reliability of conventional frontal cephalogram and the 3D cephalometry. The correlation coefficient of the intra-observer reliability ranged from 0.23-0.99 (average = 0.71) for the conventional frontal radiograph and from 0.42-0.93 (average = 0.79) for the 3D models (53).

In 2011, Yanez *et al*. published a study on asymmetry index, using patients CT data. The results revealed the intra-observer error to be 0.78, 1.05 and 1.07 mm for x, y, and z coordinates. The errors of the linear and angular measurement were 1.36 and 0.91°, respectively (57).

Damstra *et al*. 2011c, presented a study on the morphometric method to determine the midsagittal plane on 14 dry human skulls. No statistically significant difference was found between the measurements (p=0.25-0.97). The agreement was high (r=0.85-1.00) and the method error was small (mean=0.39 mm; 95% CI=0.31-0.47 mm) (30).

Table 2.5 Landmark Identification: accuracy/reproducibility/precision

Authors	Type of study	Sample size	Reference method	M&M	Observers	Statistical method	Results according to authors	Level of evidence
Richtsmeier *et al.* 1995	*In vitro*	10 dry skulls	Polhemus 3Space table-top digitizer	- CT - Image software version 1.47 - 35 craniofacial landmarks	1 observer	Precision, repeatability, ANOVA, accuracy	Precision: average difference < 0.5 mm Precision between 2 images: low average error Repeatability: along X axis = 98.5% along Y axis > 99.5% Accuracy of linear measurement: average difference = 1-2 mm	Low
Lagravère *et al.* 2009	*In vivo*	24 patients after maxillary expansion	None	- CBCT: - AMIRA© software - 24 craniometric anatomic landmarks	5 observers (Principal x5 Others x1)	Intra- and inter-observer reliability: ICC, average mean differences, ANOVA	Intra-observer: ICC > 0.80 Inter-observer: ICC > 0.80 Mean measurement differences: Intra-observer < 1.5 mm, Inter- > intra- observer	Low
Ludlow *et al.* 2009	*In vitro*	20 presurgical orthodontic patients	None	- CBCT - Lat ceph - Dolphin 3D© software version 10.5 - 24 ceph landmarks	5 observers x 1	Precision, ODM, DEO, ANOVA, paired *t* test	ANOVA: every effect and the 1° interactions between effects: sig diff (p <0.05) DEO > ODM Overall correlation = 0.98 DEO and ODM of radiographic modality and landmark: sig diff (p<0.0001)	Low
De Oliveira *et al.* 2009	*In vivo*	12 orthognathic surgery patients	None	- CBCT - Dolphin 3D© software - 30 landmarks	3 observers x 3	ANOVA, ICC	Intra-observer: ICC ≥ 0.9 (85.55%) Inter-observer: ICC ≥ 0.9 (65.55%)	Low
Chien *et al.* 2009	*In vivo*	10 patients	None	- CBCT - Digital lat ceph - Dolphin© Imaging 10.0 software - Dolphin 3D - 27 landmarks	6 observers x 2	Linear model, the best estimate of true values, absolute value of difference, standard error, ICC	Inter-observer difference of 2D > 3D (p <0.05) Inter-observer: 3D ICC: 0.64-1.00 2D ICC: 0.35-1.00 Intra-observer: 3D ICC: 0.70-1.00 2D ICC: 0.57-1.00	Low
Lagravère *et al.* 2010	*In vivo*	10 adolescent patients	None	- CBCT - Digital lat ceph - AMIRA© software - 18 landmarks	3 observers Principal x 3 Others x 1	Intra- and inter-observer reliability (ICC)	Inter-observer: ICC > 0.90 Intra-observer: ICC > 0.90 Mean landmark difference: Lat ceph ~ 1 mm CBCT > 1 mm	Low

Table 2.5 continued

Authors	Type of study	Sample size	Reference method	M&M	Observers	Statistical method	Results according to authors	Level of evidence
Olszewski *et al.* 2010	*In vivo*	13 patients	None actual reference. Stated the possibility of calculated reference standard based on the index test	- Spiral CT - ACRO 3D© software - 44 reference landmarks (22 from 3D-ACRO and 22 from 3D-Swennen)	2 observers x 2	Intra- and inter-observer mean distance (reconstructed mean log)	Intra-observer: 3D-ACRO = 1.21±1.04 mm 3D-Swennen = 1.31±1.04 mm (comparison: p=0.17 NS) Inter-observer: 3D-ACRO = 1.80±1.04 mm 3D-Swennen = 2.46±1.04 mm (comparison: p=0.000000002) Intra- and inter-observer difference: 3D-ACRO =1.49±1.06 mm 3D-Swennen = 1.88±1.06 mm Reproducibility: 3D-ACRO > 3D-Swennen (p=0.0027)	Low
Titiz *et al.* 2011	*In vivo*	20 patients	None	- CT - VoXim© 6.1 software - 28 landmarks	4 observers x 2	Descriptive statistics, ANOVA	Intra-observer: 0.52 mm Inter-observer: 0.22 mm	Low
Shibata *et al.* 2012	*In vivo*	10 patients	None	- CBCT - Digital lat ceph - VG Studio MAX 1.1 software - Anatomical coordinate system 1, 2, 3, 4	6 observers x 2 Principal x 3 and averaged the coordinates (x, y, z) as the initial coordinates.	95% confidence ellips, reproducibility of the coordinate systems (ellipsoid volume)	The volumes of ellipsoids in systems 2,4 < 1, 3: sig diff Reproducibility: > in system 2,4 Less ellipsoid volume: landmarks at greater distances from each other	Low
Schlicher *et al.* 2012	*In vitro*	19 patients	None	- CBCT - Dolphin imaging© 10.1 software - 32 landmarks	9 observers	Average coordinates of all observers for each landmark*, Consistency**, precision***	Average consistency = 1.64 mm Average precision = 0.87 mm NS between observers The most consistent: Sella turcica (0.50 mm) The most precise: Sella turcica (0.23 mm) The most inconsistent: porion-right (2.72 mm) The most imprecise: orbitale-right (1.81 mm)	Low

Table 2.5 continued

Authors	Type of study	Sample size	Reference method	M&M	Observers	Statistical method	Results according to authors	Level of evidence
Zamora *et al.* 2012	*In vivo*	15 patients	None	- CBCT - Dolphin© imaging 10.1 software - 41 landmarks	2 observers x 3	Reproducibility: ANOVA, multiple comparison, ICC, Pearson correlation coefficient	Intra-observer: ICC ≥ 0.99 Inter-observer: ICC ≥ 0.99 (best frequency on axis Z) The average SD of all landmarks = 1.0 mm, average relative error 1.3%.	Low
Hassan *et al.* 2012	*In vivo*	10 patients	None	- CBCT - Dolphin 3D© software - 22 ceph landmarks (Swennen)	11 observers x 2 3D x 2 3D+MPR	Mixed model design, Fisher's *F*-test, Cronbach's α for inter-observer reliability, precision†	Precision: 3D+MPR > 3D ($p = 0.0001$): sig diff more precise in 6 of 22 landmarks Intra-observer: 3D+MPR > 3D Inter-observer: 3D+MPR > 3D Precision: ranged between 0.29±0.17 and 2.82±7.53	Low
Olszewski *et al.* 2008	*In vitro*	15 dry skulls	Calculated reference standard based on the index test	- Spiral CT - Low-dose CT protocol - ACRO 3D© software - 12 ceph landmarks	2 observers x 2	Non-parametric test, accuracy, reliability	Intra-observer mean distances: high-dose < low-dose ($p = 0.37$) Inter-observer mean distances: high-dose < low-dose ($p = 0.03$)	Moderate
Olszewski *et al.* 2012	*In vitro*	10 dry skulls	Calculated reference standard based on the index test	- CBCT - Maxilim© software - 24 osseous landmarks	2 observers x 2	Reproducibility	Intra-observer mean distance: CBCT < low-dose CT (p=0.000075) Inter-observer mean distance: CBCT < low-dose CT (p=0.00087)	Moderate

* Average coordinates of all observers for each landmark = the centroid for the particular landmark
** Consistency = the mean of the measurements of how far the landmarks were from the centroid by all observers
*** Precision = SD of the distances from the centroid
† Precision = the absolute difference between an observer's repeated measurements and the mean of all measurements per landmark

Table 2.6 Measurement: accuracy/reliability

Authors	Type of study	Sample size	Reference method	M&M	Observers	Statistical method	Results according to authors	Level of evidence
Waitzman *et al.* 1992	*In vivo*	100 patients	None	- CT - 15 measurements	2 observer x 2	Pearson product-moment correlation coefficient (r)	Intra-observer: r ≥ 0.93 Inter-observer: 85% r > 0.85 15% r ≥ 0.74	Low
Periago *et al.* 2008	*In vitro*	23 dry skulls	Electronic digital caliper (3 times by 2 observers)	- CBCT - Dolphin 3D© software - 14 craniometric anatomic landmarks - 20 orthodontic linear measurements	2 observer x 3	Accuracy, intra-observer reliability, ICC, paired *t*-test	Intra-observer: ICC skull measurements =0.99±0.08 ICC CBCT = 0.98±0.02 Skull measurement > CBCT (p<0.001) Mean % measurement error: CBCT = 2.31%±2.11% Skull measurement = 0.63%± 0.51% CBCT > Skull measurement (p <0.001) Mean % difference: skull vs 3D-based measurements = 1.13% (SD ± 1.47%)	Low
Brown *et al.* 2009	*In vitro*	19 dry skulls	Electronic digital caliper (3 times by 2 observers)	- CBCT - Dolphin 3D© software - 24 craniometric anatomic landmarks - 16 linear measurements	1 observer x 3	Intra-observer reliability: absolute mean error (± SD), Wilks lambda multivariate test (P ≤.05), Sidak adjustment for multiple comparisons	Mean absolute error: Between scan settings: NS Average skull absolute error: marked reference points < unmarked reference Mean difference in CBCT: 9 ↓ measurements: 3.1±0.12 mm - 0.56±0.07 mm 1 ↑ measurement: 3.3±0.12 mm CBCT sequences: NS	Low
Nalcaci *et al.* 2010	*In vivo*	10 patients	None	- Spiral CT - Mimics© 9.0 software - Lat ceph - 18 ceph landmarks - Angular measurements	2 observers x 2	Intra-observer reproducibility: Dahlberg's formula, Wilcoxon matched-pairs signed rank test (α=0.05)	Inter-observer: method error 0.35°-0.65°, NS 2D vs 3D: sig diff in some measurements (P < 0.05)	Low
Van Vlijmen *et al.* 2010	*In vitro*	40 dry skulls	None	- CBCT - Lat ceph - Maxilim© software - 17 hard tissue landmarks - 10 angular and 2 linear ceph measurements	1 observer x 5	Pearson correlation coefficient, paired *t*-test	Intra-observer: 0.69-0.98 Standard error: Lat ceph < 3D model (9 of 12measurements) Reproducibility: Lat ceph > 3D models Average difference: –3.12 to 0.83.	Low

Table 2.6 continued

Authors	Type of study	Sample size	Reference method	M&M	Observers	Statistical method	Results according to authors	Level of evidence
Van Vlijmen *et al.* 2011	*In vitro*	40 dry skulls	None	- 2 CBCTs - Maxilim© software - 14 ceph variables (12 angles and 2 linear ratios)	1 observer x 5	Pearson correlation coefficient, measurement error, non-parametric statistics	Intra-observer: i-CAT = 0.42-0.98 Iluma 0.43 - 0.99 Reproducibility: Iluma > i-Cat, sig diff (8 measurements)	Low
Damstra *et al.* 2011a	*In vivo*	25 patients	None	- CBCT - SimPlant Ortho© software - 13 unilateral landmarks - 5 bilateral landmarks - 3 planes	2 observers x 2	The standard error, ANOVA, SDD for intra-observer and inter-observer measurement errors, intra- and inter-observer reliability: ICC, Shapiro-Wilks tests, nonparametric tests, Wilcoxon signed rank tests	Intra-observer: ICC 0.86-0.99. Inter-observer: ICC > 0.88 except for palatal plane-mandibular plane (ICC, 0.76) SDD between observers: similar Measurement error: Angular = 0.88-6.29 mm Linear = 1.33-3.56 mm	Low
Olmez *et al.* 2011	*In vitro*	13 dry skulls	6-inch digital caliper	- Multi-slice CT - Mimics© 9.0 software - Lateral and frontal cephalograms with metal markers - 18 ceph landmarks - 29 measurements (17 lateral and 12 frontal) - 3 groups	1 observer x 1	one-way ANOVA, Tukey Honestly Significant Difference tests, paired *t*-test, Dahlberg's formula	Computer-assisted 3D vs physical: NS Conventional 2D vs physical: sig diff The greatest magnification = Nasion-Menton distance on 2D (14.6%), ($p<0.01$) The greatest enlargement = distance between the zygomaticomaxillary sutures on 2D (16.2%), ($p<0.01$)	Low
Damstra *et al.* 2011b	*In vitro*	10 dry skulls		- CBCT - Lat ceph - SimPlant Ortho© Pro 2.0 software - Viewbox© version 3.1.1.13 software - Spherical metal markers	1 observer x 2 (on the 2nd radiographs)	Dahlberg's formula for ME, ICC, mean values, Wilcoxon signed rank tests	Intra-observer: ICC 2D > 0.97 ICC 3D > 0.88 2D vs 3D: NS (p = 0.41–1.00). Mean ME < 0.61	Low

Table 2.6 continued

Authors	Type of study	Sample size	Reference method	M&M	Observers	Statistical method	Results according to authors	Level of evidence
Gribel *et al.* 2011a	*In vitro*	25 dry skulls	Digital caliper	- CBCT - Lat ceph - SimPlant Ortho© Pro 2.0 software - Ten fiducial markers - 12 ceph landmarks - 10 linear measurements	1 observer x 2	ME: ICC, ANOVA	ME: CBCT ICC = 0.99 Direct measurement ICC = 0.98 lat ceph ICC = 0.98 CBCT vs direct measurements: NS (ANOVA, p>0.05). Direct vs ceph: sig diff (Tukey test, p<0.05).	Low
Gribel *et al.* 2011b	*In vivo*	13 patients	None	- CBCT - Lat ceph - Mimics© version 8.13 software - 6 points - 2 angular and 4 linear measurements - 4 groups: 1) ceph measurement 2) magnification correction 3) algorithm correction 4) CBCT measurement	2 observers x 2	Dahlberg's formula, mean values, R-ANOVA, post-hoc comparison with Bonferroni corection	Intra-observer: ceph 0.5 mm CBCT 0.2 mm Group 1 vs group 4: sig diff (for 3 measurements) (p<0.05) Group 2: ↑differences Group 3 vs group 4: NS	Low
Lopes *et al.* 2008	*In vitro*	28 dry skulls	Beyond Crysta-C9168 series 900 device for 3D coordinates	- Multi-slice CT - Craniometric anatomical points 6 angular measurements	2 observers x 2	Precision, accuracy	Inter-observer: NS Intra-observer: NS Difference physical vs 3D: -3.16% to -0.10%	Moderate
Cavalcanti *et al.* 2004	*In vitro*	13 cadaver heads	Electromagnetic 3 Space™ digitizer	- Spiral CT - Vitrea© version 2.3 software - Anthropometric anatomical points	2 observers x 2	Mean absolute error percentage, SD, CI, intra- and inter-observer reliability, ANOVA	Intra- vs inter-observer: NS Imaging vs physical: NS Standard error 0.45-1.44% % Error: physical vs 3D Bone = 0.83% Soft tissue = 1.78%	Moderate

↑, higher; ↓, lower

Table 2.7 Facial asymmetry

Authors	Type of study	Sample size	Reference method	M&M	Observers	Statistical method	Results according to authors	Level of evidence
Van Vlijmen *et al.* 2009	*In vitro*	40 dry skulls	None	- Ceph frontal radiographs - CBCT - Viewbox©software - Maxilim© software - 10 conventional hard-tissue ceph landmarks - 12 ceph variables	1 observer x 2	Paired *t*-test, intra-observer reliability (Pearson correlation coefficient)	Intra-observer: Frontal radiograph ICC = 0.71 3D model ICC = 0.79 Conventional frontal vs CBCT: sig diff for 11 of 12 measurements	Low
Yanez *et al.* 2011	*In vivo*	21 subjects - Control group (n=10) - Asymmetrical group (n=11)	None	- Multi-slice helical CT - VirSSPA© software - Asymmetry index	1 observer x 2	Mean, SD, 95% CI, Intra-observer error: *t*- test, difference between 2 groups: *t*-test for independent samples, Shapiro-Wilk test for normality (p<0.05), Pearson correlation coefficient	Intra-observer error: X = 0.78, Y = 1.05, Z = 1.07 mm linear measurement =1.36 mm angular measurement = 0.91° Intra-observer: NS Control group: The greatest asymmetry index: gonion The most stable: Anterior nasal spine	Low
Damstra *et al.* 2011c	*In vitro*	14 dry skulls - Visible asymmetry group (n=5) - No visible asymmetry group (n=9)	None	- CBCT - SimPlant®Ortho Pro 2.1 software - Hard tissue landmarks - Morphometric method to determine the midsagittal plane	1 observer x 2	Wilcoxon signed-rank sum test, Pearson correlation coefficient, standard error of measurement (SEM), ANOVA, smallest detectable difference	NS in intra-observer measurements (p=0.25-0.97) The agreement was high (r=0.85-1.00). Small method error: mean=0.39 mm; 95% CI=0.31-0.47 mm.	Low

Other topics

Five publications that could not be categorized into any topics above are reported in Table 2.8. Two publications: Olszewski *et al*. (2007) (45) and Lagravère *et al*. (2011) (37) reached the moderate level of evidence. Other studies did not meet the criteria because the reference standard was missing and were therefore considered as low level of evidence.

Olszewski *et al*. transformed Delaire's 2D cephalometric analysis into a 3D version. The authors validated the system on 26 dry skulls. For the intra-observer reliability, the ICC, found for 2D X-ray was 0.60-0.91 and the ICC for 3D CT was 0.97-1.00. When looking at the inter-observer reliability, the ICC varied from 0.13 to 0.84 and from 0.94 to 1.00, respectively. In the 3D CT, the user accuracy (absolute difference) was between 0.75 mm (±0.05) and 0.99 mm (±0.08). There were no statistically significant differences found between the physical measurements and the measurements in ACRO 3D® software (45).

Later on, Lagravère *et al*. (2011) published an article on the reliability and accuracy in locating several foramina in the cranial base by CBCT images. The ICC values were found to be > 0.93 and 0.92 for intra- and inter-observer reliability, respectively. From this study, the authors concluded that the foramen spinosum, ovale, and rotundum, as well as hypoglossal canal could be considered as acceptable landmarks to be used in establishing reference coordinate systems for future 3D superimposition analysis (37).

In 2006, Swennen and colleagues presented a new 3D cephalometric reference system and tested the accuracy and reliability of this analysis. The intra-observer measurement error was less than 0.88 mm, 0.76 mm and 0.84 mm for horizontal, vertical and transversal orthogonal measurements, respectively. The inter-observer measurement error was less than 0.78 mm, 0.86 mm and 1.26 mm for horizontal, vertical and transversal orthogonal measurements, respectively (17).

Park *et al*. proposed a new type of cephalometric analysis by using 3D CT in 2006 (46). The authors reported that there was no statistically significant difference when the data were compared with the Korean norm values. All landmarks were reproducible and no significant intra-observer error (p>0.01) was found (46).

Tulunoglu *et al*. 2011 (52) compared the consistency of orthodontic measurements performed on lateral and frontal cephalograms and 3D CT images of cleft lip and palate (CLP) patients. The ICC values were very high for both 2D (0.94-0.99) and 3D measurements (0.88-0.99). Significant differences were found between the measurements from 2D and from 3D methods (52).

2.5 Discussion

Summary of Evidence

No publication reported diagnostic thinking efficacy or therapeutic efficacy.

Meta-analysis was not possible because there was a lack of primary studies and the heterogeneity of the studies. This review was therefore limited to a qualitative descriptive analysis. Based on the QUADAS tools, 6 publications have reached the moderate level of evidence, therefore it is considered that there is limited research-based evidence on 3D cephalometry.

The most common reason for exclusion of publications was inadequate sample size (samples less than 10) (Fig 2.1). As the sample size is important for meaningful statistics, we determined minimum sample size equal to 10 as an inclusion criterium.

The reported research findings were most frequently on landmark identification and measurement accuracy. The results of the observer performance were reported in almost all studies. The reliability and reproducibility of the methods and the observers were highly interesting as these are the main factors influencing the cephalometric analysis. It was shown that the 3D landmark identification and measurements were as reliable or more reliable than traditional 2D cephalometric measurements (29,34,35,39) but there was not always full agreement (39,54). This may depend on the method and analysis, selected in the studies. Even different machine selection may play a role in the difference between the measurements found (55). Different landmarks have shown differences in their reliability, reproducibility and precision in the 3D space (49,50,58).

Table 2.8 Other topics

Authors	Study topic	Type of study	Sample size	Reference method	M&M	Observers	Statistical method	Results according to authors	Level of evidence
Park *et al.* 2006	To proposes a ceph analysis, using 3D CT	*In vivo*	30 patients	None	- CT - Vworks© 4.0, Vsurgery software - 19 ceph landmarks	1 observer x 5 2 sessions	Reproducibility, Korean normal averages (*t*-test, *P* < 0.01), Wilcoxon 2-sample test	Comparison with the Korean Norm: NS Intra-observer: NS, p >0.01.	Low
Swennen *et al.* 2006	To present a new 3D ceph method	*In vivo*	20 OMF patients	None	- Multi-slice CT - Maxilim© version 1.3.0 software - 14 skeletal landmarks - 42 orthogonal measurements	2 observers x 2	Method error*, Inter-observer error**, reliability (squared correlation coefficients: r^2)	Intra-observer error: Horizontal < 0.88 mm Vertical = 0.76 mm Transversal = 0.84 mm Inter-observer error: Horizontal < 0.78 mm Vertical = 0.86 mm Transversal =1.26 mm Intra-observer reliability: r^2> 50% Inter-observer reliability: r^2> 50%	Low
Tulunoglu *et al.* 2011	Cleft lip and palate (CLP) 2D vs 3D	*In vivo*	15 patients with CLP	None	- CT - Lat & frontal ceph - Mimics© version 10.02 software - McNamara, Steiner, Frontal analyses	1 observer x 2	Reliability: ICC, Mann Whitney U tests to identify differences between 2D and 3D groups	Inter-observer: ICC 2D = 0.94-0.99 3D = 0.88-0.99 Frontal: 2D>3D sig diff McNamara: sig diff Steiner: sig diff	Low
Olszewski *et al.* 2007	3D ceph craniofacial analysis	*In vitro*	26 dry skulls	3D instrument to assess 3D position (x, y, z)	- Lat ceph - Spiral CT - ACRO 3D© software - Delaire's ceph analysis	2 observers x 2	Reproducibility, accuracy	Intra-observer: ICC 2D = 0.60-0.90 ICC 3D CT = 0.97-1.00 Inter-observer: ICC 2D = 0.13-0.84 ICC 3D CT = 0.94-1.00 User accuracy of 3D (absolute diff): 0.75mm (±0.05) to 0.99mm (±0.08)	Moderate
Lagravère *et al.* 2011	Cranial base foramen	*In vitro*	10 dry skulls	Gutta percha placed at landmarks	- CBCT - AMIRA© software - 4 references foramen landmark	3 observers (Principal x3 Others x1)	Accuracy, intra- and inter-observer reliability: ICC	Intra-observer ICC > 0.93 Inter-observer ICC > 0.92 Accuracy: large average mean difference (max. 3.60 mm for foramen rotundum)	Moderate

*Method error = SD of the differences between duplicate measurements of each observer (x_1-x_2, y_1-y_2) (intra-observer error)
**Inter-observer error = SD of the mean of differences between the averages of the paired duplicate data ($x = x_1 + x_2)/2$; $y = y_1 + y_2)$ /2) measured by each investigator

Several researchers have reported studies on facial asymmetry and a few studies were included in this review (30,53,57). 3D imaging offers a better representation of the real morphology of the skulls unlike in the lateral cephalogram, where left and right structures are superimposed on each other. Frontal cephalograms or postero-anterior views have been used for decades to evaluate symmetry of facial structures but 3D cephalometry has recently been reported to prove its validity although the evidence is still very limited.

Research-based evidence on 3D cephalometry was found to be limited. More evidence was found for measurement accuracy and reproducibility of landmark identification but still there is not enough evidence about 3D cephalometry in other aspects.

Limitations

Cephalometry is a widely used method in orthodontics and orthognathic surgery. A variety of research topics were identified such as landmark identification, linear and angular measurements, facial asymmetry, cleft lip and cleft palate, introductions of new analyses and the transformation from the traditional 2D analysis to the new 3D analysis. This made it difficult to perform a systematic review as topics, statistical tests and methods were too diverse. Therefore a meta-analysis could not be performed.

In general, cephalometric analysis is used to analyse the craniofacial structures of the patient and its results have an impact on treatment planning. Cephalometry is not a direct method to diagnose the conditions of the patients, yet it offers the details of the patients' craniofacial structures, and thus reveals diagnostic information helpful in determining orthodontic treatment planning. To perform this systematic review, the authors based the procedure of the systematic review on diagnostic accuracy as it shows the most similarity.

A cephalometric analysis is basically performed on radiographs, either 2D or 3D. Osseous landmarks both on the skull surface and inside the skull are identified on the images. As a result, it is impossible to check the real landmark positions in patients. The reference standard can only be used in an *in vitro* study, which is not an ideal study type to report the diagnostic efficacy evidence. A cadaver study could overcome this problem, but the sample size will be limited. Studies on patients can only show the observer performance and reliability of the methods as direct physical skeletal measurements are not possible. Although in some publications the reference standards were calculated based on the measurements on the images, it is not preferable according to the QUADAS tool (25).

Another limitation in *in vivo* studies is the ethical issue on radiation safety for orthodontic patients. Although CBCTs offer 3D images with less radiation dose than the multi-slice CT, it is still too high to perform a controlled trial comparing 2D versus 3D cephalometry.

Within the limitations, mentioned above, the authors have tried to adapt the inclusion criteria and protocol of the present systematic review to cover all the evidence provided by current publications. The protocol, used in this study, is not as restricted as the standard one as described by Fryback and Thornbury (20). When a study did not use a reference standard, it was not excluded immediately but could still meet the low-level of evidence if the study reached other criteria.

Non-English articles were searched during the literature search and study selection, but they were not further considered in the present systematic review. From 571 publications that were retrieved, 48 non-English publications were found (9 Chinese, 2 Dutch, 15 French, 12 German, 1 Hungarian, 3 Italian, 5 Japanese, 1 Polish). Titles and abstracts of these publications were checked for the inclusion criteria. It was found that all articles did not pass these criteria with reasons: not related to 3D cephalometry [33], review literature [5], no quantitative analysis [4], method not clearly described [2], abstract not available [4]. Therefore, it is very unlikely to identify other relevant non-English publications than included in this review.

3D cephalometry and the future

There are several concerns using 3D cephalometric analysis and these concerns can also affect how future studies should be conducted. First concern is related to the selection criteria and thus to outlining when to perform 3D cephalometry. Discussion is going on regarding case selection and the necessity of 3D cephalometry because radiation exposure plays a role in this decision making process. With the current evidence, it cannot be concluded that 3D cephalometry should be performed on all orthodontic patients. Guidelines and recommendations on CBCT for dental and maxillofacial radiology by the European Commission are available and should be followed (59). Recently, new guidelines were proposed by the by the American Academy of Oral and Maxillofacial Radiology (AAOMR) to provide clinicians and more specifically orthodontic specialists some guidance and recommendations in using cone-beam CT (60).

The radiation dose is a very important issue as most orthodontic patients are children and adolescents who are more sensitive to radiation exposure (61,62). The radiation dose, received from the CBCTs, is strongly related to FOV size and also dependent on the specific CBCT machine (61). This also acts as a difficulty in conducting research on 3D cephalometry. To obtain a large FOV CT or CBCT scan is difficult because of the ethical concern. Most studies with suitable gold standard were performed *in vitro* which is not fully accepted as evidence as already mentioned above in the *limitations.* In the *in vitro* studies, more effort should be done to simulate real human conditions such as the use of water as soft tissue attenuation, which was done only in a few studies, or to develop a material that mimics soft tissue shape and density to make analysis on the soft tissues possible.

At this point, 3D cephalometric analyses were mostly based on their former 2D versions. Further tests should be done to evaluate the reliability and accuracy of these 2D transferred to 3D methods and to investigate whether the norm values from 2D cephalometry can still be used in these new 3D analyses.

Three-dimensional cephalometry is fairly new as a research topic. More studies are highly required to provide more evidence on the accuracy and the efficacy of this potentially innovative method. As for the future, researchers should concentrate more on the materials and methods of their 3D cephalometric studies, standardizing protocols, using larger sample sizes and employing more optimal statistical methods for dataset evaluation. Studies on diagnostic thinking efficacy (testing whether 3D cephalometry is helpful for diagnosis) and therapeutic efficacy (testing whether 3D cephalometry is helpful for treatment planning and the management of the patients) (20) should also be accomplished to offer more concrete evidence on the benefits of 3D cephalometry for orthodontic treatment planning and patients.

2.6 Conclusions

This systematic review reveals that there is still limited research-based evidence on 3D cephalometry. Specific research methodology needs to be developed to be able to perform more standardized diagnostic accuracy studies by using patients' data.

2.7 References

1. Hofrath H. Bedeutung der Röntgenfern und Abstands Aufnahme für die Diagnostik der Kieferanomalien. *Fortschr Orthod*. 1931;1:231-58.
2. Broadbent BH. A new x-ray technique and its application to orthodontia. *Angle Orthod*. 1931;1:45-66.
3. Baumrind S, Frantz RC. The reliability of head film measurements. 2. Conventional angular and linear measures. *Am J Orthod*. 1971;60:505-17.
4. Baumrind S, Frantz RC. The reliability of head film measurements. 1. Landmark identification. *Am J Orthod*. 1971;60:111-27.
5. Bjork A, Solow B. Measurement on radiographs. *J Dent Res*. 1962;41:672-83.
6. Connor SE, Arscott T, Berry J, Greene L, O'Gorman R. Precision and accuracy of low-dose CT protocols in the evaluation of skull landmarks. *Dentomaxillofac Radiol*. 2007;36:270-6.
7. Olszewski R, Reychler H, Cosnard G, Denis JM, Vynckier S, Zech F. Accuracy of three-dimensional (3D) craniofacial cephalometric landmarks on a low-dose 3D computed tomograph. *Dentomaxillofac Radiol*. 2008;37:261-7.
8. Olszewski R, Frison L, Wisniewski M, Denis JM, Vynckier S, Cosnard G, *et al.* Reproducibility of three-dimensional cephalometric landmarks in cone-beam and low-dose computed tomography. *Clin Oral Investig*. 2013;17:285-92.

9. Kumar V, Ludlow JB, Mol A, Cevidanes L. Comparison of conventional and cone beam CT synthesized cephalograms. *Dentomaxillofac Radiol*. 2007;36:263-9.
10. Moshiri M, Scarfe WC, Hilgers ML, Scheetz JP, Silveira AM, Farman AG. Accuracy of linear measurements from imaging plate and lateral cephalometric images derived from cone-beam computed tomography. *Am J Orthod Dentofacial Orthop*. 2007;132:550-60.
11. Cattaneo PM, Bloch CB, Calmar D, Hjortshoj M, Melsen B. Comparison between conventional and cone-beam computed tomography-generated cephalograms. *Am J Orthod Dentofacial Orthop*. 2008;134:798-802.
12. van Vlijmen OJ, Berge SJ, Swennen GR, Bronkhorst EM, Katsaros C, Kuijpers-Jagtman AM. Comparison of cephalometric radiographs obtained from cone-beam computed tomography scans and conventional radiographs. *J Oral Maxillofac Surg*. 2009;67:92-7.
13. Kumar V, Ludlow J, Soares Cevidanes LH, Mol A. In vivo comparison of conventional and cone beam CT synthesized cephalograms. *Angle Orthod*. 2008;78: 873-9.
14. Grayson B, Cutting C, Bookstein FL, Kim H, McCarthy JG. The three-dimensional cephalogram: theory, technique, and clinical application. *Am J Orthod Dentofacial Orthop*. 1988;94:327-37.
15. Adams GL, Gansky SA, Miller AJ, Harrell WE, Jr., Hatcher DC. Comparison between traditional 2-dimensional cephalometry and a 3-dimensional approach on human dry skulls. *Am J Orthod Dentofacial Orthop*. 2004;126:397-409.
16. Chenin DL. 3D cephalometrics: the new norm. *Alpha Omegan*. 2010;103:51-6.
17. Swennen GR, Schutyser F, Barth EL, De Groeve P, De Mey A. A new method of 3-D cephalometry Part I: the anatomic Cartesian 3-D reference system. *J Craniofac Surg*. 2006;17:314-25.
18. Farronato G, Farronato D, Toma L, Bellincioni F. A synthetic three-dimensional craniofacial analysis. *J Clin Orthod*. 2010;44:673-8; quiz 88.
19. Kau CH, Richmond S, Palomo JM, Hans MG. Three-dimensional cone beam computerized tomography in orthodontics. *J Orthod*. 2005;32:282-93.

20. Fryback DG, Thornbury JR. The efficacy of diagnostic imaging. *Med Decis Making*. 1991;11:88-94.
21. Deeks JJ, Bossuyt PM, Gatsonis C, editors. Cochrane Handbook for Systematic Reviews of Diagnostic Test Accuracy. Version 1.0: The Cochrane Collaboration; 2010. Available from: http://srdta.cochrane.org/handbook-dta-reviews.
22. Higgins JPT, Green S, editors. Cochrane Handbook for Systematic Reviews of Interventions. Version 5.1.0 [updated March 2011]: The Cochrane Collaboration; 2011. Available from: http://www.cochrane-handbook.org/.
23. Jaeschke R, Guyatt G, Sackett DL. Users' guides to the medical literature. III. How to use an article about a diagnostic test. A. Are the results of the study valid? Evidence-Based Medicine Working Group. *JAMA*. 1994;271:389-91.
24. Jaeschke R, Guyatt GH, Sackett DL. Users' guides to the medical literature. III. How to use an article about a diagnostic test. B. What are the results and will they help me in caring for my patients? The Evidence-Based Medicine Working Group. *JAMA*. 1994;271:703-7.
25. Whiting P, Rutjes AW, Reitsma JB, Bossuyt PM, Kleijnen J. The development of QUADAS: a tool for the quality assessment of studies of diagnostic accuracy included in systematic reviews. *BMC Med Res Methodol*. 2003;3:25.
26. Liberati A, Altman DG, Tetzlaff J, Mulrow C, Gotzsche PC, Ioannidis JP*, et al.* The PRISMA statement for reporting systematic reviews and meta-analyses of studies that evaluate healthcare interventions: explanation and elaboration. *BMJ*. 2009;339:b2700.
27. Brown AA, Scarfe WC, Scheetz JP, Silveira AM, Farman AG. Linear accuracy of cone beam CT derived 3D images. *Angle Orthod*. 2009;79:150-7.
28. Cavalcanti MG, Rocha SS, Vannier MW. Craniofacial measurements based on 3D-CT volume rendering: implications for clinical applications. *Dentomaxillofac Radiol*. 2004;33:170-6.
29. Chien PC, Parks ET, Eraso F, Hartsfield JK, Roberts WE, Ofner S. Comparison of reliability in anatomical landmark identification using two-

dimensional digital cephalometrics and three-dimensional cone beam computed tomography in vivo. *Dentomaxillofac Radiol*. 2009;38:262-73.

30. Damstra J, Fourie Z, De Wit M, Ren Y. A three-dimensional comparison of a morphometric and conventional cephalometric midsagittal planes for craniofacial asymmetry. *Clin Oral Investig*. 2012;16:285-94.
31. Damstra J, Fourie Z, Huddleston Slater JJ, Ren Y. Reliability and the smallest detectable difference of measurements on 3-dimensional cone-beam computed tomography images. *Am J Orthod Dentofacial Orthop*. 2011;140:e107-14.
32. Damstra J, Fourie Z, Ren Y. Comparison between two-dimensional and midsagittal three-dimensional cephalometric measurements of dry human skulls. *Br J Oral Maxillofac Surg*. 2011;49:392-5.
33. de Oliveira AE, Cevidanes LH, Phillips C, Motta A, Burke B, Tyndall D. Observer reliability of three-dimensional cephalometric landmark identification on cone-beam computerized tomography. *Oral Surg Oral Med Oral Pathol Oral Radiol Endod*. 2009;107:256-65.
34. Gribel BF, Gribel MN, Frazao DC, McNamara JA, Jr., Manzi FR. Accuracy and reliability of craniometric measurements on lateral cephalometry and 3D measurements on CBCT scans. *Angle Orthod*. 2011;81:26-35.
35. Gribel BF, Gribel MN, Manzi FR, Brooks SL, McNamara JA, Jr. From 2D to 3D: an algorithm to derive normal values for 3-dimensional computerized assessment. *Angle Orthod*. 2011;81:3-10.
36. Hassan B, Nijkamp P, Verheij H, Tairie J, Vink C, Stelt PV*, et al.* Precision of identifying cephalometric landmarks with cone beam computed tomography in vivo. *Eur J Orthod*. 2013;35:38-44.
37. Lagravere MO, Gordon JM, Flores-Mir C, Carey J, Heo G, Major PW. Cranial base foramen location accuracy and reliability in cone-beam computerized tomography. *Am J Orthod Dentofacial Orthop*. 2011;139:e203-10.
38. Lagravere MO, Gordon JM, Guedes IH, Flores-Mir C, Carey JP, Heo G*, et al.* Reliability of traditional cephalometric landmarks as seen in three-dimensional analysis in maxillary expansion treatments. *Angle Orthod*. 2009;79:1047-56.

39. Lagravere MO, Low C, Flores-Mir C, Chung R, Carey JP, Heo G, *et al.* Intraexaminer and interexaminer reliabilities of landmark identification on digitized lateral cephalograms and formatted 3-dimensional cone-beam computerized tomography images. *Am J Orthod Dentofacial Orthop*. 2010;137:598-604.
40. Lopes PM, Moreira CR, Perrella A, Antunes JL, Cavalcanti MG. 3-D volume rendering maxillofacial analysis of angular measurements by multislice CT. *Oral Surg Oral Med Oral Pathol Oral Radiol Endod*. 2008;105:224-30.
41. Ludlow JB, Gubler M, Cevidanes L, Mol A. Precision of cephalometric landmark identification: cone-beam computed tomography vs conventional cephalometric views. *Am J Orthod Dentofacial Orthop*. 2009;136:312 e1-10;discussion 12-3.
42. Tyndall DA, Kohltfarber H. Application of cone beam volumetric tomography in endodontics. *Aust Dent J*. 2012;57Suppl 1:72-81.
43. Fullmer JM, Scarfe WC, Kushner GM, Alpert B, Farman AG. Cone beam computed tomographic findings in refractory chronic suppurative osteomyelitis of the mandible. *Br J Oral Maxillofac Surg*. 2007;45:364-71.
44. Olszewski R, Tanesy O, Cosnard G, Zech F, Reychler H. Reproducibility of osseous landmarks used for computed tomography based three-dimensional cephalometric analyses. *J Craniomaxillofac Surg*. 2010;38:214-21.
45. Olszewski R, Zech F, Cosnard G, Nicolas V, Macq B, Reychler H. Three-dimensional computed tomography cephalometric craniofacial analysis: experimental validation in vitro. *Int J Oral Maxillofac Surg*. 2007;36:828-33.
46. Park SH, Yu HS, Kim KD, Lee KJ, Baik HS. A proposal for a new analysis of craniofacial morphology by 3-dimensional computed tomography. *Am J Orthod Dentofacial Orthop*. 2006;129:600 e23-34.
47. Periago DR, Scarfe WC, Moshiri M, Scheetz JP, Silveira AM, Farman AG. Linear accuracy and reliability of cone beam CT derived 3-dimensional images constructed using an orthodontic volumetric rendering program. *Angle Orthod*. 2008;78:387-95.

48. Richtsmeier JT, Paik CH, Elfert PC, Cole TM, 3rd, Dahlman HR. Precision, repeatability, and validation of the localization of cranial landmarks using computed tomography scans. *Cleft Palate Craniofac J*. 1995;32:217-27.
49. Shibata M, Nawa H, Kise Y, Fuyamada M, Yoshida K, Katsumata A*, et al.* Reproducibility of three-dimensional coordinate systems based on craniofacial landmarks. *Angle Orthod*. 2012;82:776-84.
50. Schlicher W, Nielsen I, Huang JC, Maki K, Hatcher DC, Miller AJ. Consistency and precision of landmark identification in three-dimensional cone beam computed tomography scans. *Eur J Orthod*. 2012;34:263-75.
51. Titiz I, Laubinger M, Keller T, Hertrich K, Hirschfelder U. Repeatability and reproducibility of landmarks--a three-dimensional computed tomography study. *Eur J Orthod*. 2012;34:276-86.
52. Tulunoglu O, Esenlik E, Gulsen A, Tulunoglu I. A comparison of three-dimensional and two-dimensional cephalometric evaluations of children with cleft lip and palate. *Eur J Dent*. 2011;5:451-8.
53. van Vlijmen OJ, Maal TJ, Berge SJ, Bronkhorst EM, Katsaros C, Kuijpers-Jagtman AM. A comparison between two-dimensional and three-dimensional cephalometry on frontal radiographs and on cone beam computed tomography scans of human skulls. *Eur J Oral Sci*. 2009;117:300-5.
54. van Vlijmen OJ, Maal T, Berge SJ, Bronkhorst EM, Katsaros C, Kuijpers-Jagtman AM. A comparison between 2D and 3D cephalometry on CBCT scans of human skulls. *Int J Oral Maxillofac Surg*. 2010;39:156-60.
55. van Vlijmen OJ, Rangel FA, Berge SJ, Bronkhorst EM, Becking AG, Kuijpers-Jagtman AM. Measurements on 3D models of human skulls derived from two different cone beam CT scanners. *Clin Oral Investig*. 2011;15:721-7.
56. Waitzman AA, Posnick JC, Armstrong DC, Pron GE. Craniofacial skeletal measurements based on computed tomography: Part II. Normal values and growth trends. *Cleft Palate Craniofac J*. 1992;29:118-28.
57. Yanez-Vico RM, Iglesias-Linares A, Torres-Lagares D, Gutierrez-Perez JL, Solano-Reina E. Three-dimensional evaluation of craniofacial asymmetry: an analysis using computed tomography. *Clin Oral Investig*. 2011;15:729-36.

58. Zamora N, Llamas JM, Cibrian R, Gandia JL, Paredes V. A study on the reproducibility of cephalometric landmarks when undertaking a three-dimensional (3D) cephalometric analysis. *Med Oral Patol Oral Cir Bucal*. 2012;17:e678-88.
59. European Commission. Guidelines on CBCT for Dental and Maxillofacial Radiology: Evidence Based Guidelines: Radiation Protection Publication; 2012. Available from: http://www.sedentexct.eu/content/guidelines-cbct-dental-and-maxillofacial-radiology.
60. American Academy of Oral and Maxillofacial Radiology. Clinical recommendations regarding use of cone beam computed tomography in orthodontic treatment. Position statement by the American Academy of Oral and Maxillofacial Radiology. *Oral Surg Oral Med Oral Pathol Oral Radiol*. 2013;116:238-57.
61. Pauwels R, Beinsberger J, Collaert B, Theodorakou C, Rogers J, Walker A, *et al.* Effective dose range for dental cone beam computed tomography scanners. *Eur J Radiol*. 2012;81:267-71.
62. Theodorakou C, Walker A, Horner K, Pauwels R, Bogaerts R, Jacobs R, *et al.* Estimation of paediatric organ and effective doses from dental cone beam CT using anthropomorphic phantoms. *Br J Radiol*. 2012;85:153-60.

PART II

PANORAMIC IMAGING

Chapter 3

An in vitro comparison of subjective image quality of panoramic views acquired via 2D or 3D imaging

This chapter is based on:

Pittayapat P, Galiti D, Huang Y, Dreesen K, Schreurs M, Souza PC, et al. An in vitro comparison of subjective image quality of panoramic views acquired via 2D or 3D imaging. *Clin Oral Investig*. 2013;17:293-300.

3.1 Abstract

Objectives: The objective of this study is to compare subjective image quality and diagnostic validity of cone-beam CT (CBCT) panoramic reformatting with digital panoramic radiographs.

Materials and methods: Four dry human skulls and two formalin-fixed human heads were scanned using nine different CBCTs, one multi-slice CT (MSCT) and one standard digital panoramic device. Panoramic views were generated from CBCTs in four slice thicknesses. Seven observers scored image quality and visibility of 14 anatomical structures. Four observers repeated the observation after 4 weeks.

Results: Digital panoramic radiographs showed significantly better visualization of anatomical structures except for the condyle. Statistical analysis of image quality showed that the 3D imaging modalities (CBCTs and MSCT) were 7.3 times more likely to receive poor scores than the 2D modality. Yet, image quality from NewTom VGi® and 3D Accuitomo 170® was almost equivalent to that of digital panoramic radiographs with respective odds ratio estimates of 1.2 and 1.6 at 95% Wald confidence limits. A substantial overall agreement amongst observers was found. Intra-observer agreement was moderate to substantial.

Conclusions: While 2D-panoramic images are significantly better for subjective diagnosis, 2/3 of the 3D-reformatted panoramic images are moderate or good for diagnostic purposes.

Clinical relevance: Panoramic reformattings from particular CBCTs are comparable to digital panoramic images concerning the overall image quality and visualization of anatomical structures. This clinically implies that a 3D derived panoramic view can be generated for diagnosis with a recommended 20-mm slice thickness, if CBCT data is a priori available for other purposes.

3.2 Introduction

Panoramic radiography has been used in dentistry for more than half a century (1–3). It has been widely used for screening purposes, periodontal evaluation, orthodontic treatment planning, oral surgery and also for implant treatment planning. It is considered as a very important diagnostic tool in dentistry. Even though it has been widely accepted, it still carries several down sides such as geometric distortion and superimposition of structures (4-7).

Three-dimensional images started to play an important role in oral diagnosis. First, computed tomography (CT) was introduced to the dental field in 1990s. However, because of its high radiation dose, it was not broadly used. In 1996, the first dental cone-beam computed tomography (CBCT) was invented and the technology has been developing since.

Nowadays, there are more than 30 CBCTs available on the market and their function has been developed to serve dentists' objectives. In many machines, it is possible to choose different field of views (FOV) and different resolution parameters depending on the clinical indication for producing the images. Software tools accompanying the CBCTs allow clinicians to display the 3D data in clinically suitable views, e.g., cross-sectional slices and panoramic view. Some software programs even allow 3D cephalometric analysis (8, 9). Some clinicians still refer patients for additional conventional digital panoramic radiographs and conventional lateral cephalograms despite the fact that CBCT data has already been acquired. If the panoramic images generated from three-dimensional data have equal diagnostic quality as conventional digital panoramic radiographs, then it is not necessary for clinicians to take extra conventional 2D radiographs. Patients' datasets will be more compact and the radiation dose to patients can be reduced. However, there is only little evidence that can prove if the panoramic images generated from three-dimensional data (CT or CBCT) have equal diagnostic quality as conventional digital panoramic radiographs (10-12).

The aims of this study were to compare the diagnostic validity of the panoramic view derived from different CBCTs and a multi-slice CT (MSCT) with the standard digital panoramic radiograph. The latter is meant to evaluate whether CBCT derived panoramic views could avoid making another panoramic radiograph if a CBCT is a priori available. During this particular study, inter- and intra-observer variability was also assessed.

3.3 Materials and methods

The samples consisted of four dry human skulls and two formalin-fixed human heads obtained from the collection of the Oral Imaging Center, Katholieke Universiteit Leuven. The mandibles were fixed to the skulls at the maximum occlusion by using broad tape attached from the temporal bone, crossing the inferior border of the mandible to the temporal bone of the opposite side.

Image acquisition

To acquire conventional digital panoramic images, the dry skulls were put in a plastic bucket filled with water to simulate the attenuation of soft tissue. Additional cervical spines were placed below the foramen magnum to resemble a real human cervical. The two formalin-fixed heads were put in plastic bags with additional cervical spines attached at the postero-inferior side of the bags.

The samples were put in a standard digital panoramic device (Veraviewepocs 2D®, J. Morita, Kyoto, Japan) with CCD sensor. The Frankfort horizontal plane, midline and the canine indication line were adjusted as in patients. The "standard adult" panoramic setting was selected (64 kVp, 8.9 mA 7.4 s, with pixel size 0.144 mm). All panoramic radiographs were exported as TIFF files.

The samples were also placed in a MSCT (SOMATOM® Sensation 64, Siemens, Erlangen, Germany) at the Department of Imaging and Pathology, University Hospitals Leuven, Gasthuisberg, Leuven, Belgium. The samples were placed horizontally and dry skulls were put in a different polystyrene box to be able to place the skulls horizontally with water as soft tissue simulation. Standard parameters for head and neck area were used (120 kVp, 250 mAs, voxel size 0.43 mm). The datasets were exported as Digital Imaging and Communications in Medicine (DICOM) files.

Images were taken on the samples by nine different CBCT machines as shown in Table 3.1. The large maxillofacial FOV was selected for each machine to ensure that all anatomical structures mandatory for panoramic viewing were covered. All data were exported as DICOM files.

Panoramic image generation

All DICOM data from MSCT and CBCTs were imported in OnDemand3D® software, version 1.0.8.0408 (Cybermed, Seoul, Republic of South Korea). Before generating a panoramic view, the skull position was adjusted for standardization. First, the Frankfort horizontal was checked and adjusted to be parallel with the horizontal plane. The midline of the face was adjusted to be perpendicular to the horizontal plane. From the axial view of alveolar process of the mandible (mid-root area), a curve was drawn manually starting 1 cm posterior from the most posterior border of ramus to cover the condyle in the slice. Four points were marked bilaterally within the path on each side of the jaw and one at the midline (most posterior, molar, premolar, canine and one at midline; Fig. 3.1). The curves were checked to ensure that all anatomical points of interest of both maxilla and mandible covered. After the panoramic curves were confirmed, panoramic images were generated in different slice thicknesses: 10, 15, 20, 25 mm and then saved in TIF format (Fig. 3.2). This process was performed by a 5-year-experienced dentomaxillofacial radiologist.

Table 3.1 Technical parameters of CBCT devices

CBCT	Manufacturer	FOV (cm) (D x H)	Voxel size (mm)	Voltage (kV)	mAs
3D Accuitomo 170	J. Morita, Kyoto, Japan	17 x 12	0.25	90	154
Galileos Comfort	Sirona Dental Systems, Bensheim, Germany	15 x 15	0.29	85	21
i-CAT Next Gen	Imaging Sciences International, Hatfield, PA, USA	23 x 17	0.30	120	35
Iluma Elite	Imtec (3M), Ardmore, OK, USA	21 x 14	0.19	120	152
Kodak 9500	Kodak Dental Systems, Carestream Health, Rochester, NY, USA	20 x 18	0.30	90	108
NewTom VGi	Quantitative Radiology, Verona, Italy	15 x 15	0.30	110	122[b]
Picasso Trio[a]	VATECH, Yongin, Republic of Korea	12 x 7	0.20	85	90
Scanora 3D	Soredex, Tuusula, Finland	14.5 x 13	0.25	90	48
SkyView	MyRay, Celfa Dental Group, Imola, Italy	17 x 17	0.34	90	51.5

[a] Picasso Trio® was the largest FOV from VATECH available in Europe at the time of scanning
[b] Mean exposure of six samples. The device uses automatic exposure based on density distribution of scout image

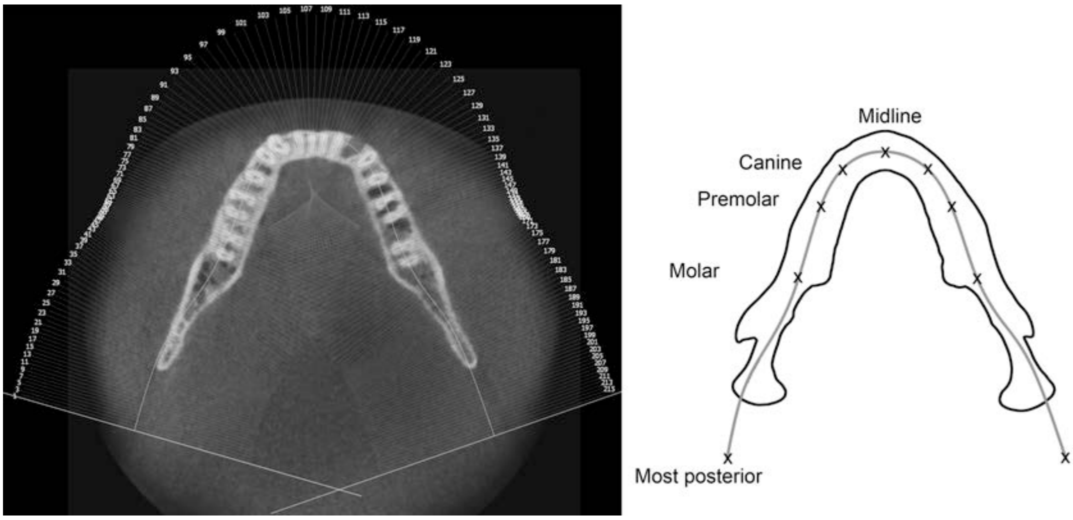

Figure 3.1 Panoramic reformatting arch, drawn on the axial view of each CBCT scan. The sketch figure on the right indicates the marking of the different curve points during the drawing process. A total of nine points were marked for one panoramic curve

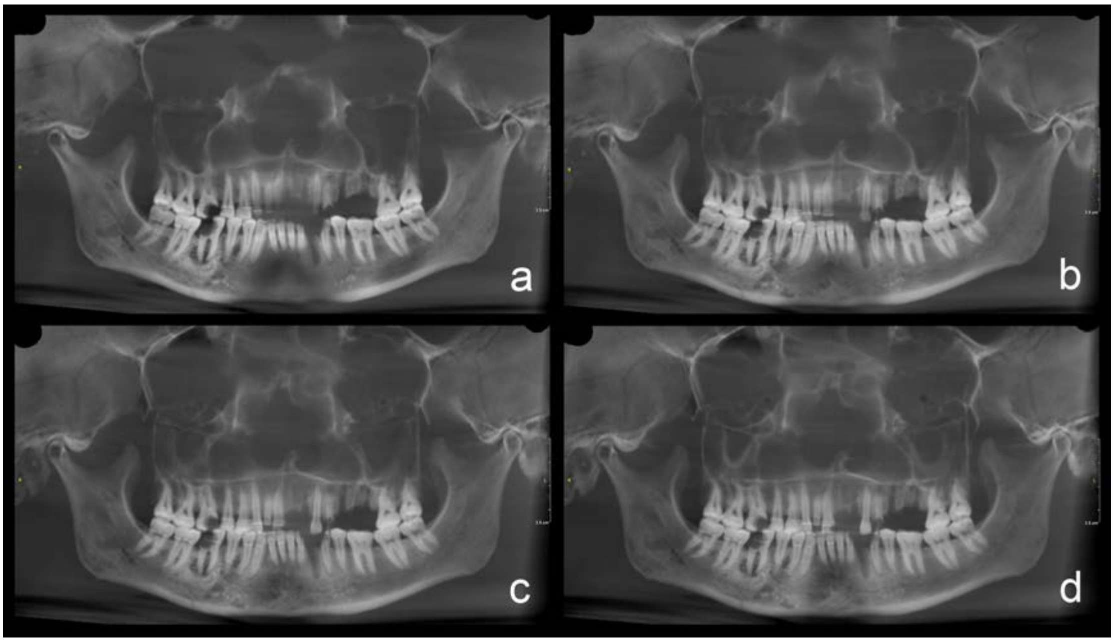

Figure 3.2 Panoramic images generated from NewTom VGi® by OnDemand3D® with different slice thicknesses (a 10 mm, b 15 mm, c 20 mm, d 25 mm)

Observation scoring technique

Seven observers were initially introduced to an instruction session in observation and scoring of panoramic images prior to the first observation. The observation was performed under standardized conditions: dimmed ambient light, with 20-inch clinical review display (MDRC-2120, Barco N.V., Kortrijk, Belgium). Digital panoramic radiographs and panoramic images generated from 3D data were randomized. Seven observers performed the observation on 238 images in total. Observers had to give scores for overall image quality and visibility of 14 anatomical landmarks: 5 in the maxilla and 9 in the mandible. The description of each score is shown in Table 3.2. Four observers repeated the observation after a 4-week interval.

Table 3.2 Scoring technique

			Description
Overall image quality	Score	1	Very poor (no diagnosis possible)
		2	Poor (diagnosis probably possible)
		3	Acceptable (diagnosis possible)
		4	Very good (diagnosis definitely possible)
Visibility of anatomical structures *Maxillary structures* Lower and anterior border of maxillary sinus Pterygomaxillary fissure/posterior border of maxillary sinus Periodontal structures (alveolar process & supporting structures) Anterior sextant/anterior teeth Posterior sextant/posterior teeth	Score	1	Significant structure not visible, no diagnosis possible
		2	Only broad details seen, diagnosis doubtful
		3	Small details visualized, diagnosis probably possible
		4	Fine details visualized, diagnosis definitely possible
Mandibular structures Condylar process (TMJ) Coronoid process Ramus Body and angle of mandible Mandibular canal Mental foramen Periodontal structures (alveolar process & supporting structures) Anterior sextant/anterior teeth Posterior sextant/posterior teeth	Possible reasons for errors	0	No reason
		1	Density/brightness/contrast is not optimal
		2	Blurring/Unsharpness
		3	Overlapping/superimposition of structures
		4	Area of interest is not included in the image
		5	Other than above

Statistical analysis

Statistical analysis was performed with SAS software (Statistical Analysis System Version 9.2, SAS Institute Inc, Cary, NC). The data was analysed while taking into account the ordering in the scores using ordinal logistic regression (OLR). OLR fits, in essence, a binary logistic regression model for each cumulative logit; therefore, odds ratios can be used for interpretation purposes (13). Intra-observer and inter-observer variability were assessed by Kappa statistics. Overall agreement was assessed using Kendall's coefficient of concordance for ordinal response.

3.4 Results

A total of 238 images were observed and scored. Substantial agreement was found for all observers at 0.63 of Kendall's coefficient of concordance. Intra-observer variability of each observer ranged from moderate to substantial (weighted Kappa 0.46–0.74). Inter-observer variability of each observer pair ranged from fair to substantial (weighted Kappa 0.32–0.62) (14).

Overall image quality

The frequency of scores for different devices, scored by all seven observers is shown in Table 3.3. The most common reason for the image error in both 2D and 3D imaging modalities as given by the observers is image blurring. An ordinal logistic regression model was fitted to this study and the results were presented in a form of odds ratio estimates with 95% Wald confidence limits. It was found that when comparing the 2D (Veraviewepocs 2D®) with the 3D (all CBCTs and the MSCT), the 3D modalities had 7.25 times more chance to receive poor score (Table 3.4).

Anatomical structures

Conventional panoramic radiograph showed superiority over panoramic imaging derived from 3D dataset except for the visualization of the condyle. Figure 3.3 shows the odds ratio estimates of different structures at 95% Wald confidence limits tested in this study. Maxillary structures yielded higher odds ratio estimates, which mean that the maxillary structures in the 3D modality were more likely to receive poor scores than the 2D images. The visualization of mandibular structures was, however, found to be almost equal to the conventional panoramic radiography (except for periodontal structure and anterior/posterior teeth sextant).

Table 3.3 Frequency table of scores for overall image quality by 7 observers

Overall image quality	Devices										
Frequency	Veraview-epocs 2D	3D Accuitomo 170	Galileos Comfort	i-CAT Next Gen	Iluma Elite	Kodak 9500	NewTom VGi	Picasso Trio	Scanora 3D	Skyview	MSCT	Total
[a]Poor	8	23	89	106	86	64	17	53	51	167	112	776
Acceptable	12	84	68	62	76	98	79	48	110	1	52	690
Good	22	61	11	0	6	6	72	11	7	0	4	200
Total	42[b]	168	168	168	168	168	168	112[c]	168	168	168	1666[d]

[a] The scores "very poor" and "poor" were collapsed into one score (poor) for computational reasons.

[b] No different slice thickness for Veraviewepocs 2D®: 6 samples x 7 observers = 42

[c] Images of 4 samples were taken by Picasso Trio®: 4 samples x 4 slice thicknesses x 7 observers = 112

[d] Total 238 images were scored, therefore the total frequency = 238 x 7 = 1666

Table 3.4 Overall image quality of 2D modality versus 3D modality

	Odds Ratio Estimates		
Effect	Point Estimate	95% Wald Confidence Limits	
3D modality vs 2D modality	7.25	4.01	13.12

Devices

The SkyView® machine received a 99.4% poor score. Therefore, it was left out from the comparison of all devices for computational reasons. When comparing the performance of different 3D devices to the standard panoramic machine, it was found that the quality of the images from NewTom VGi® and 3D Accuitomo 170® was almost equivalent to the images taken by conventional digital panoramic machine with odds ratio estimates of 1.2 and 1.6, respectively. In contrast, MSCT is performing much worse, being 29.7 times more likely to receive poor image quality score than conventional digital panoramic machine (Fig. 3.4).

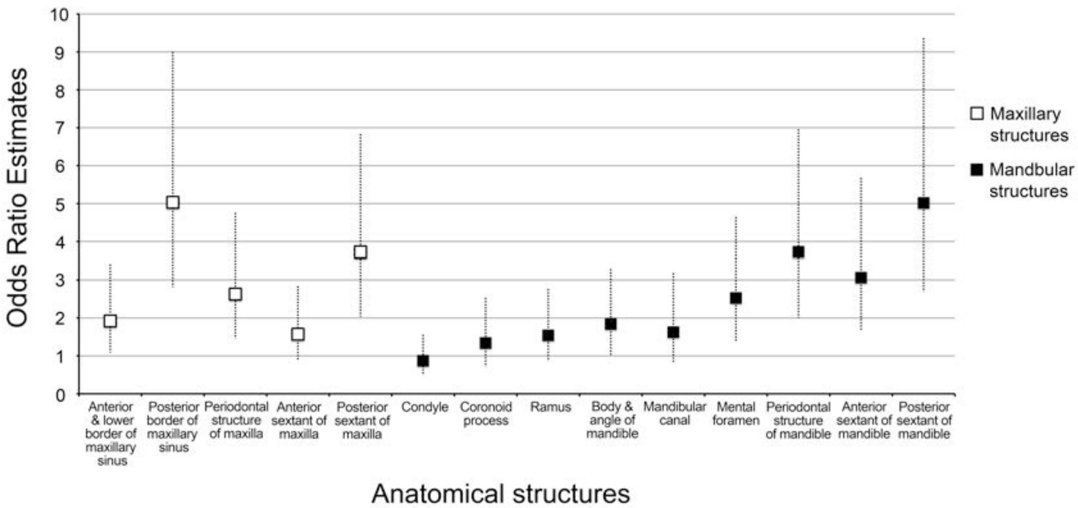

Figure 3.3 Odds ratio estimates with 95% Wald confidence limits of different anatomical structures in panoramic images generated from 3D data. The closer the odds ratio estimates to 1, the closer the visualization as compared to the panoramic radiograph from conventional 2D modality. Larger odd ratios correspond to greater differences between 2D and 3D for the visualization of this structure.

Slice thickness

Conventional digital panoramic radiographs showed significantly superior quality than all different slice thicknesses of the panoramic derived from CBCT and MSCT. Among different slice thicknesses, it was found that 20 mm is slightly better than other slice thickness settings (Point estimate at 6.56 compared to the conventional panoramic radiograph), followed by 15 mm (6.90), 10 mm (7.54) and 25 mm (8.17) consecutively.

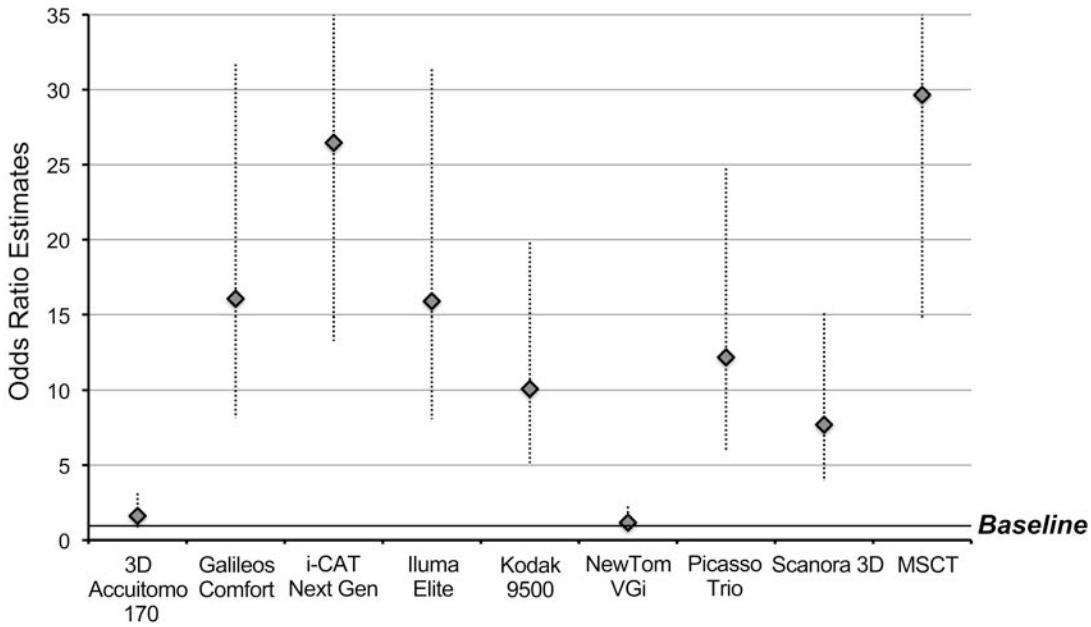

Figure 3.4 Odds ratio estimates with 95% Wald confidence limits of different devices. The baseline corresponds with the Veraviewepocs 2D®. The closer the odds ratio estimates to 1, the closer the quality as compared to the panoramic radiograph from conventional 2D modality.

3.5 Discussion

Panoramic view can be easily generated from 3D datasets. The scoring system used in this research was based on Gijbels' study published in 2000 (15), comparing image quality of direct digital and conventional panoramic radiographs. Fourteen anatomical landmarks were added in the protocol to be able to evaluate their visualization as this is very crucial for panoramic radiographic diagnosis. We found that the intra- and inter-observer agreement ranged from fair to good which proved that the methods were statistically valid.

The image quality assessment in this study is based on a subjective rating as there is no reference standard. The metal artifact assessment was not the main aim of this study; therefore, it was not evaluated separately from the overall image quality. It should also be noted that the nine included CBCT devices were compared at the level of the DICOM dataset, not using the systems' own software. One image viewing software (OnDemand3D®) was used to allow for a standardized evaluation.

Our sample size of four dry skulls and two formalin heads was rather small but to acquire images of skulls samples from different CBCT devices in different locations was a demanding task. The results of this *in vitro* study showed that conventional digital panoramic radiographs are significantly better both in overall image quality and visualization of anatomical structures.

Differences in the quality could be caused by differences in nature of the image. Conventional digital panoramic radiograph has much higher spatial resolution than both CBCTs and the medical CT. This could explain why the overall image quality of conventional digital panoramic radiograph is approximately seven times better. Furthermore, it could explain why image blurring was the most common reason for error. Indeed, as the spatial resolution for CBCT and CT images is limited, the sharpness will not be as high compared to panoramic radiographs. All CBCTs except SkyView® performed better than the MSCT, confirming the effect of spatial resolution.

The visualization of mandibular structures was slightly better than maxillary structures. The reason might be that the nature of most mandibular structures is well corticated and formed by denser bone than in the maxilla; therefore, even if the contrast and sharpness of the images were limited, the landmarks were clear enough to be used for diagnosis. For the 3D reformatted panoramic images, the minimum slice thickness (i.e. 0.2 mm) was not included in this protocol, although it may provide less blurring and improve contrast; however, it will not allow us to visualize all the teeth and other important anatomical structures. In order to cover all anatomical structures necessary for panoramic images, four slice thicknesses were selected for this study. It appeared that 20 mm thickness was slightly better than the others.

There are only a few studies that compared conventional panoramic radiographs with panoramic reformattings derived from 3D data. Pawelsik *et al.* (10) compared conventional panoramic radiographs with panoramic and crosssectional images reconstructed from the NewTom-9000® (Quantitative Radiology, Verona, Italy) in diagnosis of relationship between third molars and mandibular canals. The authors reported that the cross-sectional images had given significantly clearer perception of the mandibular nerve than the conventional panoramic radiographs although the scores of conventional panoramic images were significantly better than the reconstructed panoramic images (10). The results of the present study agree with previous results. CBCTs have been developed in the past decade; however, the resolution of conventional panoramic radiographs is still significantly superior. Nevertheless, CBCT can provide 3D views of the jaw and is useful to locate the mandibular canal in the cross-sectional slices.

Mischkowski *et al*. compared reconstructed panoramic images acquired from Galileos® (Sirona Dental Systems, Bensheim, Germany) with conventional panoramic radiographs (11). It was found that there was no significant difference in diagnostic quality between both image modalities. Image quality of reconstructed panoramic views was significantly lower than the conventional panoramic radiographs but anatomical structures except mandibular canal and alveolar ridge gingiva were better visualized in the panoramic view from CBCT. The authors concluded that the reconstructed panoramic views from CBCT were better in diagnosis of specific lesions, whereas conventional panoramic radiographs provided better image quality for a general overview. The diagnostic quality is equal for both modalities (11). This is in agreement with the present study. The image quality of conventional panoramic radiographs is higher but for the visualization of anatomical structures, the opposite results were found. This can be explained by differences in "Materials and methods". In Mischkowski's study, the reconstructed panoramic images were viewed in the Galileos software and the inspection window was used. This inspection window may have provided more visualization to specific structures and then resulted in higher scores for the anatomical landmarks. In our study, only the condyle did not show significant difference between the two imaging modalities although the image quality of some of the mandibular structures (ramus, body and angle of mandible, mandibular foramen and mandibular canal) of the 3D derived images were almost equal to the 2D system. The other reason can be that in this study, as nine CBCTs and one MSCT were tested, there could then be more variability among these devices.

In 2008, Angelopoulos *et al*. (12) published a study comparing digital panoramic radiography and CBCT for the identification of mandibular canals. The results showed that panoramic images generated from CBCT were significantly better than digital panoramic radiographs in identifying the mandibular canals (12).

This result is not in agreement with the results of the present study. The reason could be the difference in CBCT devices used in the study as well as the slice thickness. Angelopulos and coworkers (12) used 5.2-mm slice thickness which is thinner than that in our study. At this thickness, the images may be able to cover the area of mandibular canals and avoided other structures from superimposing with the canals. Instead we used 10, 15, 20 and 25 mm. This factor might affect the visibility of the mandibular canals, but the increased slice thickness could cover and show more structures both in the maxilla and the mandible.

There are two studies that were performed on the accuracy of measurements on CBCT derived panoramic images. Ludlow *et al*. compared measurements of mandibular anatomy on panoramic reconstructions from CBCT (2D) and on axial slices (3D) with the physical measurements (16). It was found that both 2D and 3D techniques provided acceptably accurate measurements of mandibular anatomy (16). In 2010, Van Elslande *et al*. reported results of the accuracy of mesio-distal root angulation projected by panoramic reconstructed from CBCT. They concluded that panoramic reconstructions on CBCT were more accurate than conventional panoramic radiography concerning mesio-distal root angulation (17). Although in the present study, measurements were not done, these two references suggested that panoramic images derived from CBCT allowed suitably accurate measurement results which are useful for orthodontic and implant treatment planning.

Radiation exposure of the cone-beam CT is still a big concern in dental field. A new report on radiation dose of different CBCT devices has been published by Pauwels *et al*. (18). The results showed that the dose received is strongly related to FOV size and also dependent on the exposure parameter. In order to gain full panoramic images, a medium to big FOV should be used; but it must be kept in mind that, at this stage, CBCT still cannot replace the use of conventional panoramic radiographs. However, if there is a diagnostic requirement for CBCT, for some devices, moderate to good quality panoramic images can be generated from existing CBCT data.

3.6 Conclusions

While 2D panoramic images are still significantly better, 2/3 of the 3D-derived panoramic images, depending on the machines, are moderate to good concerning subjective diagnosis. Furthermore, panoramic images generated from some cone-beam CT devices seem to be comparable to the conventional digital panoramic images concerning the overall subjective image quality and visualization of anatomical structures. On 3D-derived panoramics, mandibular structures tended to be more visible than the maxillary structures and 20-mm slice thickness is recommended.

The radiation dose to patients must be concerned. Conventional digital panoramic radiographs must not be replaced by CBCT images, but CBCT should be taken only if there is a clear indication.

3.7 References

1. Paatero Y. The use of a mobile source of light in radiography. *Acta Radiol.* 1948;29:221.
2. Paatero Y. A new tomographic method for radiographing curved outer surfaces. *Acta Radiol.* 1949;32:177.
3. Numata H. Consideration of the parabolic radiography of the dental arch. *J Shimazu Stud*. 1993;10:13.
4. Tronje G, Welander U, McDavid WD, Morris CR. Image distortion in rotational panoramic radiography. I. General considerations. *Acta Radiol Diagn (Stockh)*. 1981;22:295-299.
5. Tronje G, Eliasson S, Julin P, Welander U. Image distortion in rotational panoramic radiography. II. Vertical distances. *Acta Radiol Diagn (Stockh)*. 1981;22:449-455.
6. Tronje G, Welander U, McDavid WD, Morris CR. Image distortion in rotational panoramic radiography. III. Inclined objects. *Acta Radiol Diagn (Stockh)*. 1981;22:585-592.
7. Wyatt DL, Farman AG, Orbell GM, Silveira AM, Scarfe WC. Accuracy of dimensional and angular measurements from panoramic and lateral oblique radiographs. *Dentomaxillofac Radiol*. 1995;24:225-231.

8. Swennen GR, Schutyser F. Three-dimensional cephalometry: spiral multi-slice vs cone-beam computed tomography. *Am J Orthod Dentofacial Orthop*. 2006;130:410-416.
9. Chenin DL. 3D cephalometrics: the newnorm. *Alpha Omegan.* 2010;103:51-56.
10. Pawelzik J, Cohnen M, Willers R, Becker J. A comparison of conventional panoramic radiographs with volumetric computed tomography images in the preoperative assessment of impacted mandibular third molars. *J Oral Maxillofac Surg*. 2002;60:979-984.
11. Mischkowski RA, Ritter L, Neugebauer J, Dreiseidler T, Keeve E, Zoller JE. Diagnostic quality of panoramic views obtained by a newly developed digital volume tomography device for maxillofacial imaging. *Quintessence Int.* 2007;38:763-772.
12. Angelopoulos C, Thomas SL, Hechler S, Parissis N, Hlavacek M. Comparison between digital panoramic radiography and cone-beam computed tomography for the identification of the mandibular canal as part of presurgical dental implant assessment. *J Oral Maxillofac Surg.* 2008;66:2130-2135.
13. Agresti A. An introduction to categorical data analysis. 2nd ed. New Jersey: Wiley; 2007.
14. Landis JR, Koch GG. The measurement of observer agreement for categorical data. *Biometrics.* 1977;33:159-174.
15. Gijbels F, De Meyer AM, Bou Serhal C, Van den Bossche C, Declerck J, Persoons M, Jacobs R. The subjective image quality of direct digital and conventional panoramic radiography. *Clin Oral Investig.* 2000;4:162-167.
16. Ludlow JB, Laster WS, See M, Bailey LJ, Hershey HG. Accuracy of measurements of mandibular anatomy in cone beam computed tomography images. *Oral Surg Oral Med Oral Pathol Oral Radiol Endod.* 2007;103:534-542.
17. Van Elslande D, Heo G, Flores-Mir C, Carey J, Major PW. Accuracy of mesiodistal root angulation projected by cone-beam computed tomographic panoramic-like images. *Am J Orthod Dentofacial Orthop.* 2010;137:S94-99.

18. Pauwels R, Beinsberger J, Collaert B, Theodorakou C, Rogers J, Walker A, *et al*. Effective dose range for dental cone beam computed tomography scanners. *Eur J Radiol*. 2012;81:267-271.

Chapter 4

Agreement between cone-beam computed tomography images and panoramic radiographs for initial orthodontic evaluation

This chapter is based on:

Pittayapat P, Willems G, Alqerban A, Coucke W, Ribeiro-Rotta RF, Couto Souza P, Westphalen FH, Jacobs R. Agreement between cone beam computed tomography images and panoramic radiographs for initial orthodontic evaluation. *Oral Surg Oral Med Oral Pathol Oral Radiol.* 2014;117:111-9.

4.1 Abstract

Objectives: The aim of this study was to compare the agreement between cone-beam computed tomography (CBCT) and panoramic radiographs for initial orthodontic evaluation. This study was not meant to test differences between imaging modalities or to indicate superiority of one technique.

Materials and methods: Thirty-eight subjects with both panoramic and CBCT images were retrospectively collected. Eight observers answered 14 observational questions. The observation was repeated after 4 weeks.

Results: CBCT images yielded better agreement between 2 observer groups (orthodontic residents and radiologists) and better inter- and intra-observer agreement. The agreement between panoramic radiographs and CBCT scans was moderate.

Conclusions: If CBCT is a priori present in a case with justified indications, it has the potential to provide valuable diagnostic information for initial orthodontic evaluation and extra information for treatment planning. The moderate agreement between panoramic and CBCT images may indicate that the nature and amount of information gained from both imaging sources is deviant.

Clinical relevance: Although CBCT scans still cannot replace panoramic radiographs, the present study might suggest eliminating the need for a further panoramic image if a recent CBCT scan of both jaws is already available.

4.2 Introduction

Panoramic radiography has been used as an essential diagnostic tool in dentistry for more than half a century (1-3). Although with several limitations, such as geometric distortion and superimposition of anatomic structures (4-7), panoramic radiographs are still generally used in orthodontic treatment planning, in oral surgery, and in almost all dental specialties for overall screening.

Three-dimensional (3D) computed tomography (CT) images were introduced to dentistry in the 1990s, but in view of the high radiation dose, their use has been rather controversial and not widely accepted. However, since the introduction of the first cone-beam computed tomography (CBCT) systems (8), 3D imaging has started to play an increasingly important role in oral health care diagnostics. The technology of this device has been continuously developing, offering dentists spatial visibility of anatomic structures and pathology with a better image quality and also with a relatively lower radiation dose than the multi-slice CT (9). Although different guidelines and selection criteria may exist in various countries, orthodontists often seem to request a panoramic radiograph and a lateral cephalogram for initial treatment planning. Additional information about tooth eruption state, angulation of the teeth, and overall dental, periodontal, and condylar condition is often added to the clinical evaluation based on analysis of the panoramic radiograph. This type of radiograph is also used to follow up orthodontic treatment progress as well as to visualize treatment outcome and prognosis of wisdom teeth if present (10). In particular indications, conventional radiographs seem to offer insufficient information to make a diagnosis, illustrating the need for a low-dose CBCT for specific orthodontic comprehensive care, such as cases of canine impaction, root resorption, supernumerary teeth, and airway related problems (11,12). The radiation burden by CBCT, however, remains a major concern, especially in children. Studies have been conducted on different CBCT devices and different protocols to evaluate radiation dose to the patients. Dosimetric studies found that the amount of radiation dose is strongly related to the size of the field of view (FOV) and imaging parameters (e.g., resolution, rotation, milliamperage) (13,14). The latter information is crucial to apply the ALARA (as low as reasonably achievable) concept in children.

Several studies have tested the reliability of panoramic radiography for orthodontic-related issues, and some have contrasted its reliability with that of CBCT. Results show that panoramic radiographs are often unreliable in diagnosing canine impaction, third molar impaction, mesial angulation of the roots, root contact, root resorption, and supernumerary teeth. In contrast, CBCT scans could offer more reliable information and may lead to a different diagnosis and treatment plan for these specific conditions (15-24).

In a previous study, the ability of panoramic views generated from CBCT scans was compared with that of conventional digital panoramic radiographs. The results suggested that the reformatted panoramic views from some CBCT scans may be able to offer equal diagnostic quality compared with the digital panoramic images commonly used in dental practices (25). The next step would be to examine whether the full CBCT dataset has equal diagnostic quality compared with conventional digital panoramic radiographs. If the patient's preexisting CBCT data can provide orthodontists all necessary information for orthodontic treatment, then extra conventional 2D radiographs will not be required anymore, making an additional panoramic radiograph unnecessary. Patients' datasets will be more compact, and the radiation dose can be reduced.

There is only a little evidence from the literature that indicates whether CBCT data can offer better diagnostic potential, lead to improved orthodontic treatment planning, and offer orthodontists the same amount of information as they usually require from conventional panoramic radiographs (26).

The aim of this study was to compare the agreement between observers for CBCT and digital panoramic radiographs related to initial orthodontic evaluation in the situation where CBCT images are a priori requested by the orthodontist for justified indications. This study was not meant to test differences or indicate superiority of 3D imaging in general or CBCT imaging more specifically. This study was aimed to evaluate the suitability of CBCT for initial orthodontic evaluation, when a CBCT scan was indicated and a priori taken for some specific indications.

4.3 Materials and methods

Samples

Thirty-eight patients (13 males and 25 females; age range, 8-25 years; mean age, 13.2 years; standard deviation [SD], 4.2 years) were retrospectively selected from the hospital orthodontic database (Oral Imaging Center, Katholieke Universiteit Leuven, Leuven, Belgium). The selection criteria were (1) that patients had a panoramic radiograph and additional CBCT images after a panoramic radiograph had been taken (the CBCT was specifically indicated for patients with root resorption cases and for treatment planning when dealing with impacted canines); (2) that both types of images were taken within an average time interval of 3 months (range, 0-11.5 months; SD, 3.7 months); (3) that no significant pathology of the maxillofacial region (benign or malignant tumor, cleft lip or cleft palate, trauma) was present; and (4) that no significant asymmetry of the face was observed. The study protocol (reference number, ML6960) was approved by the UZ Leuven Medical Ethics Committee. The authors have read the Helsinki Declaration and have followed the guidelines in this investigation.

Imaging modalities

Panoramic radiographs were acquired from a standard digital panoramic device with CCD sensor (Veraviewepocs 2D®, J. Morita, Kyoto, Japan). The panoramic settings were selected depending on each patient (64 kilovolt peak [kVp]; 8.9 milliampere [mA]; 7.4 sec; pixel size, 0.144 mm; image size, 30 _ 15 cm). The images were collected from the hospital picture archiving and communication system by being exported as TIFF files (Tagged Image File Format).

The CBCT scans of each patient were taken with 3D Accuitomo® 170 (J. Morita) (FOV, 140 _ 100 mm; high-fidelity (Hi-Fi) mode, 90 kVp, 5 mA; scan time, 30.8 sec; voxel size, 0.25 mm). All datasets were exported as Digital Imaging and Communications in Medicine (DICOM) standard files.

Image evaluation

Eight observers (5 second-year orthodontic residents and 3 dentomaxillofacial radiologists with more than 5 years' experience) were initially introduced to an instruction and calibration session. Detailed instructions and definitions of all questions were given to all observers. The observers made an observation of 3 cases. Then the answers were checked and calibrated by the main author. All of them participated at the first observation session, and 5 observers (orthodontic residents) repeated the evaluation after a 4-week interval. Both observation sessions were performed under standardized conditions: dimmed ambient light, with 20-inch, 2-megapixel clinical review display (MDRC-2120, Barco NV, Kortrijk, Belgium).

During the observation, images from the patients were divided into 2 groups and then randomized within the group, and they were also re-randomized for the second session. In group 1, panoramic radiographs were shown to observers on the ImageJ® software, version 1.45s (National Institutes of Health, Bethesda, MD, USA) (Fig. 4.1). In group 2, the entire volumes of CBCT images were shown on the OnDemand3D® software, version 1.0.8.0408 (Cybermed, Seoul, South Korea) (Fig. 4.2). In both groups, the observers had the possibility to use all tools available in the software, including the panoramic curve tool in the OnDemand3D® application.

Questionnaire

Observers answered 14 questions related to initial orthodontic evaluation. The detailed questions and answer options are shown in Table 4.1. The tooth numbering system used in the questionnaire was the FDI World Dental Federation notation (e.g., 13 is a maxillary right canine).

Statistical analysis

Statistical analysis was performed with R software for Windows, version 2.14 (R Development Core Team, Foundation for Statistical Computing, Vienna, Austria). Agreements were assessed using Fleiss κ statistics. Data were assessed on the following aspects:

- Agreement between the radiologist group and the orthodontic resident group
- Agreement between digital panoramic radiographs and CBCT images
- Inter-observer agreement
- Intra-observer agreement

Table 4.1 Questions (Q) related to the initial orthodontic evaluation, answered by the observers

	Questions	Description	Answers
Q1	Are all permanent teeth present?	All permanent teeth including both teeth and tooth buds.	*1 Yes/ 2 No/ 3 Unidentified*
Q2	Is the sequence of eruption in upper left and upper right side symmetrical?	The same sequence of eruption applied for both left and right side of the upper jaw or not.	*1 Yes/ 2 No/ 3 Unidentified*
Q3	Is the sequence of eruption in lower left and lower right side symmetrical?	The same sequence of eruption is applied for both left and right side of the lower jaw or not.	*1 Yes/ 2 No/ 3 Unidentified*
Q4	Is the *anterior apical area (*root spacing) optimal?	The space in the area between the mesial surface of the upper right and left canines is adequate for normal eruption or not. *Yes* - The space is optimal and adequate. *Reduced* - The space is slightly reduced. This will determine the treatment plan to gain more space. *Severe* - The space is severely reduced. This will determine the treatment plan to gain more space and whether there is a need for tooth extraction.	*1 Yes/ 2 Reduced/ 3 Severe/ 4 Unidentified*
Q5	Is the *middle apical area (*root spacing) optimal?	The space in the area from the mesial surface of the upper canine to the mesial surface of the first molar is adequate for normal eruption or not. The answers are as in Q4.	*1 Yes/ 2 Reduced/ 3 Severe/ 4 Unidentified*
Q6	Is the *posterior apical are*a (root spacing) optimal?	The space in the area from the mesial surface of the upper first molar to the distal surface of the upper third molar is adequate for normal eruption or not. The answers are as in Q4.	*1 Yes/ 2 Reduced/ 3 Severe/ 4 Unidentified*
Q7	Is the path of eruption of #13 optimal?	The optimal path of eruption is when the upper canine replaces the primary canine vertically without deviating to the mesial or distal side.	*1 Yes/ 2 No/ 3 Unidentified*
Q8	Is the path of eruption of #23 optimal?	The optimal path of eruption is when the upper canine replaces the primary canine vertically without deviating to the mesial or distal side.	*1 Yes/ 2 No/ 3 Unidentified*
Q9	Is there impaction risk of #13 and #23?	Impaction is defined as a suboptimal path of eruption, the canine has not erupted when the dental age is more than 13 years old, complete canine root formation without eruption, or insufficient mesio-distal space.	*1 Yes/ 2 No/ 3 Unidentified*
Q10	Can the upper right canine (#13) be localized?	Localization of the upper right canine in relation to the dental arch.	*1 Buccal/ 2 Middle/ 3 Palatal/ 4 Unidentified*
Q11	What is the angulation of upper right canine (#13) to the midline?	The angle is formed by a line on the midline bisecting the jaw in two and a line through the cusp and the apex bisecting the canine along its long axis (Fig. 4.3) (19, 27-30).	*1 Category A: 0-22.5° to the midline* *2 Category B: 22.6-45.0° to the midline* *3 Category C: 45.1-67.5° to the midline* *4 Category D: 67.6-90.0° to the midline*
Q12	Is there pathological root resorption at the upper right lateral incisor (#12)?	Detection of a resorption defect on the upper right lateral incisor root.	*1 Yes/ 2 No/ 3 Unidentified*
Q13	Is there impaction risk of premolar and molars?	The impaction risk is classified when: the path of eruption is not optimal, complete root formation without eruption, insufficient mesio-distal space.	*1 Yes/ 2 No/ 3 Unidentified*
Q14	Is there impaction risk of third molars?	The impaction risk is classified when: the path of eruption is not optimal, complete root formation without eruption, insufficient mesio-distal space.	*1 Yes/ 2 No/ 3 Unidentified*

Figure 4.1 Panoramic radiograph of a 10-year-old boy from group 1

Figure 4.2 The CBCT image of the same patient as in Figure 4.1, viewed on the OnDemand3D® software. During the observation, the observers could view the entire CBCT volume in axial, coronal, and sagittal slices and could potentially draw a panoramic curve to create a reformatted panoramic view, as shown in this Figure. The thickness of reformatted panoramic views could be adjusted. This Figure shows a reformatted panoramic view with a 20-mm thickness. (CBCT, cone beam computed tomography.)

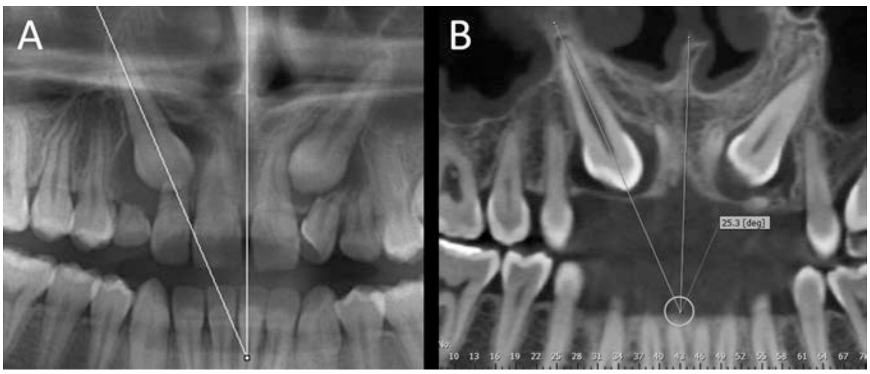

Figure 4.3 The angular measurement performed in question 11 on a panoramic radiograph (A) and on a CBCT image (B). The angle was formed by a line on the midline bisecting the jaw in two and a line through the cusp and the apex bisecting the canine along its long axis. (CBCT, cone beam computed tomography.)

4.4 Results

Agreement between observer groups

A high agreement was found between the orthodontic resident group and the radiologist group. The agreement was higher in the CBCT image group than in the panoramic group, with the Fleiss κ being 1.0 and 0.9 ($p<0.0001$), respectively.

Agreement between 2 imaging modalities

A moderate agreement for all observers (Fleiss κ, 0.5; $p<0.0001$) was observed when comparing the 2 image modalities (group 1, panoramic; group 2, CBCT) (31). The Fleiss κ was slightly higher in the orthodontic resident group (0.54) than in the radiologist group (0.45) ($p<0.0001$).

More detailed results of the questionnaire per question and the frequency of all answers given to all questions are shown in Table 4.2. It was found that for question 10 (localization of the upper right canine), the agreement between the 2D and 3D modalities was only slight (Fleiss κ, 0.2; $p<0.0001$) (31). Other questions that received fair agreement (Fleiss k, 0.2-0.4) were questions 4, 5, and 6 (apical area of frontal, middle, and posterior region), 11 (angulation of the upper right canine), 12 (root resorption of the upper right lateral incisor), and 14 (impaction risk of third molars).

Intra- and Inter-observer agreement

The intra-observer agreement was substantial and was slightly better for the CBCT than the panoramic images (Fleiss κ, 0.71 and 0.65 ($p<0.0001$), respectively). Moderate agreement was found in the inter-observer analysis. The Fleiss κ tended to be higher for the CBCT (0.5) than for the panoramic images (0.4) ($p<0.0001$).

Table 4.2 Agreement between group 1 panoramic and group 2 CBCT per question for all observers and frequency of all answers in percentage with standard error

		Fleiss k	*P*-value	Image modality	% Answer 1, (SE)	% Answer 2, (SE)	% Answer 3, (SE)	% Answer 4, (SE)
					Yes	*No*	*Unidentified*	
Q1	Are all permanent teeth present?	0.6	<0.0001	Panoramic	55.6, (1.2)	39.1, (1.0)	5.3, (0.4)	
				CBCT	54.3, (1.3)	44.7, (1.1)	1.0, (0.2)	
Q2	Is the sequence of eruption of *upper* Left and upper Right side symmetrical?	0.6	<0.0001	Panoramic	46.7, (1.2)	32.9, (1.0)	20.4, (0.8)	
				CBCT	39.8, (1.3)	43.8, (1.2)	16.4, (0.8)	
Q3	Is the sequence of eruption of *lower* Left and *lower* Right side symmetrical?	0.6	<0.0001	Panoramic	53.0, (1.2)	16.4, (0.8)	30.6, (1.0)	
				CBCT	48.7, (1.3)	19.7, (0.9)	31.6, (1.0)	
					Yes	*Reduced*	*Severe*	*Unidentified*
Q4	Is the *anterior apical area* of the upper jaw optimal?	0.3	<0.0001	Panoramic	58.5, (2.8)	31.9, (3.4)	8.9, (2.6)	0.7, (0.8)
				CBCT	71.1, (2.6)	23.0, (3.3)	4.9, (2.0)	1.0, (1.0)
Q5	Is the *middle apical area* of the upper jaw optimal?	0.2	<0.0001	Panoramic	48.4, (2.9)	36.8, (3.4)	11.8, (2.8)	3.0, (1.7)
				CBCT	74.7, (2.5)	24.0, (3.5)	1.0, (1.0)	0.3, (0.6)
Q6	Is the *posterior apical* area of the upper jaw optimal?	0.4	<0.0001	Panoramic	31.2, (2.7)	45.7, (3.2)	16.5, (3.1)	6.6, (2.3)
				CBCT	37.5, (2.8)	49.7, (3.3)	9.9, (2.7)	2.9, (1.7)
					Yes	*No*	*Unidentified*	
Q7	Is the path of eruption of #13 optimal?	0.4	<0.0001	Panoramic	56.9, (1.2)	34.2, (1.0)	8.9, (0.6)	
				CBCT	43.4, (1.3)	48.0, (1.2)	8.6, (0.6)	
Q8	Is the path of eruption of #23 optimal?	0.6	<0.0001	Panoramic	40.8, (1.2)	52.3, (1.1)	6.9, (0.5)	
				CBCT	47.0, (1.3)	46.4, (1.2)	6.6, (0.5)	
Q9	Is there impaction risk of #13 and #23?	0.5	<0.0001	Panoramic	76.0, (1.0)	20.7, (0.8)	3.3, (0.4)	
				CBCT	72.7, (1.1)	25.0, (1.0)	2.3, (0.3)	
					Buccal	*Middle*	*Palatal*	*Unidentified*
Q10	Can #13 be localized?	0.2	<0.0001	Panoramic	4.9, (1.2)	51.3, (2.9)	16.1, (2.7)	27.7, (3.6)
				CBCT	15.8, (2.1)	59.5, (3.0)	24.7, (3.5)	0.0, (0.0)
					0-22.5° to M	*22.6-45.0° to M*	*45.1-67.5° to M*	*67.6-90.0° to M**
Q11	What is the angulation of #13 to the midline (M)?	0.3	<0.0001	Panoramic	79.0, (2.3)	17.4, (3.2)	3.6, (1.8)	0.0, (0.0)
				CBCT	68.1, (2.7)	25.3, (3.4)	6.3, (2.3)	0.3, (0.6)
					Yes	*No*	*Unidentified*	
Q12	Is there any pathological root resorption at #12?	0.3	<0.0001	Panoramic	10.5, (1.8)	65.5, (2.8)	24.0, (3.5)	
				CBCT	10.9, (1.8)	81.9, (2.3)	7.2, (2.4)	
Q13	Is there impaction risk of premolar and molars?	0.5	<0.0001	Panoramic	28.6, (1.1)	67.8, (1.0)	3.6, (0.4)	
				CBCT	20.4, (1.0)	76.3, (1.0)	3.3, (0.4)	
Q14	Is there impaction risk of third molars?	0.4	<0.0001	Panoramic	67.8, (2.7)	9.8, (2.3)	22.4, (3.5)	
				CBCT	61.9, (2.8)	12.8, (2.5)	25.3, (3.5)	

4.5 Discussion

The present study found only a moderate agreement between CBCT images and digital panoramic radiographs when questions related to the initial orthodontic evaluation had to be answered.

In this study, panoramic and CBCT images of the patients were collected retrospectively. The patients were selected from the database of patients who had images from both modalities taken. The patients included in this study had CBCT scans acquired in the clinic according to the treating doctor's specified exposure parameters. The patients were not intentionally overexposed for this study. The patients often had problems with impacted canines or third molars, thus the population of this study was not distributed to people with normal oral condition. Although patients with oral and maxillofacial tumor, cleft lip and cleft palate, and trauma were discarded, there still might have been some potential bias to this study.

As the results have shown, a high agreement was found between the 2 observer groups, and the agreement was higher when visualizing the CBCT images compared with the panoramic images. This was not unforeseen, because the CBCT images should offer more precise and realistic volume data when comparing with the panoramic images that are actually 2D shadows of the jaws. Evaluation of the dentomaxillofacial region on CBCT images should give more reliable answers to the questions. This supports the fact that both inter- and intra-observer agreement were higher in the CBCT group.

Questions were raised when comparing the 2 image modalities, because only a moderate agreement was observed. The Fleiss κ was slightly higher in the orthodontic resident group. This implied that there were some points for which panoramic and CBCT images resulted in different answers to the questions, or, to put it another way, they provided different information. The agreement was then inspected closely to see which questions had less agreement, and the results are shown in Table 4.2.

Some questions showed low or slight agreement (e.g., for question 10, Fleiss κ = 0.2; $p<0.0001$) (Table 4.2). In question 10, the observers were asked to localize the upper right canine. In all cases, the canine could be localized in the CBCT images, but in the panoramic radiographs, the observers could only localize in 72.3% of the cases, and in reality, the judgment of the location may not always be the true location, because the panoramic radiographs provide only 2D aspects and do not show the real bucco-palatal dimension (Table 4.2). The results of this study are similar to previous evidence on managing canine impaction (19, 20,28).

Studies found that 3D imaging was advantageous in the management of impacted canines (28) and that the CBCT was more sensitive than conventional radiography for canine localization (19). The findings from Botticelli *et al*. (20) indicated that CBCT increased precision in the localization of the canines and improved the estimation of the space conditions in the arch. The latter resulted in a difference in diagnosis and treatment planning from the 2D imaging approach (20).

Some questions showed fair agreement (Fleiss κ = 0.2-0.4) (31). These were questions about apical area (questions 4, 5, and 6), angulation of the upper right canine (question 11), root resorption of the upper right lateral incisor (question 12), and the impaction risk of third molars (question 14). Some questions (especially questions 4, 5, and 6) are indeed rather subjective and cannot be truly objectified. Therefore, they probably had a large influence on the level of agreement. On the other hand, the authors decided to include these questions because they are often asked by orthodontists during the initial evaluation.

Questions 4 to 6 asked the observers to evaluate the space at the apical areas. As mentioned, the nature of these questions is rather subjective, and in this study, true distance measurements could not be performed as a gold standard; therefore, it was impossible to verify which answers were correct for each case. It is expected that 3D CBCT scans will give the answer that is closer to the real situation than panoramic radiographs, which have more distortion from their image geometry. However, in this study, only the agreement between the 2 imaging modalities could be tested.

To be able to answer question 11, the observers had to use the angular measuring tools, in both the ImageJ and the OnDemand3D® software (Fig. 4.3), and then select the angle categories from 1 to 4 (Table 4.2). However, the image geometry of the panoramic radiograph might influence the angular measurements. Patient positioning in the panoramic radiographic machine can influence the occlusal plane or the smile curve of the panoramic radiographs and therefore can result in only a fair agreement between the 2 imaging modalities (21,32). The results of the present study were also supported by the results from Alqerban *et al.* (19) in 2011, who reported a significant difference in upper canine angulation to the midline between a digital panoramic radiograph and a medium-FOV CBCT (19).

In question 12, the observers were asked to report any pathologic root resorption on the upper right lateral incisor. Fair agreement was found (Fleiss κ = 0.3). In the panoramic group, 24.0% of all the answers were categorized as "unidentified," in contrast to only 7.2% in the CBCT group (Table 4.2). This may be explained by the fact that in panoramic radiographs, the observers can only visualize the teeth in 2 dimensions. Superimposition of the anatomic structures and teeth might camouflage any root resorption in panoramic images, contrary to the situation in CBCT images, where the observers can look for the presence of root resorption on every side of the tooth. This result should be read with some caution. When root resorption was severe, it was obvious in both panoramic radiography and CBCT. In contrast, when it came to mild resorption cases, studies found that CBCT is more sensitive than panoramic radiography (15,16).

So far, several articles related to root resorption and 3D imaging have been published (15,16,19,33-35). Before the introduction of CBCT, studies compared conventional panoramic radiography with CT. Such comparisons found lower reliability of panoramic radiography for diagnosing incisor root resorption associated with impacted canines (33,34). When looking at the CBCT devices, studies also found that CBCT scans were more accurate than panoramic radiographs for detecting root resorption (15,16,19). In the study by Dudic *et al*. (16), it was found that "no resorption" was observed more in panoramic radiographs than in CBCT, but mild resorption cases were observed more in CBCT, in agreement with the results of the present study (16).

Results from another study by Alqerban *et al*. (35) indicated that high image quality was important for detecting root resorption, and the CBCT systems had high accuracy in the detection of the severity of root resorption (35).

The question related to the impaction risk of third molars (question 14) showed fair agreement (Fleiss κ = 0.4; $p<0.0001$). The reason might be the nature of the question, which was rather subjective. Another reason might be the age of the patients included in this study. The mean age was approximately 13 years; neither the jaws nor the third molars were fully developed, and for this reason, it was difficult to answer whether there was an impaction risk of the third molars. As a prediction, this resulted in fair agreement.

Although several studies have found additional value in CBCT, a systematic review on the use of CBCT in orthodontic treatment published in 2012 had interesting findings (26). It was found that there is still limited evidence that CBCT offers better diagnostic potential or leads to improved treatment planning and a more predictable or superior treatment outcome than conventional imaging modalities. Only some specific studies on airway diagnostics provide sound scientific data suggesting that CBCT can add value (26). There is little evidence to support a role of CBCT in the initial orthodontic evaluation.

The present study did not aim to establish the superiority of any imaging modalities but instead was trying to evaluate whether both imaging modalities offer the essential information needed for an initial orthodontic diagnostic evaluation. The study did not aim to compare the observers' reply to the real case findings (clinical standard). Even though this could be regarded as a limitation, this study has found that the cone beam computed tomography showed its ability to give all necessary information for initial orthodontic evaluation. With moderate agreement between 2D and 3D imaging modalities, it suggested that the information gained from CBCT scans might not be similar to the information usually gained from panoramic radiographs. In the observation of the detailed results, CBCT offered a greater depth of information about the patient's condition. Further studies should be performed on the accuracy of the radiographic findings, by comparing CBCT and panoramic radiography with a gold standard and by evaluating whether the differential findings using 2D vs 3D imaging modalities could influence treatment planning and treatment outcome in orthodontic treatment.

Radiation to the patients

The present study was a retrospective study, and all images were acquired before data collection. Both CBCT and panoramic images were referred by orthodontists with justified indications. The radiation dose received from CBCT is strongly related to FOV size and also dependent on the exposure (13,14). For children it is crucial that dental CBCT examinations should be fully justified over conventional radiography. New guidelines and recommendations on CBCT for dental and maxillofacial radiology are now available and should be followed (36). One recently published set of recommendations by the American Academy of Oral and Maxillofacial Radiology (37) stated that CBCT in orthodontic treatment should be justified on an individual basis, based on clinical presentation, and the position statement should be periodically revised to reflect new evidence. A proper radiation regimen is highly recommended, and it is emphasized to keep the radiation dose to the patient as low as reasonably achievable.

4.6 Conclusions

In this questionnaire-based study, moderate agreement on initial orthodontic evaluation was found between CBCT images and panoramic radiographs. This does not mean that the information received from CBCT images is either incorrect or unreliable; rather, it simply means that it deviated from the information gained from panoramic radiographs. If a priori present, CBCT imaging has the potential to provide valuable diagnostic information for initial orthodontic evaluation and also to add extra information for orthodontic treatment planning. Yet proper justification and the ALARA concept should be meticulously followed.

4.7 References

1. Numata H. Consideration of the parabolic radiography of the dental arch. *J Shimazu Stud*. 1933;10:13.
2. Paatero Y. The use of a mobile source of light in radiography. *Acta Radiol*. 1948;29:221.

3. Paatero Y. A new tomographic method for radiographing curved outer surfaces. *Acta Radiol*. 1949;32:177.
4. Tronje G, Welander U, McDavid WD, Morris CR. Image distortion in rotational panoramic radiography. I. General considerations. *Acta Radiol Diagn (Stockh)*. 1981;22:295-9.
5. Tronje G, Eliasson S, Julin P, Welander U. Image distortion in rotational panoramic radiography. II. Vertical distances. *Acta Radiol Diagn (Stockh)*. 1981;22:449-55.
6. Tronje G, Welander U, McDavid WD, Morris CR. Image distortion in rotational panoramic radiography. III. Inclined objects. *Acta Radiol Diagn (Stockh)*. 1981;22:585-92.
7. Wyatt DL, Farman AG, Orbell GM, Silveira AM, Scarfe WC. Accuracy of dimensional and angular measurements from panoramic and lateral oblique radiographs. *Dentomaxillofac Radiol*. 1995;24:225-31.
8. Mozzo P, Procacci C, Tacconi A, Martini PT, Andreis IA. A new volumetric CT machine for dental imaging based on the cone-beam technique: preliminary results. *Eur Radiol*. 1998;8:1558-64.
9. Loubele M, Bogaerts R, Van Dijck E, Pauwels R, Vanheusden S, Suetens P, *et al*. Comparison between effective radiation dose of CBCT and MSCT scanners for dentomaxillofacial applications. *Eur J Radiol.* 2009;71:461-8.
10. Proffit WR, Fields HW, Jr., Sarver DM. Contemporary Orthodontics. 4th ed. St.Lois, MO: Mosby Elsevier; 2007.
11. Kau CH, Richmond S, Palomo JM, Hans MG. Three-dimensional cone beam computerized tomography in orthodontics. *J Orthod.* 2005;32:282–93.
12. Mah JK, Huang JC, Choo H. Practical applications of cone-beam computed tomography in orthodontics. *J Am Dent Assoc*. 2010;141:7S-13S.
13. Pauwels R, Beinsberger J, Collaert B, Theodorakou C, Rogers J, Walker A, *et al*. Effective dose range for dental cone beam computed tomography scanners. *Eur J Radiol*. 2012;81:267-71.
14. Theodorakou C, Walker A, Horner K, Pauwels R, Bogaerts R, Jacobs R. Estimation of paediatric organ and effective doses from dental cone beam CT using anthropomorphic phantoms. *Br J Radiol*. 2012;85:153-60.

15. Alqerban A, Jacobs R, Souza PC, Willems G. In-vitro comparison of 2 cone-beam computed tomography systems and panoramic imaging for detecting simulated canine impaction-induced external root resorption in maxillary lateral incisors. *Am J Orthod Dentofacial Orthop*. 2009;136:764 e1-11.
16. Dudic A, Giannopoulou C, Leuzinger M, Kiliaridis S. Detection of apical root resorption after orthodontic treatment by using panoramic radiography and cone-beam computed tomography of super-high resolution. *Am J Orthod Dentofacial Orthop*. 2009;135:434-7.
17. Haney E, Gansky SA, Lee JS, Johnson E, Maki K, Miller AJ, *et al*. Comparative analysis of traditional radiographs and cone-beam computed tomography volumetric images in the diagnosis and treatment planning of maxillary impacted canines. *Am J Orthod Dentofacial Orthop*. 2010;137:590-7.
18. Leuzinger M, Dudic A, Giannopoulou C, Kiliaridis S. Root-contact evaluation by panoramic radiography and cone-beam computed tomography of super-high resolution. *Am J Orthod Dentofacial Orthop*. 2010;137:389-92.
19. Alqerban A, Jacobs R, Fieuws S, Willems G. Comparison of two cone beam computed tomographic systems versus panoramic imaging for localization of impacted maxillary canines and detection of root resorption. *Eur J Orthod*. 2011;33:93-102.
20. Botticelli S, Verna C, Cattaneo PM, Heidmann J, Melsen B. Two- versus three-dimensional imaging in subjects with unerupted maxillary canines. *Eur J Orthod*. 2011;33:344-9.
21. Bouwens DG, Cevidanes L, Ludlow JB, Phillips C. Comparison of mesiodistal root angulation with posttreatment panoramic radiographs and cone-beam computed tomography. *Am J Orthod Dentofacial Orthop*. 2011;139:126-32.
22. Ghaeminia H, Meijer GJ, Soehardi A, Borstlap WA, Mulder J, Vlijmen OJ, *et al*. The use of cone beam CT for the removal of wisdom teeth changes the surgical approach compared with panoramic radiography: a pilot study. *Int J Oral Maxillofac Surg*. 2011;40:834-9.

23. Anthonappa RP, King NM, Rabie AB, Mallineni SK. Reliability of panoramic radiographs for identifying supernumerary teeth in children. *Int J Paediatr Dent*. 2012;22:37-43.
24. Neves FS, Souza TC, Almeida SM, Haiter-Neto F, Freitas DQ, Bóscolo FN. Correlation of panoramic radiography and cone beam CT findings in the assessment of the relationship between impacted mandibular third molars and the mandibular canal. *Dentomaxillofac Radiol*. 2012;41:553-7.
25. Pittayapat P, Galiti D, Huang Y, Dreesen K, Schreurs M, Souza PC, *et al*. An in vitro comparison of subjective image quality of panoramic views acquired via 2D or 3D imaging. *Clin Oral Investig*. 2013;17:293-300.
26. van Vlijmen OJ, Kuijpers MA, Bergé SJ, Schols JG, Maal TJ, Breuning H, *et al*. Evidence supporting the use of cone-beam computed tomography in orthodontics. *J Am Dent Assoc*. 2012;143:241-52.
27. Liu DG, Zhang WL, Zhang ZY, Wu YT, Ma XC. Localization of impacted maxillary canines and observation of adjacent incisor resorption with cone-beam computed tomography. *Oral Surg Oral Med Oral Pathol Oral Radiol Endod*. 2008;105:91-8.
28. Walker L, Enciso R, Mah J. Three-dimensional localization of maxillary canines with cone-beam computed tomography. *Am J Orthod Dentofacial Orthop*. 2005;128:418-23.
29. Ericson S, Kurol J. Resorption of maxillary lateral incisors caused by ectopic eruption of the canines. A clinical and radiographic analysis of predisposing factors. *Am J Orthod Dentofacial Orthop*. 1988;94:503-13.
30. Ericson S, Kurol J. Radiographic examination of ectopically erupting maxillary canines. *Am J Orthod Dentofacial Orthop*. 1987;91:483-92.
31. Landis JR, Koch GG. The measurement of observer agreement for categorical data. *Biometrics*. 1977;33:159-74.
32. Peck JL, Sameshima GT, Miller A, Worth P, Hatcher DC. Mesiodistal root angulation using panoramic and cone beam CT. *Angle Orthod.* 2007;77:206-13.
33. Schmuth GP, Freisfeld M, Köster O, Schüller H. The application of computerized tomography (CT) in cases of impacted maxillary canines. *Eur J Orthod.* 1992;14:296-301.

34. Freisfeld M, Dahl IA, Jäger A, Drescher D, Schüller H. X-ray diagnosis of impacted upper canines in panoramic radiographs and computed tomographs. *J Orofac Orthop.* 1999;60:177-84.
35. Alqerban A, Jacobs R, Fieuws S, Nackaerts O; SEDENTEXCT Project Consortium, Willems G. Comparison of 6 cone-beam computed tomography systems for image quality and detection of simulated canine impaction-induced external root resorption in maxillary lateral incisors. *Am J Orthod Dentofacial Orthop*. 2011;140:e129-39.
36. European Commission. Guidelines on CBCT for Dental and Maxillofacial Radiology: Evidence Based Guidelines. Radiation Protection Publication 2012; Available from: http://www.sedentexct.eu/content/guidelines-cbct-dental-and-maxillofacial-radiology.
37. American Academy of Oral and Maxillofacial Radiology. Clinical recommendations regarding use of cone beam computed tomography in orthodontics. Position statement by the American Academy of Oral and Maxillofacial Radiology. *Oral Surg Oral Med Oral Pathol Oral Radiol*. 2013;116:238-57.

PART III

CEPHALOMETRIC IMAGING

Chapter 5

Accuracy of linear measurements using 3 imaging modalities: two lateral cephalograms and one 3D model from CBCT data

---

This chapter is based on:

Pittayapat P, Bornstein MM, Imada TSN, Coucke W, Lambrichts I, Jacobs R. Accuracy of linear measurements using 3 imaging modalities: two lateral cephalograms and one 3D model from CBCT data. *Eur J Orthod*. 2014. (in press)

5.1 Abstract

Background: The aim of this study was to evaluate the accuracy of linear measurements on 3 imaging modalities: lateral cephalograms from a cephalometric machine with a 3-meter source-to-mid-sagittal-plane distance (SMD), from a machine with 1.5-meter SMD and 3D models from CBCT data.

Materials and methods: Twenty-one dry human skulls were used. Lateral cephalograms were taken, using 2 cephalometric devices: one with a 3-meter SMD and one with a 1.5-meter SMD. CBCT scans were taken by 3D Accuitomo® 170 and 3D surface models were created in Maxilim® software. Thirteen linear measurements were completed twice by 2 observers with a 4-week interval. Direct physical measurements by a digital calliper were defined as the gold standard. Statistical analysis was performed.

Results: Nasion-Point A was significantly different from the gold standard in all methods. More statistically significant differences were found on the measurements of the 3-meter SMD cephalograms in comparison to the other methods. Intra- and inter-observer agreement based on 3D measurements were slightly better than others.

Limitations: Dry human skulls without soft tissues were used. Therefore, the results have to be interpreted with caution, as they do not fully represent clinical conditions.

Conclusions: 3D measurements resulted in a better observer agreement. The accuracy of the measurements based on CBCT and 1.5-meter SMD cephalogram was better than a 3-meter SMD cephalogram. These findings demonstrated the linear measurements accuracy and reliability of 3D measurements based on CBCT data when compared to 2D techniques. Future studies should focus on the implementation of 3D cephalometry in clinical practice.

5.2 Introduction

A cephalometric analysis is a key element in orthodontic diagnostics. First introduced by Hofrath in Germany and Broadbent in the United States, this radiographic technique has been widely accepted as a standard tool for orthodontic treatment planning (1, 2). Traditionally, the technique is performed on a two-dimensional lateral cephalogram, which does not represent the full dimensions of the human face, and also has disadvantages such as geometric distortion and superimposition of anatomical structures. In the past, a cephalogram with a long distance between X-ray source and mid-sagittal plane of the patient's face (3 to 4 meters) was used. This type of machine allows more parallel X-ray beams, leading to less magnification of the images and possibly less radiation dose to the patient, when paired with sensitive image receptors (3-6). Today, most of the machines on the market combine panoramic and cephalometric radiographic options within one single device. The design of these machines is more compact, which allows for a 1.5-meter distance between the X-ray source and the mid-sagittal plane of the patient's face (7).

In recent years, 3D imaging modalities, especially cone-beam computed tomography (CBCT), have played an important role in dentistry because of lower radiation doses compared to the multi-slice CT (MSCT) and their availability in the dental offices (8). In orthodontics, 3D images have overcome the obstacle of 2D images by allowing orthodontists to visualize craniofacial structures without superimposition and distortion (9-11). Several publications have shown that the accuracy of 3D measurements is good or even superior to the measurements performed on lateral cephalograms (12-15). However, no investigation has directly compared the measurements from both left and right sides of the images. Furthermore, no study has compared measurements on images from a traditional cephalometric device with a long source-to-mid-sagittal-plane distance (SMD).

The aim of this study was to evaluate the accuracy of linear measurements on 3 different imaging modalities for cephalometric analysis: lateral cephalograms from a cephalometric device with a 3-meter SMD, lateral cephalograms from a device with a 1.5-meter SMD, and 3D models from cone-beam computed tomographic data.

5.3 Materials and methods

Sample

In total, 21 dry human skulls with present upper and lower first incisors and first molars were collected from the Department of Anatomy, Hasselt University, Diepenbeek, Belgium. Mandibles were attached to the skulls by taping around them starting from the temporal area of one side to the other. The occlusion was fixed at the maximum intercuspation. The study protocol (reference number: ML6960, BE322201010078) was approved by the UZ Leuven Medical Ethics Committee.

Imaging modalities

Three sets of radiographic images, 2 different types of lateral cephalograms and 1 CBCT, were acquired. First, lateral cephalograms of the dry skulls were taken by a 3-meter SMD cephalometric machine with DX104 Comet tube (COMET, 3175 Flamatt, Switzerland; 70 kVp, 32-40 mAs) at the University of Bern, Bern, Switzerland. Photostimulable phosphor plates, size 24x30 cm (Digora PCT system, Soredex, Tuusula, Finland) were used as image receptors. Second, lateral cephalograms were taken on the same samples by a digital cephalometric device with 1.5-meter SMD equipped with complementary metal-oxide-semiconductor (CMOS) sensor (Cranex® 3D, Soredex, Tuusula, Finland; 81 kVp, 10 mA, 16 sec). The dry skulls were placed in both devices and fixed with ear rods. The Frankfort horizontal plane was adjusted to be parallel to the floor. Left and right sides were recorded by the main operator according to the anatomical structures without placing any radiopaque markers on the skulls during image acquisition. Last, CBCT scans were taken on the same skulls with a CBCT device (3D Accuitomo® 170, J. Morita, Kyoto, Japan) with the largest field of view: diameter 170 x height 120 mm (High-Fidelity / Hi-Fi mode: 90 kVp, 154 mAs, voxel size 0.25 mm.). A 1.7 mm thick copper filter was attached to the machine during image acquisition to simulate soft tissue attenuation.

The two sets of lateral cephalograms were exported and stored in TIFF. The radiographs were then imported to Adobe® Photoshop CS4 (Adobe Systems Incorporated, San José, CA, USA) and prepared for observation. A letter “L” was placed on each image (both 1.5-meter SMD group and 3-meter SMD group) close to the angle of mandible to indicate the left side (Fig. 5.1). CBCT data were exported to DICOM then imported to Maxilim® software (Medicim NV, Sint-Niklaas, Belgium). 3D surface models were created for all samples.

Cephalometric measurements

Ten cephalometric landmarks (Table 5.1) resulting in a total of thirteen cephalometric linear measurements were included in this study (Table 5.2). Linear measurements including lateral landmarks were performed on both right and left sides.

The measurements of 2D lateral cephalometric groups: 1.5-meter SMD group and 3-meter SMD group, were done on Adobe® Photoshop CS4 (Fig. 5.2). The digital cephalograms were calibrated by means of visible rulers and ear rods in the images. For the 3D group, all measurements were performed on Maxilim® software (Fig. 5.2).

Two observers (dentomaxillofacial radiologists with more than 5 years of experience, one being the main operator) were initially calibrated in a separate session. Detailed instructions over the landmark definitions and software manipulation were given intensively. The observers completed each set of measurements twice with a 4-week interval.

Gold standard

Direct physical measurements of all 13 measurements were done on the skulls 3 times by the main operator using a digital calliper (ABSOLUTE® digimatic calliper, Mitutoyo, Kawasaki, Japan) and were regarded as a gold standard.

Table 5.1 Definition of the cephalometric landmarks used in the present study

Landmark	Abbreviation	Definition
Nasion	N	The midpoint of the frontonasal suture
Anterior Nasal spine	ANS	The most anterior midpoint of the anterior nasal spine of the maxilla
Point A	A	The point of maximum concavity in the midline of the alveolar process of the maxilla
Point B	B	The point of maximum concavity in the midline of the alveolar process of the mandible
Menton	Me	The most inferior midpoint of the chin on the outline of the mandibular symphysis
Posterior Nasal spine	PNS	The most posterior midpoint of the posterior nasal spine of the palatine bone
Basion	Ba	The most anterior point of the foramen magnum
Sigmoid notch	SmN	The most concave point of each sigmoid notch of the mandible
Gonion	Go	The point at each mandibular angle that is defined by dropping a perpendicular from the intersection of the tangent lines to the posterior margin of the mandibular vertical ramus and inferior margin of the mandibular body to horizontal ramus
Condylion	Co	The most superior point of each mandibular condyle

Table 5.2 Definition of the cephalometric linear measurements performed in the present study

Linear measurement	Definition
N-ANS	Distance in mm between N and ANS
N-A	Distance in mm between N and A
N-B	Distance in mm between N and B
N-Me	Distance in mm between N and Me
ANS-Me	Distance in mm between ANS and Me
ANS-PNS	Distance in mm between ANS and PNS
Ba-PNS	Distance in mm between Ba and PNS
SmN-Go (right and left)	Distance in mm between SmN and Go of each side
Go-Co (right and left)	Distance in mm between Go and Co of each side
Go-Me (right and left)	Distance in mm between Go and Me of each side

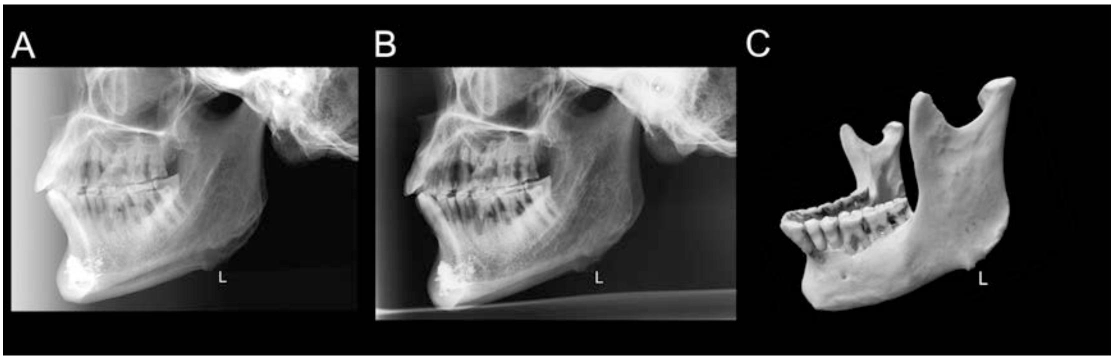

Figure 5.1 A letter "L" was placed on the image close to the angle of the mandible to indicate the left side. A) a lateral cephalogram from a cephalometric device with 1.5-meter SMD; B) a lateral cephalogram from a cephalometric device with 3-meter SMD. C) a photograph of the same mandible as on the images.

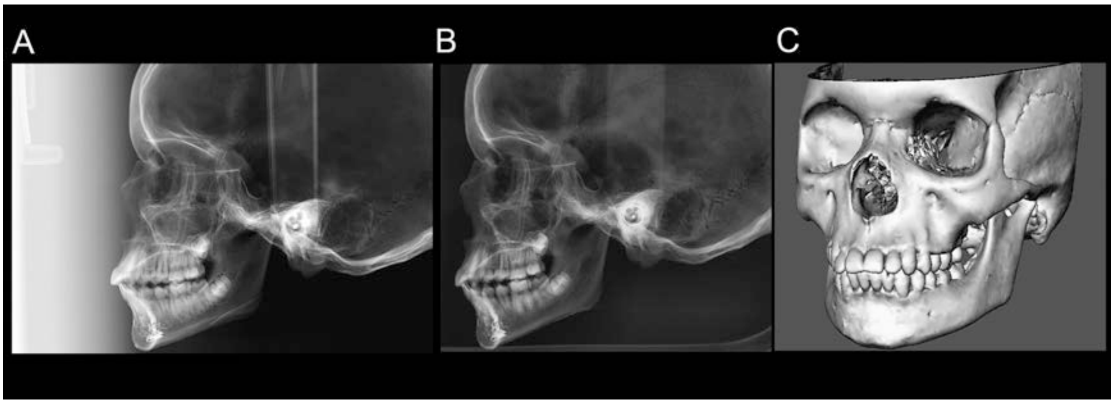

Figure 5.2 Examples of images from all radiographic devices used in the present study: A) lateral cephalogram from a cephalometric device with 1.5-meter SMD with a visible ruler that was used for image calibration; B) lateral cephalogram from a cephalometric device with 3-meter SMD. In this image, the diameter of the ear rod was used for image calibration; C) 3D surface model constructed from CBCT data, viewed on Maxilim® software. 3D measurements were performed by placing digital landmarks on the model. Subsequently, the software calculated the preset linear measurements and the values were recorded.

Statistical analysis

All data were placed in Excel files. Statistical analysis was performed with R 2.14 software© for Windows (R Development Core Team, ©R Foundation for Statistical Computing, Vienna, Austria).

The accuracy of the measurements was evaluated, comparing each cephalometric method with the gold standard. The *measurement accuracy* was defined as the closeness of the measured value to the gold standard value. The *measurement reliability* was also tested, reflecting the variability of the repeated measurements by the same or different observers.

First, the mean value of three measurements of the gold standard was calculated and the same was done for the two datasets of the two observers. Subsequently, a linear least-squares regression model was built between the gold standard and each of the cephalometric methods, and orthogonal linear regression models were used to compare each data set of the two cephalometric methods.

The inter- and intra-observer variability of the cephalometric methods was evaluated by means of linear mixed models. The gold standard was taken as an explanatory variable, the observer as a random factor and the measurements obtained by the different observers as dependent variables.

5.4 Results

Summary statistic was performed and the results are shown in Table 5.3. The biggest deviation can be observed on Go-Me (Table 5.3).

Comparison with the gold standard

3D measurements showed statistically significant differences (p<0.05) from the gold standard for N-A and SmN-Go left. A statistically significant difference (p<0.05) of N-A measurement was found for the 1.5-meter SMD group. For lateral cephalogram with 3-meter SMD, statistically significant differences (p<0.05) were observed for N-A, N-B, N-Me, Go-Me right, Go-Me left and Go-Co left measurements (Table 5.4).

Comparison between cephalometric techniques

When comparing 3D measurements with measurements on both 2D cephalograms, statistically significant differences (p<0.05) were found for all measurements except N-ANS. When comparing between measurements on the 1.5-meter SMD group and 3-meter SMD group, all measurements were statistically significantly different (p<0.05).

Table 5.3 Summary statistics showing the results of the cephalomertic measurements (in mm) of the three radiographic modalities and the gold standard: a deviation of more than 5 mm from the gold standard was found for measurements on 2D lateral cephalograms, involving both midline and lateral landmarks (Go-Me).

Measurements	Gold standard				3-meter SMD group				1.5-meter SMD group				3D group			
	Ave	SD	Min	Max	Ave	SD	Min	Max	Ave	SD	Min	Max	Ave	SD	Min	Max
N-ANS	44.95	3.66	37.70	50.94	43.99	3.55	36.45	51.13	44.48	3.59	36.75	52.09	45.42	3.66	37.40	52.30
N-A	50.15	4.51	41.53	58.10	48.10	3.70	40.28	56.74	48.97	3.84	40.44	55.82	49.98	4.02	41.90	57.30
N-B	86.78	7.95	70.49	99.55	83.74	7.12	68.38	97.20	85.06	7.55	69.77	99.24	85.35	7.70	69.30	100.00
N-Me	103.97	10.32	86.08	122.47	102.39	9.80	84.14	121.29	103.49	10.05	84.90	122.65	104.43	9.94	85.70	122.60
ANS-Me	60.74	7.64	47.91	73.66	60.00	7.35	46.04	73.98	60.81	7.60	47.18	74.61	60.46	7.48	47.00	74.70
ANS-PNS	48.07	2.68	43.57	53.85	44.98	2.89	39.88	53.56	47.12	2.89	41.74	53.03	47.28	2.85	41.70	53.30
Ba-PNS	40.73	3.46	34.73	47.42	42.02	6.02	34.79	73.53	41.93	3.73	34.32	52.04	41.08	3.41	35.20	47.90
SmN-Go right	38.13	5.31	27.92	47.31	36.66	6.25	25.03	67.02	36.56	5.02	26.28	47.08	37.89	5.14	27.20	47.60
SmN-Go left	38.81	5.20	28.25	48.83	37.51	6.09	24.85	67.02	38.96	5.93	27.85	61.24	37.70	4.94	27.60	47.70
Go-Co right	51.54	6.00	37.86	59.44	48.12	6.10	36.74	59.60	49.45	5.81	36.65	61.04	50.56	6.01	35.10	60.50
Go-Co left	52.52	6.65	38.69	64.37	49.12	5.94	36.74	62.89	51.51	6.67	37.34	66.47	50.16	6.31	33.90	61.70
Go-Me right	77.71	6.43	64.52	88.83	62.80*	5.61	49.65	75.97	64.17*	5.86	52.84	75.92	77.86	6.94	62.80	92.20
Go-Me left	76.70	6.43	63.42	88.82	61.89*	5.43	49.89	75.18	63.56*	6.19	49.66	75.95	77.86	7.10	62.80	95.70

*Measurements > 5 mm different from the gold standard

Table 5.4 Comparison of linear measurements using radiographic data with the gold standard: statistically significant differences (defined as $p<0.05$) of N-A were observed for all modalities. The measurements of the 3-meter SMD group showed more significant differences than the other 2 imaging groups.

Measurements	3-meter SMD group		1.5-meter SMD group		3D group	
	p-value of Intercept	*p*-value of Slope	*p*-value of Intercept	*p*-value of Slope	*p*-value of Intercept	*p*-value of Slope
N-ANS	0.624	0.361	0.588	0.453	0.57	0.696
N-A	0.004*	0.001*	0.014*	0.006*	0.028*	0.026*
N-B	0.065	0.01*	0.163	0.08	0.496	0.327
N-Me	0.2	0.038*	0.323	0.261	0.13	0.193
ANS-Me	0.51	0.199	0.424	0.439	0.994	0.735
ANS-PNS	0.607	0.813	0.504	0.4	0.243	0.376
Ba-PNS	0.522	0.672	0.227	0.346	0.534	0.789
SmN-Go right	0.547	0.333	0.519	0.175	0.202	0.163
SmN-Go left	0.405	0.253	0.706	0.668	0.141	0.04*
Go-Co right	0.797	0.298	0.606	0.295	0.748	0.51
Go-Co left	0.091	0.017*	0.486	0.354	0.364	0.099
Go-Me right	0.98	0.006*	0.598	0.056	0.209	0.195
Go-Me left	0.664	0.003*	0.611	0.166	0.242	0.158

* $p<0.05$

Observer agreement

Inter- and intra-observer variability of the 3D measurements was expressed as a percentage of coefficients of variability (CV). Inter-observer variability of 3D measurements (5.7%) was lower than the other methods (6.5% for 3-meter SMD and 6.1% for 1.5-meter SMD cephalograms), which could be interpreted as a higher reproducibility for the measurements using CBCT images. For intra-observer variability, CV of 3D was shown to be between 2.4-3%, and also lower than the 2D methods (2.9-6% for 3-meter SMD and 3.6-4.1% for 1.5-meter SMD cephalograms). Therefore, the intra-observer agreement of 3D measurements was better than the two 2D measurements from both cephalometric devices.

5.5 Discussion

In the present study, the accuracy of linear measurements using 3 different types of imaging modalities for cephalometry was assessed and comparisons of measurements among the techniques were performed. Although there are several publications that have evaluated the accuracy and compared measurements between 2D and 3D imaging techniques, there is, to the best of our knowledge, no publication in English that included cephalograms from a 3-meter source-to-image-receptor distance.

Dry human skulls were used as *in vitro* subjects in this study to account for the fact that several different imaging modalities had to be taken on the same samples, and thus it was unethical to use patients for this type of study. Although the skulls could not represent real human anatomy including soft tissues, this model offered some advantages. Direct measurements on hard tissue were possible unlike using real human subjects, and these were later used as gold standard. A 1.7 mm thick copper filter was used to mimic soft tissue attenuation during image acquisition to prevent any overexposures.

Cephalometric landmarks selected for this study included midline landmarks and lateral landmarks, both on the right and left side. Although only 1 measurement will be used for a lateral cephalogram in clinical situations, measurements of both sides were used in the present investigation in order to directly compare 3D with 2D measurements. No fiducial marker was placed prior to image acquisition. This was done in order to mimic the real clinical situation, as landmark identification is one of the variables affecting the intra- and inter-observer agreement. With marker placement in an experiment, this clinical observer bias might be largely eliminated.

Considering the imaging modalities used in the present study, 2D and 3D images are different in nature. 2D imaging systems, in this study the lateral cephalograms, are based on projecting shadows of anatomical structures on the image receptors. In 2D, structures aligned obliquely to the image receptor will result in distorted shadows on lateral cephalograms. These shadows are usually measured and used for cephalometric analysis. In this study, the effect of the SMD distance of two devices was evaluated, yet another factor that might influence magnification of 2D cephalometric radiographs is the distance from the mid-sagittal plane to the image receptor. In the current experimental set-up, both machines had a very similar 15 cm distance from the mid-sagittal plane to the image receptor, minimizing this secondary magnification bias.

On the other hand, for the 3D modality (CBCT), the image data were acquired and quantified in voxels, forming a realistic volume, which is definitely different from the 2D projection. This is one of the biggest advantages of 3D over the 2D imaging as it can capture structures with their real dimensional relationship. As a result, 3D image data, representing anatomical structures without any geometric distortion, can be measured. The linear distances in this study were defined as direct distances on 3D models, not orthogonal distances or distances created by projecting a 3D structure on a plane, which is the principle of 2D lateral cephalography. The purpose of this study design was to compare the measurements on 2D and 3D imaging modalities using their full capacity. Thus, a comparison of measurements by creating 2D projections from 3D data was avoided. Therefore, measurements with lateral landmarks are expected to exhibit the most pronounced differences between 2D and 3D imaging, which was demonstrated by Go-Me values on lateral cephalograms that significantly deviated from the gold standard and 3D measurements in the present study.

For the accuracy evaluation, it was found that the accuracy of measurements on 3-meter SMD cephalograms was lower than the other two groups with 6 measurements exhibiting statistically significant differences when compared to the gold standard (Table 5.3). There was no English publication found to directly compare the results of the present study, but it was found in a few publications that the accuracy of 3D measurements was better than measurements on lateral cephalograms (16-18). In 2010, Varghese *et al*. published results on the accuracy of CT and digital cephalometric measurements. The results showed the accuracy of CT measurements was better than the 2D lateral cephalograms (16). Olmez *et al*. found that there were no significant differences between the computer-assisted 3D and physical measurements, while the 2D measurements showed significant differences when compared to the physical measurements (17). Gribel *et al*. investigated the accuracy and reliability of measurements on lateral cephalograms and CBCT (18). No statistically significant difference was found between CBCT measurements and the gold standard. However, for the lateral cephalograms, all measurements were statistically significantly different from the gold standard (18).

N-A was the only measurement that was statistically significantly different from the gold standard for all types of imaging techniques. This can be explained from previous studies published on landmark identification. It has been demonstrated in other investigations that point A (Table 5.1) was less reliable in terms of landmark identification (19-22). The position of the landmark situated on a curved surface such as the concavity of the alveolar process for point A may affect the accuracy of the identification more than a landmark situated on a small pointed area like ANS (19). This surely affected the accuracy of linear measurements in this study, when one of the landmarks was less reliable and more difficult to define or prone to subjectivity. Interestingly, Perillo *et al*. stated that the lack of precision in identification of landmarks might not, on average, preclude cephalometric diagnosis (20).

It was speculated at the beginning of the study that measurements involving both a midline landmark (Me) and a lateral landmark (Go) would result in a statistically significant difference when compared to the gold standard. However, the results of the present study showed significant differences only for the 3-meter SMD cephlometric group, but not for the 1.5-meter SMD group. Table 5.3 shows deviations of the measurements of the 1.5-meter SMD group from the gold standard values, but when the regression model was applied, the results were not statistically significant except for the N-A measurements (Table 5.4).

The comparison of all techniques with each other showed significant differences in almost all measurements in all pairs of techniques. This could mean that although the measurements were accurate when comparing to the gold standard, the measurements were actually significantly different when comparing between the techniques. As shown in Table 5.3, some measurements including the lateral landmarks were highly deviated among cephalometric techniques but when compared to the gold standard, the result was not statistically significantly different.

The results of the 3-meter SMD cephalometric group were rather unexpected because the system should have provided a less to none magnified lateral cephalogram, thus the midline measurements should have been close to those obtained from gold standard physical measurements. One reason that could help explain this circumstance was the quality of the phosphor imaging plate. From the exposure parameter applied to the device, it did not give the image optimal brightness, contrast and sharpness. This might have affected the landmark identification process. The images were calibrated properly by using the diameter of the ear rod as a reference - so this could be excluded as a possible factor affecting the measurement values.

The results of this study showed that the observer agreement of measurements on 3D models was slightly superior to the agreement of measurements on 2D lateral cephalograms, regardless of the type of the cephalometric device. This finding was in line with results published by previous studies. A study done by Gribel *et al*. showed that measurements on 3D images (intraclass correlation coefficient (ICC) = 0.99) were as reliable as the measurements on 2D images (ICC = 0.98) (18). On the other hand, Damstra *et al*. found the ICC of the 2D measurements on lateral cephalograms (ICC > 0.97) to be higher than the ICC of 3D measurements (ICC > 0.88), but there was no statistically significant difference between the two methods (23).

Although in a study by Van Vlijmen *et al*., the result was in the opposite direction (24). It was found that the intra-observer reliability of the measurements on the conventional cephalometric radiographs was higher compared with the intra-observer reliability of measurements on the 3D models. The authors suggested 2 factors possibly affecting the results: the learning curve in 3D tracing and the added third dimension of the image (24). In the present study, an intensive calibration of the observers was performed prior to the measurements, in order to be familiar with the software and landmark definition both in 2D and 3D. The results were therefore improved.

The results of the present investigation showed that inter-observer agreement is lower than the intra-observer agreement. This was expected, as observer performance can be affected by several factors such as background experiences, the familiarity of the observers to the software and the ability to identify landmarks according to the definitions. A calibration session was conducted prior to the observation to minimize the effect of these factors.

To acquire CBCT images on real patients, dental CBCT examinations should be fully justified over conventional X-ray imaging and dose optimisation by field of view (FOV) collimation and low dose settings should be achieved (8, 25). Large FOV CBCTs should be used only when full indication and justification for the benefit of the patient is applied, as the radiation dose received from the CBCTs is strongly related to FOV size and also dependent on the specific CBCT machine (8). Recent guidelines on orthodontic use of CBCT imaging were published by the American Academy of Oral and Maxillofacial Radiology (AAOMR) (26). Furthermore, guidelines and recommendations on CBCT use for dental and maxillofacial radiology have been made available by the European Commission to offer clinicians and orthodontists some guidance and recommendations (27). In general, the selection of radiographic imaging should be based on initial clinical evaluation and must be justified based on individual need without being considered “routine” (26, 28). Especially when treating children and young adults, the decision to perform a CBCT examination must be based on the patient’s history, clinical examination, available radiographic imaging, and the presence of a clinical condition for which the benefits of the diagnosis and/or treatment plan outweigh the potential risks of exposure to radiation (26, 28). Therefore, 3D cephalometric analysis and 3D orthodontic treatment planning should only be performed when their benefits to the patients in specific cases can overcome the radiation risk.

5.6 Conclusions

This study has confirmed the knowledge on the accuracy of linear cephalometric measurements of 2D and 3D images. Although the results did not show that 3D measurements were more accurate than the 2D standard digital lateral cephalograms (1.5-meter SMD), the results did confirm that 3D measurements were more reliable than measurements on 2D images.

5.7 References

1. Hofrath H. Bedeutung der Röntgenfern und Abstands Aufnahme für die Diagnostik der Kieferanomalien. *Fortschr Orthod*. 1931;1:231-58.
2. Broadbent BH. A new x-ray technique and its application to orthodontia. *Angle Orthod*. 1931;1:45-66.
3. Bourriau J, Bidange G, Foucart JM. Les erreurs de mesure en céphalométrie 2D. *Orthod Fr.* 2012;83:23-36.
4. Jacobs R, Velders XL. Pre-implantair röntgendiagnostiek. Handboek voor Tandheelkundige Praktijk 1997. p. C37-I.
5. Gijbels F, Sanderink G, Wyatt J, Van Dam J, Nowak B, Jacobs R. Radiation doses of collimated vs non-collimated cephalometric exposures. *Dentomaxillofac Radiol*. 2003;32:128–33.
6. Gonzalez L, Fernandez R, Ziraldo V, Vano ER. Reference level for patient dose in dental skull lateral teleradiography. *Br J Radiol*. 2004;77:735–9.
7. Proffit WR, Fields HW, Jr., Sarver DM. Contemporary Orthodontics. 4th ed. St.Lois, MO: Mosby Elsevier; 2007.
8. Pauwels R, Beinsberger J, Collaert B, Theodorakou C, Rogers J, Walker A, *et al*. Effective dose range for dental cone beam computed tomography scanners. *Eur J Radiol*. 2012;81:267-71.
9. Kau CH, Richmond S, Palomo JM, Hans MG. Three-dimensional cone beam computerized tomography in orthodontics. *J Orthod*. 2005;32:282-93.
10. Mah, JK, Huang, JC, Choo H. Practical applications of cone-beam computed tomography in orthodontics. *J Am Dent Assoc*. 2010;141:7S-13S.

11. van Vlijmen OJ, Kuijpers MA, Bergé SJ, Schols JG, Maal TJ, Breuning H, *et al*. Evidence supporting the use of cone-beam computed tomography in orthodontics. *J Am Dent Assoc*. 2012;143:241-52.
12. Cavalcanti MG, Rocha SS, Vannier MW. Craniofacial measurements based on 3D-CT volume rendering: implications for clinical applications. *Dentomaxillofac Radiol*. 2004;33:170-6.
13. Periago DR, Scarfe WC, Moshiri M, Scheetz JP, Silveira AM, Farman AG. Linear accuracy and reliability of cone beam CT derived 3-dimensional images constructed using an orthodontic volumetric rendering program. *Angle Orthod*. 2005;78:387-95.
14. Brown AA, Scarfe WC, Scheetz JP, Silveira AM, Farman AG. Linear accuracy of cone beam CT derived 3D images. *Angle Orthod*. 2009;79:150-7.
15. Pittayapat P, Limchaichana-Bolstad N, Willems G, Jacobs R. Three-dimensional cephalometric analysis in orthodontics: a systematic review. *Orthod Craniofac Res*. 2014;17:69-91.
16. Varghese S, Kailasam V, Padmanabhan S, Vikraman B, Chithranjan A. Evaluation of the accuracy of linear measurements on spiral computed tomography-derived three-dimensional images and its comparison with digital cephalometric radiography. *Dentomaxillofac Radiol*. 2010;39:216-23.
17. Olmez H, Gorgulu S, Akin E, Bengi AO, Tekdemir I, Ors F. Measurement accuracy of a computer-assisted three-dimensional analysis and a conventional two-dimensional method. *Angle Orthod*. 2011;81:375-82.
18. Gribel BF, Gribel MN, Frazao DC, McNamara JA, Jr, Manzi FR. Accuracy and reliability of craniometric measurements on lateral cephalometry and 3D measurements on CBCT scans. *Angle Orthod*. 2011;81:28-37.
19. Baumrind S, Frantz RC. The reliability of head film measurements. 1. Landmark identification. *Am J Orthod*. 1971;60:111-27.
20. Perillo M, Beideman R, Shofer F, Jacobsson-Hunt U, Higgins-Barber K, Laster L, Ghafari J. Effect of landmark identification on cephalometric measurements: guidelines for cephalometric analyses. *Clin Orthod Res*. 2000;3:29-36.

21. Kazandjian S, Kiliaridis S, Mavropoulos A. Validity and reliability of a new edge-based computerized method for identification of cephalometric landmarks. *Angle Orthod*. 2006;76:619-24.
22. Chien PC, Parks ET, Eraso F, Hartsfield JK, Roberts WE, Ofner S. Comparison of reliability in anatomical landmark identification using two-dimensional digital cephalometrics and three-dimensional cone beam computed tomography in vivo. *Dentomaxillofac Radiol*. 2009;38:262-73.
23. Damstra J, Fourie Z, Ren Y. Comparison between two-dimensional and midsagittal three-dimensional cephalometric measurements of dry human skulls. *Br J Oral Maxillofac Surg*. 2011;49:392-5.
24. van Vlijmen OJ, Maal T, Berge SJ, Bronkhorst EM, Katsaros C, Kuijpers-Jagtman AM. A comparison between 2D and 3D cephalometry on CBCT scans of human skulls. *Int J Oral Maxillofac Surg*. 2010;39:156-60.
25. Theodorakou C, Walker A, Horner K, Pauwels R, Bogaerts R, Jacobs R, Consortium SP. Estimation of paediatric organ and effective doses from dental cone beam CT using anthropomorphic phantoms. *Br J Radiol*. 2012;85, 153-60.
26. American Academy of Oral and Maxillofacial Radiology. Clinical recommendations regarding use of cone beam computed tomography in orthodontic treatment. Position statement by the American Academy of Oral and Maxillofacial Radiology. *Oral surg Oral med Oral pathol Oral radiol*. 2013;116:238-57.
27. European Commission. Guidelines on CBCT for Dental and Maxillofacial Radiology: Evidence Based Guidelines. Radiation Protection Publication 2012; Available from: http://www.sedentexct.eu/content/guidelines-cbct-dental-and-maxillofacial-radiology.
28. American Dental Association Council on Scientific Affairs. The use of cone-beam computed tomography in dentistry: an advisory statement from the American Dental Association Council on Scientific Affairs. *J Am Dent Assoc*. 2012;143:899-902.

Chapter 6

Reproducibility of sella turcica landmark in 3 dimensions using a sella turcica specific reference system

This chapter is based on:

Pittayapat P, Jacobs R, Odri G, Vasconcelos KdeF, Willems G, Olszewski R. Reproducibility of sella turcica landmark in 3 dimensions using a sella turcica specific reference system. *Submitted.*

6.1 Abstract

Objective: To assess the reproducibility of sella turcica landmark in 3 dimensions by using a new sella turcica specific landmark reference system.

Materials and methods: Thirty-two cone-beam computed tomographic scans (3D Accuitomo® 170) were retrospectively collected. The three-dimensional (3D) data were exported into DICOM and imported to Maxilim® software to create 3D surface models. Five observers identified four osseous landmarks to create the reference frame and then identified two sella turcica landmarks. Coordinates (x, y, z) of each landmark were exported. The observations were repeated after 4 weeks. Statistical analysis was performed.

Results: The intra-observer mean precision of all landmarks was < 1 mm. For the sella turcica landmarks, intra-observer mean precision ranged from 0.43 (SD 0.34) mm – 0.51 (SD 0.46) mm. The intra-observer reproducibility was generally good. The overall inter-observer mean precision was < 1 mm. Inter-observer reproducibility of sella turcica landmarks was good with > 50% of the precision in locating the landmark below 1 mm.

Conclusions: A newly developed reference system offers high precision and reproducibility for sella turcica identification in 3 dimensions. This method has the potential to increase the reliability of the whole cephalometric analysis and other angular measurements related to the sella point.

6.2 Introduction

A cephalometric analysis is an essential part of the orthodontic treatment planning. One analysis is comprised of several cephalometric landmarks. Longitudinal growth evaluation of an individual and orthodontic treatment outcome can be assessed through superimposition of structures on the lateral cephalogram.

The sella turcica landmark is one of the most commonly used cephalometric landmarks. This landmark is located at the center of the pituitary fossa in the cranial base. The morphology of the sella turcica has been described by several authors (1-7). Literature showed that there are variations in the shape and size of the sella turcica in adults (7). The sella turcica can be classified into 3 segments: an anterior wall, the floor and the posterior wall (dorsum sellae). The shape can vary from round, oval, which are the most common, and flat (1).

Traditionally, cephalometric tracing is performed on a lateral cephalogram. The technique was first introduced by Hofrath (8) in Germany and Broadbent (9) in the United States. Although the technique was widely accepted as a standard tool for orthodontic treatment planning for several decades, it has shown several disadvantages because of the geometric distortion and superimposition of structures on the radiographs.

Recently, 3D imaging modalities such as computed tomography (CT) and cone-beam computed tomography (CBCT) have played an important role in dentistry. CBCT offers relatively lower radiation doses than multi-slice CT (MSCT) (10); therefore, it has become very popular for maxillofacial diagnosis and treatment planning. In orthodontics, 3D images allow orthodontists to visualize craniofacial structures in 3 dimensions without the superimposition of anatomical structures (11-13). This modality proves to be useful in several orthodontic aspects, one of which is the three-dimensional cephalometry.

3D cephalometry offers orthodontists the opportunity to identify cephalometric landmarks in 3 dimensions with the aid of the 3D image viewing software (14,15). Several publications have shown the advantages of this technique over the traditional 2D cephalometric analysis especially for the accuracy of the measurements (16,17) and the landmark identification reproducibility (18-20).

In 3D maxillofacial software, the sella point is usually identified based on 2D cephalometric images generated from 3D data either from CT or CBCT (14). In literature, it was shown that the results of sella point identification in this technique was good (21-23); however, a question was raised whether the sella landmark identified on the generated 2D image truly refers to the real 'geometric center' of the sella turcica especially in the situation where the shape of the sella turcica is not within normal range. No solid method on how to identify the sella turcica, which is a floating landmark in nature, on real 3D surface models was published (20). Therefore, the aim of this study was to assess the reproducibility of identifying the sella turcica landmark in three dimensions by using a newly developed reference system.

6.3 Materials and methods

The study protocol (reference number: ML6960, BE322201010078) was approved by the UZ Leuven Medical Ethics Committee. The authors have read the Helsinki Declaration and have followed the guidelines in this investigation.

Thirty-two patients (11 males and 21 females, age range 8.8-76.7 years (mean 26.0, SD 21.6 years) were retrospectively selected from the hospital database. The selection criteria were: (1) Patients with CBCT images; (2) The sella turcica was present in the images; (3) No significant pathology of the maxillofacial region; (4) No significant asymmetry of the face; (5) No significant anatomical variation at the sella turcica and sphenoidal region.

The CBCT scans of each patient were taken with 3D Accuitomo® 170 (J. Morita, Kyoto, Japan) with the minimum field of view (FOV) of 140 x 100 mm (90 kVp, mAs, voxel size 0.25 mm.) CBCT data were exported from i-Dixel® software (J. Morita, Kyoto, Japan) in digital imaging and communications in medicine (DICOM) format and then imported into Maxilim® software (Medicim NV, Sint-Niklaas, Belgium). 3D surface models for all subjects were created using full CBCT volume with 0.5 mm sub-sampling of voxels. The threshold was set between 276 and 476 to segment the hard tissues for the 3D models. The models were then saved and randomized.

Reference frame

A reference system was created in Maxilim® software with the purpose to identify the geometric center or mid-point of the sella turcica. The reference frame was composed of 6 landmarks (4 operator-indicated landmarks, 2 software-calculated landmarks) and 2 sella turcica landmarks which were indicated on 2 different vertical planes, created from the reference system (Table 6.1) (Fig. 6.1).

Table 6.1 Landmarks used in this reference system with their definitions

Landmarks	Definition
Anterior clinoid process right (ACP-R)	The tip of anterior clinoid process of the right side
Anterior clinoid process left (ACP-L)	The tip of anterior clinoid process of the left side
Apex of the petrous part of the temporal bone right (APT-R)	The apex of the petrous part of the temporal bone of the right side
Apex of the petrous part of the temporal bone light (APT-L)	The apex of the petrous part of the temporal bone of the left side
Mid ACP	A point in the middle between right and left ACP indicated by the software
Mid APT	A point in the middle between right and left APT indicated by the software
Sella turcica on a plane through Mid ACP (Sella 1)	The sella turcica identified on a vertical plane that passed through Mid ACP and perpendicular to a plane created by Mid ACP, APT-R and APT-L
Sella turcica on a plane through Mid APT (Sella 2)	The geometric center of the sella turcica identified on a vertical plane that passed through Mid APT and perpendicular to a plane created by Mid APT, ACP-R and ACP-L

Image evaluation

Five observers (two 3rd year orthodontic residents, two dentomaxillofacial radiologists with 5 and 8 years experience and one maxillofacial surgeon with 20 years experience) were initially introduced to an instruction and calibration session that allowed the observers to understand the definitions of landmarks and to be familiar with the software.

During the observation, the observers had to identify 6 landmarks (Table 6.1). Coordinates (x, y, z) of each landmark were exported to Excel files. The observation was repeated after 4 weeks to provide the data for intra-observer evaluation.

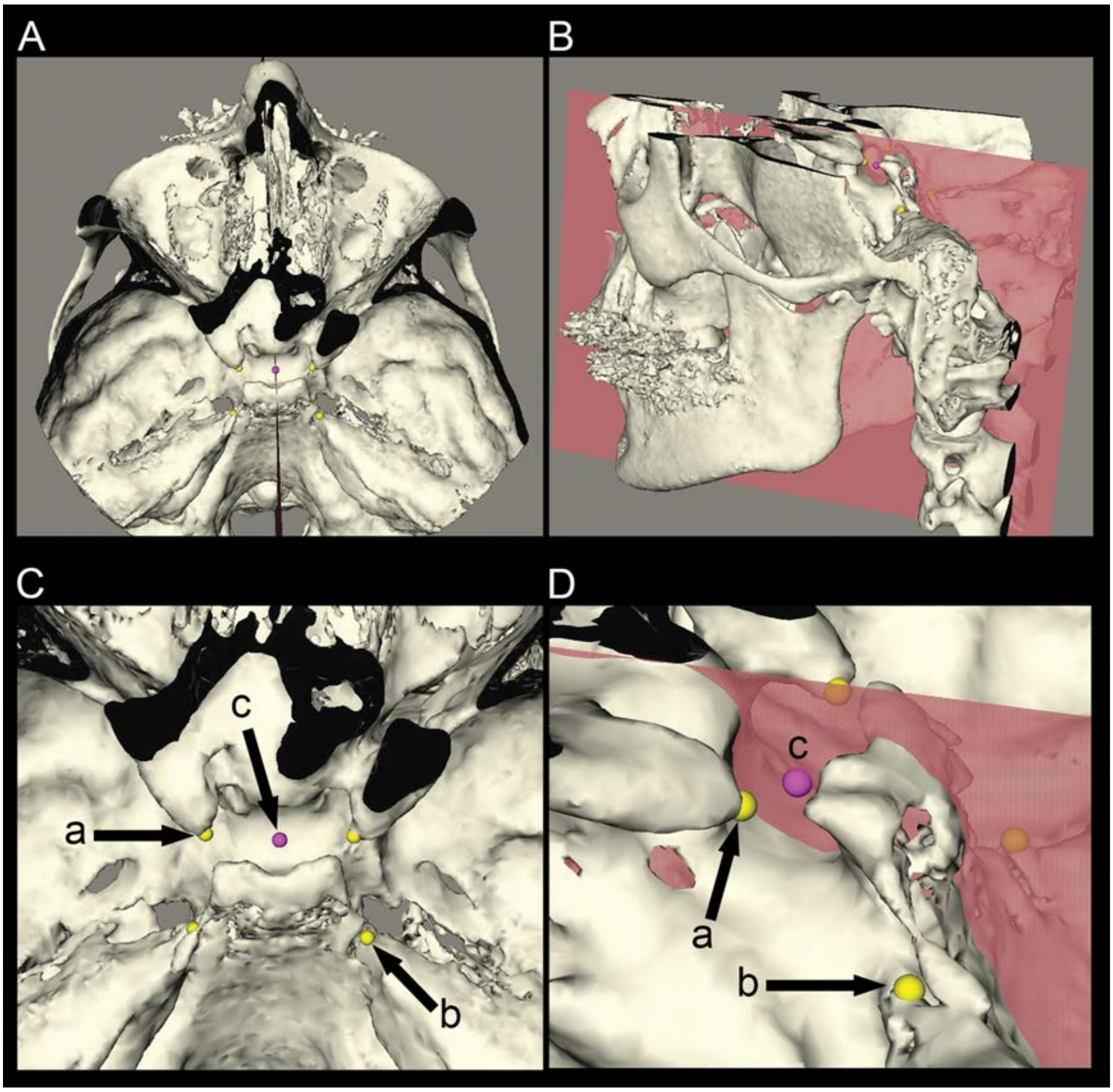

Figure 6.1 A and B show a top and an oblique overview of a 3D model of one patient, respectively. In this figure, a reference was created by locating 4 landmarks (anterior clinoid process (ACP) right and left, apex of the petrous part of the temporal bone right (APT) right and left). C is a close-up of the top view (A), showing landmarks that form the reference system: a. anterior clinoid process (ACP) right and left, b. apex of the petrous part of the temporal bone right (APT) right and left and c. one of the sella turcica landmark. D is a close-up of the oblique view, showing landmarks a, b and c. The sella turcica (c) was located on one of the vertical planes created from the reference system in Maxilim® software.

Statistical analysis

Coordinates (x, y, z) of 6 operator indicated landmarks were exported and put in Excel files. For each pair of landmarks placed by the observers, the Euclidean distance (d) between the 2 points was calculated by the formula:

$$d = \sqrt{\{(x_1-x_2)^2+(y_1-y_2)^2+(z_1-z_2)^2\}}$$

Point 1 coordinate: (x_1, y_1, z_1) = coordinate at time point 1 or coordinate from observer 1
Point 2 coordinate: (x_2, y_2, z_2) = coordinate at time point 2 or coordinate from observer 2
(These are also applied for coordinates from observer 3, observer 4 and observer 5.)

In this study, *the precision* was defined as "the mean distance of all subjects of a specific landmark". *Intra-observer precision* was defined as "the mean distance of all subjects of a specific landmark for each observer". *Inter-observer precision* was defined as "the mean distance of all subjects of a specific landmark for each pair of observers".

The reproducibility was defined as "the percentage of precision values". The intra- and inter-observer reproducibility was categorized into 3 levels, determined as the percentage of the precisions < 0.5 mm, < 1 mm, and > 1 mm.

Parametrical tests were used for statistical analysis because the data were normally distributed.

Intra-observer precision

A multiple paired *t*-test was performed on the transformed variable with Bonferonni correction ($p<0.005$) to determine the difference of the intra-observer precision between observers for each landmark. ANOVA with a Tukey post-hoc test was used to compare the means of the intra-observer precision between landmarks for each observer.

Inter-observer precision

All the possible distances between the 2 points of each pair of observers were calculated; therefore, there were 4 distance values for each subject, each landmark and each observer.

A multiple paired *t*-test with Bonferroni correction was performed to compare the 4 distances cited above. None of the comparisons reached a statistical significance, thus all these distances were joined together.

Mean values of the precision of each anatomical landmark, between each pair of observers, were evaluated by a multiple paired *t*-test with Bonferroni correction

(p<0.0011). ANOVA with a Tukey post-hoc test was calculated to compare the means of the precision between landmarks for each pair of observers.

6.4 Results

The results showed that all distances were positive and normally distributed.

Intra-observer precision and reproducibility

The results of the intra-observer precision are shown in Table 6.2. The intra-observer mean precision of all landmarks were < 1 mm. The best mean precision was 0.23 mm (SD 0.39) for ACP-L. The poorest mean precision was 0.96 mm (SD 1.76) for APT-R. For sella tucica landmarks (Sella 1 and Sella 2), intra-observer mean precision ranged from 0.43 (SD 0.34) mm – 0.51 (SD 0.46) mm.

The comparison between the intra-observer precision of each observer, using multiple paired *t*-test on the transformed variable with Bonferonni correction (p<0.005), showed significant differences in ACP-R, ACP-L and APT-L. This implied that ACP-R, ACP-L and APT-L, identified by some observers, were significantly more precise than others.

The intra-observer reproducibility (Table 6.3) of landmarks was generally good (more than 50% of mean distance is < 1 mm) but APT-L in one observer showed 53.1% of precisions above 1 mm. Sella 1 and Sella 2 showed good intra-observer reproducibility for all observers, with only 6.3-15.6% of mean distance above 1 mm (Table 6.3).

Inter-observer precision and reproducibility

No statistically significant difference was found when comparing precision values of each observer at 2 time points by using a multiple paired *t*-test with Bonferroni correction (p<0.0083). Therefore, the data were joined together without taking the time point into account.

Table 6.2 Intra-observer precision (mm)

	Observer 1		Observer 2		Observer 3		Observer 4		Observer 5	
	Mean	SD	Mean	SD	Mean	SD	Mean	SD	Mean	SD
ACP-R	0.28	0.35	0.36	0.32	0.59	0.49	0.33	0.44	0.46	0.43
ACP-L	0.23	0.39	0.30	0.46	0.57	0.50	0.37	0.38	0.38	0.42
APT-R	0.49	0.74	0.60	1.02	0.76	1.38	0.96	1.76	0.70	1.06
APT-L	0.40	0.83	0.45	0.73	0.96	1.24	0.82	0.78	0.75	1.02
Sella 1	0.49	0.41	0.43	0.34	0.51	0.39	0.40	0.40	0.42	0.46
Sella 2	0.46	0.38	0.55	0.45	0.51	0.46	0.35	0.37	0.44	0.43

Table 6.3 Intra-observer precision reproducibility for each observer.
Percentage of precisions: < 0.5 mm, 0.5-1 mm and > 1 mm.

	Observer 1			Observer 2			Observer 3			Observer 4			Observer 5		
	< 0.5	0.5-1	> 1	< 0.5	0.5-1	> 1	< 0.5	0.5-1	> 1	< 0.5	0.5-1	> 1	< 0.5	0.5-1	> 1
ACP-R	75.0	18.75	6.25	71.88	28.13	0	31.25	53.13	15.63	71.88	15.63	12.50	59.38	25.00	15.63
ACP-L	75.00	18.75	6.25	62.50	34.38	3.13	40.63	37.50	21.88	59.38	37.50	3.13	68.75	21.88	9.38
APT-R	75.00	18.75	6.25	71.88	28.13	0	31.25	53.13	15.63	71.88	15.63	12.50	59.38	25.00	15.35
APT-L	59.38	21.88	18.75	56.25	28.13	15.63	25.00	21.88	53.13*	21.88	34.38	43.75	31.25	25.00	43.75
Sella 1	53.13	34.38	12.50	56.25	34.38	9.38	53.13	37.50	9.38	71.88	18.75	9.38	50.00	43.75	6.25
Sella 2	65.63	28.13	6.25	43.75	40.63	15.63	46.88	46.88	6.25	71.88	18.75	9.38	50.00	43.75	6.25

* >50% of precisions > 1 mm

The results of the inter-observer precision are shown in Table 6.4. For most landmarks the inter-observer mean precision was < 1 mm except APT-R and APT-L that showed the mean precision > 1 mm for most pairs of observers.
Significant differences between each pair of observers for all anatomical landmarks were found (p<0.0011) and thus implied that the inter-observer precision and reproducibility was observer dependent.

Table 6.4 Inter-observer precision (mm) for every pair of observers (O)

	ACP-R		ACP-L		APT-R		APT-L		Sella 1		Sella 2	
	M	SD	M	SD	M	SD	M	SD	M	SD	M	SD
O1/2	0.55	0.55	0.44	0.51	0.84	1.46	0.62	1.26	0.67	0.53	0.63	0.57
O1/3	0.45	0.53	0.44	0.47	0.79	1.00	0.79	1.17	0.68	0.6	0.70	0.61
O1/4	0.62	0.57	0.66	0.53	1.93*	1.89	1.58*	1.39	0.78	0.63	0.76	0.65
O1/5	0.44	0.51	0.48	0.52	0.88	1.18	0.81	1.03	0.76	0.61	0.68	0.6
O2/3	0.53	0.57	0.53	0.48	1.04*	1.12	0.87	1.16	0.59	0.48	0.62	0.50
O2/4	0.59	0.63	0.57	0.54	1.62*	1.77	1.32*	1.19	0.53	0.45	0.58	0.51
O2/5	0.55	0.55	0.47	0.47	1.19*	1.30	1.03*	1.13	0.65	0.53	0.65	0.55
O3/4	0.64	0.59	0.59	0.53	1.82*	1.91	1.63*	1.53	0.66	0.53	0.62	0.52
O3/5	0.57	0.53	0.56	0.51	0.85	1.06	0.98	1.06	0.85	0.69	0.56	0.45
O4/5	0.45	0.46	0.44	0.46	1.99*	1.82	2.03*	1.71	0.71	0.57	0.70	0.55

* mean precision > 1 mm

For each pair of observers, an ANOVA with a Tukey post-hoc test was also performed to compare the means of the precision values between landmarks. It was found that for all pairs of observers, the precision of ACP-R and ACP-L were significantly better than other landmarks. For most pairs of observers, the precision of Sella 1 and Sella 2 were better compared to that of APT-L and APT-R, and sometimes as good as ACP-L and ACP-R.
The inter-observer reproducibility in percentage is shown in Table 6.5. The reproducibility was good to very good for ACP-R and ACP-L (only 9.4-30.5% of mean precisions > 1 mm). The reproducibility of APT left and right was poorer (36.7-90.6% of mean precisions > 1 mm). The reproducibility of 2 sella turcica landmarks (Sella 1 and Sella 2) was shown to be good (7.8-37.5% of mean precisions > 1 mm).

Table 6.5 Inter-observer reproducibility for every pair of observers (O).

Percentage of precisions: < 0.5 mm, 0.5-1 mm and > 1 mm.

	ACP-R			ACP-L			APT-R			APT-L			Sella 1			Sella 2		
	<0.5	0.5-1	>1	<0.5	0.5-1	>1	<0.5	0.5-1	>1	<0.5	0.5-1	>1	<0.5	0.5-1	>1	<0.5	0.5-1	>1
O1/2	47.66	31.25	21.09	57.03	25.78	17.19	32.03	21.09	46.88	42.19	21.09	36.72	28.91	48.44	22.66	32.81	42.97	24.22
O1/3	57.03	25.78	17.19	50.78	39.84	9.38	28.13	35.16	36.72	28.91	27.34	43.75	28.13	46.88	25.00	25.78	46.88	27.34
O1/4	32.03	39.84	28.13	31.25	45.31	23.44	5.47	10.16	84.38*	6.25	11.72	82.03*	21.09	44.53	34.38	25.78	37.50	36.72
O1/5	53.91	33.59	12.50	52.34	34.38	13.28	22.66	37.50	39.84	27.34	25.78	46.88	21.09	41.41	37.50	25.78	45.31	28.91
O2/3	42.97	40.63	16.41	45.31	35.94	18.75	16.41	30.47	53.13*	26.56	25.00	48.44	33.59	51.56	14.84	32.81	51.56	15.63
O2/4	43.75	25.78	30.47	35.16	44.53	20.31	7.81	16.41	75.78*	9.38	21.88	68.75*	47.66	42.19	10.16	38.28	43.75	17.97
O2/5	43.75	35.16	21.09	48.44	41.41	10.16	13.28	21.09	65.63*	13.28	37.50	49.22	30.47	50.00	19.53	29.69	46.09	24.22
O3/4	34.38	35.16	30.47	38.28	39.84	21.88	5.47	18.75	75.78*	5.47	7.03	87.50*	26.56	53.13	20.31	34.38	50.00	15.63
O3/5	40.63	41.41	17.97	41.41	40.63	17.97	24.22	30.47	45.31	20.31	26.56	53.13*	37.50	51.56	10.94	40.63	51.56	7.81
O4/5	53.13	33.59	13.28	48.44	42.19	9.38	4.69	9.38	85.94*	3.13	6.25	90.63*	22.66	52.34	25.00	22.66	55.47	21.88

* >50% of precisions > 1 mm

6.5 Discussion

The current study investigated the precision and reproducibility of landmarks incorporated in a new reference system which was developed in order to precisely indicate the sella turcica landmark in 3D.

CBCT scans of patients were collected retrospectively. No age limitation was set in the study criteria although age may be one of the factors that can cause variations in the sella turcica region. In the inclusion criteria, it was stated that there must be no variation at the sella and sphenoidal regions, as from literature, bridging of the sella turcia or calcification of the interclinoid ligament (ICL) occurs in 1.1-13% of the normal population (24-26). This also implies that the system developed in the present study should only be used in patients without sella variations.

Bony resorption of the posterior part may occur which might result in difficulty in identifying the border of the sella turcica. The results of this study showed that for some landmarks (APT, Sella), the precision was case sensitive. This might be because of the fact that in CBCT scans of some patients, the landmarks and bony structures were more difficult to visualize and also in some CBCTs, image noises were more obvious.

Selection of the CBCT devices might also be a key factor in performing 3D cephalometry as this may affect the image quality and the quality of the 3D computed surface model. In this present study, data were retrospectively collected and the number of device was limited to one. The CBCT data was tested for compatibility with Maxilim® software.

The Maxilim® software showed a minor limitation while segmenting 3D surface models. The software does not allow the operator to reduce any image artifacts or noises. Thus while selecting the hard tissue threshold to create a surface model, some unwanted soft tissue parts and artifact were included in the 3D model. This gave the observers some difficulties in viewing the images of some patients whose CBCT showed more noises and artifacts.

The reference system created in this study was comprised of 4 operator-indicated landmarks, 2 software-calculated landmarks and 2 sella turcica landmarks on 2 different vertical planes (Table 6.1). The landmarks used in the system were carefully selected to be able to precisely identify the center of the pituitary fossa. All landmarks forming the vertical planes are located adjacent to the sella turcica so the planes were not affected by variations of other craniofacial structures.

In this study, an upper limit of 1 mm was chosen as a clinical relevance level. There was no scientific evidence that proved whether 1 mm is the real clinical standard. Yet, it is usually presumed that larger differences may cause an unacceptable difference in measurements, thus may alter the cephalometric analysis results (20,27).

The results showed that both intra- and inter-observer precision of all landmarks were moderate to very good although for some landmarks (APT), the precision was poorer especially for inter-observer precision but even with this poorer precision, it did not alter much how the observers indicated the sella points on these vertical planes.

The intra-observer precision was slightly better than the inter-observer precision. This trend was expected as the examiner factor is one of the factors that may influence the result in observational study. The difference in background of the observers, the familiarity of the observers to the software and the ability to identify landmarks according to the definition might play a role. A calibration session was performed to minimize this effect as much as possible.

In this study, two of the observers (observer 1 and 2) had more experience in using Maxilim® software prior to the observations. This effect could still be observed in the results. There were significant differences of intra-observer precision between observers for some landmarks (ACP and APT) and that 2 observers (observer 1 and 2) could identify the landmarks more precisely. Also while evaluating inter-observer precision, significant differences between each pair of observers for all anatomical landmarks were found, implying that the inter-observer precision was observer dependent. These findings may indicate that more calibration sessions should be performed in the future study related to new software or the observers should be selected based on their experience when it is possible.

The overall reproducibility of all landmarks was good. ACP was the most reproducible, followed by 2 sella landmarks and the least reproducible was the

APT (left and right) (highest % of precisions > 1 mm). There was no difference in using either Sella 1 or Sella 2. Sella 2 on a vertical plane, passing through mid-APT is recommended because ACP points were more reproducible thus better to be used separately.

Some authors have published results of 3D landmark reproducibility by using different methods. However, no similar sella-specific reference system was evaluated prior to this study. Therefore, their results cannot be directly compared with the results from the present study.

In 2008, Marumatsu *et al*. (28) reported the plotting reproducibility of landmarks on 3D-CT using the 95% confidence ellipse method. The methodology of this study is different from the present study as the landmarks were located only on the axial views of the CT images of one phantom head. The reproducibility of sella turcica was reported to have some variations (28).

Another study was conducted by de Oliveira *et al*. (23) to evaluate 3D landmark identification. The results showed high intraclass correlation coefficient of both intra- and inter-observer assessments. The authors concluded that 3D landmark identification using CBCT could offer reproducible data if a protocol for operator training and calibration was followed (23). In the present study, the calibration session was done and the landmark definitions were carefully defined.

In orthodontics, sella turcica (S) is utilized as a reference point to evaluate longitudinal growth of the patients and also evaluate the treatment results by superimposing several lateral cephalogram and comparing angles e.g. SNA (sella-nasion-point A) and SNB (sella-nasion-point B). Further studies should be conducted to integrate this sella reference system into 3D cephalometric analysis and assess how this system may influence the angular measurements and the results of several 3D cephalometric analyses.

6.6 Conclusions

The sella turcica landmark is one of the most important cephalometric landmarks although it is a floating landmark in nature. Identifying the sella turcica by using a newly developed reference system offers high precision and reproducibility in 3-dimensions, without being based on 2D images derived from 3D data.

6.7 References

1. Teal JS. Radiology of the adult sella turcica. *Bull Los Angeles Neurol Soc.* 1977;42:111-174.
2. Axelsson S, Storhaug K, Kjaer I. Post-natal size and morphology of the sella turcica. Longitudinal cephalometric standards for Norwegians between 6 and 21 years of age. *Eur J Orthod.* 2004;26:597-604.
3. Andredaki M, Koumantanou A, Dorotheou D, Halazonetis DJ. A cephalometric morphometric study of the sella turcica. *Eur J Orthod.* 2007;29:449-456.
4. Alkofide EA. The shape and size of the sella turcica in skeletal Class I, Class II, and Class III Saudi subjects. *Eur J Orthod.* 2007;29:457-463.
5. Alkofide EA. Sella turcica morphology and dimensions in cleft subjects. *Cleft Palate Craniofac J.* 2008;45:647-653.
6. Brock-Jacobsen MT, Pallisgaard C, Kjaer I. The morphology of the sella turcica in monozygotic twins. *Twin Res Hum Genet.* 2009;12:598-604.
7. Kjaer I. Sella turcica morphology and the pituitary gland--a new contribution to craniofacial diagnostics based on histology and neuroradiology. *Eur J Orthod.* 2012, in press.
8. Hofrath H. Bedeutung der Röntgenfern und Abstands Aufnahme für die Diagnostik der Kieferanomalien. *Fortschr Orthod.* 1931;1:231-258.
9. Broadbent BH. A new x-ray technique and its application to orthodontia. *Angle Orthod.* 1931;1:45-66.
10. Pauwels R, Beinsberger J, Collaert B, Theodorakou C, Rogers J, Walker A, *et al*. Effective dose range for dental cone beam computed tomography scanners. *Eur J Radiol.* 2012;81:267-271.
11. Kau CH, Richmond S, Palomo JM, Hans MG. Three-dimensional cone beam computerized tomography in orthodontics. *J Orthod.* 2005;32:282-293.
12. Mah JK, Huang JC, Choo H. Practical applications of cone-beam computed tomography in orthodontics. *J Am Dent Assoc.* 2010;141:7S-13S.
13. van Vlijmen OJ, Kuijpers MA, Bergé SJ, Schols JG, Maal TJ, Breuning H, *et al*. Evidence supporting the use of cone-beam computed tomography in orthodontics. *J Am Dent Assoc.* 2012;143:241-252.

14. Swennen GR, Schutyser F, Barth EL, De Groeve P, De Mey A. A new method of 3-D cephalometry Part I: the anatomic Cartesian 3-D reference system. *J Craniofac Surg.* 2006;17:314-325.
15. Olszewski R, Cosnard G, Macq B, Mahy P, Reychler H. 3D CT-based cephalometric analysis: 3D cephalometric theoretical concept and software. *Neuroradiology.* 2006;48:853-862.
16. Periago DR, Scarfe WC, Moshiri M, Scheetz JP, Silveira AM, Farman AG. Linear accuracy and reliability of cone beam CT derived 3-dimensional images constructed using an orthodontic volumetric rendering program. *Angle Orthod.* 2008;78:387-395.
17. Brown AA, Scarfe WC, Scheetz JP, Silveira AM, Farman AG. Linear accuracy of cone beam CT derived 3D images. *Angle Orthod.* 2009;79:150-157.
18. Olszewski R, Tanesy O, Cosnard G, Zech F, Reychler H. Reproducibility of osseous landmarks used for computed tomography based three-dimensional cephalometric analyses. *J Craniomaxillofac Surg.* 2010;38:214-221.
19. Olszewski R, Frison L, Wisniewski M, et al. Reproducibility of three-dimensional cephalometric landmarks in cone-beam and low-dose computed tomography. *Clin Oral Investig.* 2013;17:285-292.
20. Pittayapat P, Limchaichana-Bolstad N, Willems G, Jacobs R. Three-dimensional cephalometric analysis in orthodontics: a systematic review. *Orthod Craniofac Res.* 2014;17:69-91.
21. Schlicher W, Nielsen I, Huang JC, Maki K, Hatcher DC, Miller AJ. Consistency and precision of landmark identification in three-dimensional cone beam computed tomography scans. *Eur J Orthod.* 2012;34:263-275.
22. Chien PC, Parks ET, Eraso F, Hartsfield JK, Roberts WE, Ofner S. Comparison of reliability in anatomical landmark identification using two-dimensional digital cephalometrics and three-dimensional cone beam computed tomography in vivo. *Dentomaxillofac Radiol.* 2009;38:262-273.
23. de Oliveira AE, Cevidanes LH, Phillips C, Motta A, Burke B, Tyndall D. Observer reliability of three-dimensional cephalometric landmark identification on cone-beam computerized tomography. *Oral Surg Oral Med Oral Pathol Oral Radiol Endod.* 2009;107:256-265.

24. Bergland RM, Ray BS, Torack RM. Anatomical variations in the pituitary gland and adjacent structures in 225 human autopsy cases. *J Neurosurg.* 1968;28:93-99.
25. Cederberg RA, Benson BW, Nunn M, English JD. Calcification of the interclinoid and petroclinoid ligaments of sella turcica: a radiographic study of the prevalence. *Orthod Craniofac Res.* 2003;6:227-232.
26. Meyer-Marcotty P, Reuther T, Stellzig-Eisenhauer A. Bridging of the sella turcica in skeletal Class III subjects. *Eur J Orthod.* 2010;32:148-153.
27. Durao AR, Pittayapat P, Rockenbach MI, *et al*. Validity of 2D lateral cephalometry in orthodontics: a systematic review. *Prog Orthod.* 2013;14:31.
28. Muramatsu A, Nawa H, Kimura M. Reproducibility of maxillofacial anatomic landmarks on 3-dimensional computed tomographic images determined with the 95% confidence ellipse method. *Angle Orthod.* 2008;78:396-402.

Chapter 7

A new mandible-specific landmark reference system for three-dimensional cephalometry

This chapter is based on:

Pittayapat P, Jacobs R, Odri G, Kwon MS, Lambrichts I, Willems G, Politis C, Olszewski R. A new mandible-specific landmark reference system for three-dimensional cephalometry. *Submitted.*

7.1 Abstract

Objectives: To develop a 3D landmark reference system that is specific for mandibular midline cephalometric landmarks and to assess its reproducibility and the reproducibility of the mandibular midline cephalometric landmarks.

Materials and methods: Cone-beam computed tomography (CBCT) scans (3D Accuitomo® 170) were performed on 26 dry human skulls. The CBCT data were exported into DICOM and imported to Maxilim® software to create 3D surface models. The reference system was composed of five landmarks: two mandibular foramina, two molar landmarks and one interincisive landmark. Three observers used a new landmark reference system to identify four mandibular cephalometric landmarks: Point B, Pogonion, Gnathion and Menton. The coordinates (x, y, z) of each landmark were exported to Excel. The observations were repeated after 4 weeks. Statistical analysis was performed.

Results: The intra-observer median precision in locating all landmarks ranged between 0.17-0.61 mm. The intra-observer reproducibility was generally good with a precision under 1 mm in >50% of the measurements. The overall median inter-observer precision was 0.26-2.30 mm. The mandibular foramina showed the best inter-observer reproducibility. The general inter-observer reproducibility was moderate to good except for Pogonion and Point B.

Conclusion: A newly developed reference system offered good precision and generally good to moderate reproducibility for mandibular midline cephalometric landmark identification in three dimensions.

7.2 Introduction

Cephalometric analysis is an essential part of orthodontic treatment planning. This technique was first introduced by Hofrath (1) in Germany and Broadbent (2) in the United States. It is traditionally performed on a lateral cephalogram and a frontal cephalogram. Although this widely accepted technique has been used as a standard tool for orthodontic treatment planning for several decades, a disadvantage of the technique is geometric distortion and the superimposition of structures on a radiograph (3,4).

A cephalometric analysis comprises several cephalometric landmarks. Mandibular midline landmarks are important elements in many cephalometric analyses. The landmarks in this region are Point B (B), Pogonion (Pog), Gnathion (Gn), and Menton (Me). These important landmarks are used to define mandibular planes and to investigate the relationship of the mandible to the maxilla. These landmarks are part of angular measurements such as Sella-Nasion-Point B and Nasion-Pogonion to the Frankfort horizontal plane. They are also used to analyze the vertical relationship of the jaws (Sella-Nasion to Gonion-Gnathion) and to analyze the inclination of the lower incisors to the mandibular plane (incisor mandibular plane angle) (5).

Three-dimensional imaging modalities, especially cone-beam computed tomography (CBCT), have become important diagnostic tools in dentistry. CBCT generates a lower radiation dose than that of multi-slice CT (MSCT) (6) and produces detailed images of the dentition and maxillofacial region. Therefore, CBCT has become very popular for use in maxillofacial diagnosis and treatment planning. Three-dimensional images allow orthodontists to accurately visualize craniofacial structures in all dimensions, without the superimposition of anatomic structures (7-9). This modality is useful in orthodontic cases such as canine impaction, root resorption, sleep disorders, orthognathic surgery, and also in three-dimensional cephalometry.

Three-dimensional cephalometry allows clinicians to identify cephalometric landmarks in three dimensions with the aid of 3D image viewing software (10,11). Several studies have shown the advantages of this technique over traditional 2D cephalometric analysis (12-15).

When using 3D maxillofacial software, the mandibular midline landmarks are usually identified based on 2D cephalometric images generated from a 3D dataset (10). Studies have demonstrated the reliability and accuracy of 3D cephalometric landmark identification, including B, Pog, Gn, and Me (16-18). However, it is not clear if these landmarks, identified on the generated 2D image, refer to the appropriate midsagittal plane of the mandible because the reference system provided by several studies used landmarks that are not related to the mandible (19). No accurate method or system that allows the operator to identify mandibular midline landmarks on 3D models without generating 2D lateral cephalometric views has been described (19).
Therefore, the aim of this study was first to develop a 3D reference system that is specific for mandibular midline landmarks and to assess its reproducibility and the reproducibility of mandibular midline cephalometric landmarks.

7.3 Materials and methods

Samples

Twenty-six dry human skulls with present upper and lower first incisors and first molars were collected from the Department of Anatomy, Hasselt University, Diepenbeek, Belgium. The mandibles were attached to the skulls by taping from the temporal area of both sides. The occlusion was fixed at the maximum intercuspation. The study protocol (reference number: ML6960, BE322201010078) was approved by the UZ Leuven Medical Ethics Committee, University Hospitals Leuven, KU Leuven. The authors have read the Helsinki Declaration and have followed the guidelines in this investigation.

Imaging modalities

CBCT scans of the samples were taken using 3D Accuitomo® 170 (J. Morita, Kyoto, Japan) with the largest field of view: 170 mm diameter x 120 mm height (High-Fidelity mode: 90 kVp, 154 mAs, voxel size 0.25 mm.). A 1.7-mm-thick copper filter was attached to the machine during image acquisition to simulate soft tissue attenuation. CBCT data were exported to Digital Imaging and Communications in Medicine (DICOM) files then imported to Maxilim® software version 2.3.0.3 (Medicim NV, Sint-Niklaas, Belgium). A 3D surface model was created for each sample using the full CBCT volume with 0.5 mm sub-sampling of voxels. The threshold was set at 276 to segment the hard tissues for the 3D models.

Reference frame

A reference system was created in the Maxilim® software to identify the mandibular midline cephalometric landmarks. The reference frame was composed of 5 mandibular landmarks and 4 mandibular midline cephalometric landmarks that were indicated on a vertical plane created from the reference system (Table 7.1) (Fig. 7.1).

Two observers (one Dentomaxilofacial radiologist with 8 years of experience and one oral and maxillofacial surgeon with 20 years of experience) were initially calibrated in a calibration session. Detailed instructions about landmark definition and software manipulation were given. The observers completed each set of observations twice with a 4 week-interval.

Table 7.1 Definitions of the landmarks and planes used in the reference system

Name	Definition
Landmarks	
Mandibular foramen right and left (MF-R, MF-L)	The point at the superior margin of the mandibular foramen
Molar right and left (M-R, M-L)	The point located on the alveolar crest at the area perpendicular to the lingual fissure of the mandibular first molar
Interincisive (II)	The point located at the alveolar crest in the middle between two mandibular central incisors
Point B (B)	The intersection between the midsagittal plane and the most posterior point of the anterior surface of the mandibular symphysis
Pogonion (Pog)	The intersection between the midsagittal plane and the most anterior point of the mandibular symphysis
Gnathion (Gn)	The intersection between the midsagittal plane and the the most anteroinferior point of the mandibular symphysis, bisecting the angle between Pog and Me
Menton (Me)	The intersection between the midsagittal plane and the lowest point of the mandibular symphysis
Planes	
Horizontal plane	The plane formed by MF-R, MF-L and II landmarks
Vertical plane	The plane passing through M-R, M-L and perpendicular to the horizontal plane
Mandibular midsagittal plane	The plane passing through II and perpendicular to the horizontal and vertical planes

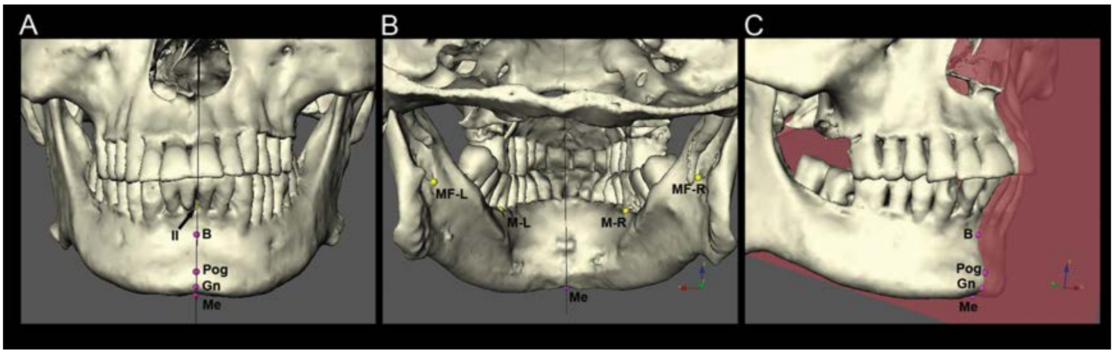

Figure 7.1 The mandibular landmark reference system. A is the anterior view of the 3D model of a sample, showing identified landmarks: II, B, Pog, Gn and Me located on a midsagittal plane that created from the reference system. B shows the posterior view of the sample with landmarks: MF-R, MF-L, M-R, M-L, and Me. C is the oblique view with 25% transparent of the midsagittal plane, showing B, Pog, Gn and Me.

Statistical analysis

The coordinates (x, y, z) of the landmarks were exported into Excel files. For each pair of landmarks identified by the observers, the Euclidean distance (d) between the 2 points in 3D space was calculated by the formula:

$$d = \sqrt{\{(x_1-x_2)^2+(y_1-y_2)^2+(z_1-z_2)^2\}}$$

Point 1 coordinate: (x_1, y_1, z_1) = coordinate at time point 1 or coordinate from observer 1

Point 2 coordinate: (x_2, y_2, z_2) = coordinate at time point 2 or coordinate from observer 2

Non-parametrical tests were used because the distribution of the data was not normal.

The distance between point 1 (1^{st} observation) and point 2 (2^{nd} observation) was used to determine the intra-observer precision. The intra-observer precision of each landmark was defined as “the median distance of all samples”. The intra-observer precision between observers and the intra-observer precision between landmarks was compared using the multiple Wilcoxon’s test with Bonferroni’s correction ($p<0.0054$ and $p<0.0014$, respectively).

To determine the inter-observer precision 4 possible distances between the 2 points of each observer were calculated for each landmark. The multiple Wilcoxon’s test with Bonferroni correction ($p<0.0083$) was performed to compare the 4 distances. None of the comparisons reached a statistical significant level, thus all distances were joined together. The inter-observer precision for each landmark was defined as "the median distance of all samples of these 4 measures". The inter-observer precision between landmarks was compared by a multiple Wilcoxon's test with Bonferroni's correction ($p<0.0014$). Reproducibility was presented as a percentage and categorized into three levels defined as the percentage of the precision in locating the landmark by < 0.5 mm, < 1 mm, or ≥ 1 mm. Good, moderate, and poor reproducibility were defined as when >50% of the precision in locating the landmark were < 1 mm, 51-75% were > 1 mm, and when >75% were >1 mm, respectively.

7.4 Results

Intra-observer precision and reproducibility

No statistically significant difference was found when comparing the precision between the two observers. When examining the intra-observer precision in locating the landmarks, the right and left mandibular foramina (MF-R, MF-L) were located with significantly better precision than all other landmarks ($p<0.0001$).

The median intra-observer precision was < 1 mm for all landmarks (Table 7.2). The landmarks that were located the most precisely were the mandibular foramina. Point B (B) showed the highest maximum value at 3.47 mm (median 0.48 mm).

The intra-observer reproducibility is shown in Table 7.3. All the landmarks were located with >50% of the precision in locating the landmarks < 1 mm. The right and left mandibular foramina (MF-R, MF-L) were the most reproducibly located landmarks with >90% of the precision in locating the landmarks < 0.5 mm.

Inter-observer precision and reproducibility

The median inter-observer precisions in locating the landmarks are presented in Table 7.4. Comparison of the inter-observer precision between landmarks showed that MF-R (0.28 mm) and MF-L (0.26 mm) were significantly better than other landmarks ($p<0.001$). The median precision in locating Pog was significantly poorer than those of the landmarks ($p<0.001$).

The inter-observer reproducibility is shown in Table 7.5. All landmarks resulted in > 50% of the precision in locating the landmark below 1 mm except for Pog, Gn, Me, and B. MF-R and MF-L showed the best inter-observer reproducibility with > 70% of the precision in locating the landmark below 0.5 mm. The distribution of the inter-observer precision of Pog, Gn, Me, and B (2 observers, 2 times) are shown in Figure 7.2. It was observed that the precision distribution mostly ranged between 1-3.5 mm. However, a few measurements had a precision of 5 mm (Fig. 7.2).

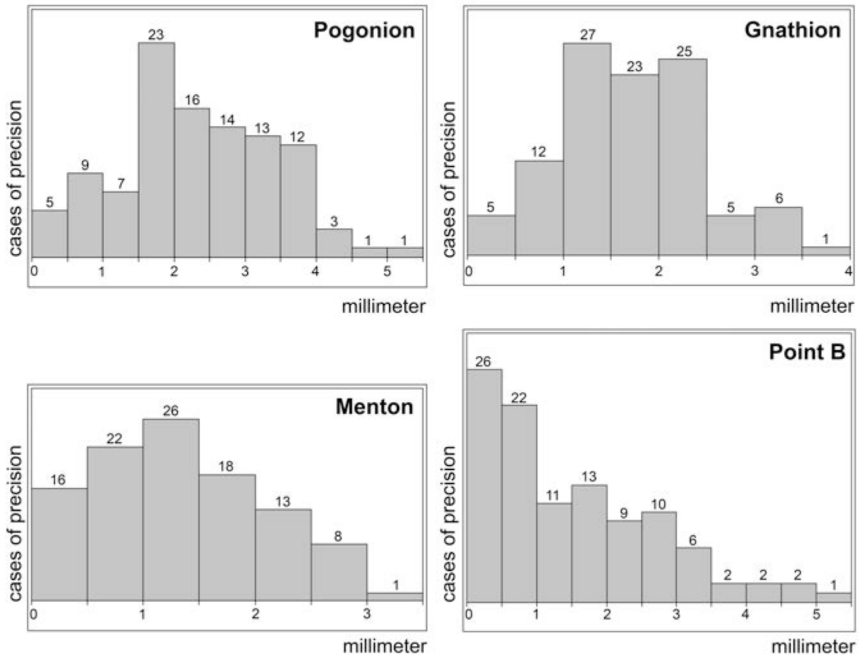

Figure 7.2 The distribution of the inter-observer precision in locating Pogonion (Pog), Gnathion (Gn), Menton (Me), and Point B (B). The precision distribution of Pog ranged mostly between 1.5-4 mm. For Gnathion, the precision ranged between 1-2.5 mm. For Me, the precision ranged from 0-3 mm and lastly for B, the precision ranged from 0-3.5 mm. The precision of the measurements ranged up to 5.5 mm.

Table 7.2 Intra-observer precision (mm)

Landmarks	Median	Min	Max
MF-R	0.23	0.03	1.25
MF-L	0.17	0.03	1.67
II	0.33	0.06	2.31
M-R	0.47	0.07	2.18
M-L	0.61	0.06	2.59
Me	0.40	0.09	2.19
Pog	0.41	0.11	1.95
Gn	0.41	0.07	1.67
B	0.48	0.03	3.47

Table 7.3 Intra-observer reproducibility, showing percentage (%) of the precision in locating the landmark < 0.5 mm, 0.5-1 mm and > 1 mm.

Landmarks	% precision		
	< 0.5	0.5-1	> 1
MF-R	92.3	5.8	1.9
MF-L	92.3	7.7	0.0
II	61.5	30.8	7.7
M-R	55.8	26.9	17.3
M-L	40.4	40.4	19.2
Me	69.2	21.2	9.6
Pog	57.7	23.1	19.2
Gn	59.6	32.7	7.7
B	50.0	21.2	28.9

Table 7.4 Inter-observer precision (mm)

Landmarks	Median	Minimum	Maximum
MF-R	0.28	0.01	1.30
MF-L	0.26	0.02	1.08
II	0.71	0.03	2.80
M-R	0.80	0.12	2.85
M-L	0.60	0.02	1.98
Me	1.41	0.11	3.05*
Pog	2.30	0.22	5.01*
Gn	1.61	0.12	3.74*
B	1.16	0.06	5.00*

* The maximum inter-observer precision value >3 mm

Table 7.5 Inter-observer reproducibility, showing percentage (%) of the precision in locating the landmark < 0.5 mm, 0.5-1 mm and > 1 mm.

Landmarks	% precision		
	< 0.5	0.5-1	> 1
MF-R	74.0	24.0	1.9
MF-L	80.8	17.3	1.9
II	34.6	31.7	33.7
M-R	21.2	49.0	29.8
M-L	39.4	34.6	26.0
Me	15.4	21.2	63.5
Pog	4.8	8.7	86.5*
Gn	4.8	11.5	83.7*
B	25.0	21.2	53.9

* >75%

7.5 Discussions

The present study investigated the precision and reproducibility of locating landmarks used in a new reference system developed to precisely indicate important mandibular cephalometric landmarks in three dimensions. The results showed good intra-observer precision and reproducibility in locating the landmarks and moderate to good inter-observer precision and reproducibility in locating the landmarks, except for Pog and B.

In the present 3D cephalometric study, dry human skulls were used to represent human subjects. A limitation in using dry human skulls is the lack of soft tissue; therefore, they may not represent real human anatomical structures. Due to ethical concerns about exposing healthy human subjects to ionizing radiation, it is generally accepted to use dry skulls in cephalometric studies. The main focus of the present study was on hard tissue landmarks, thus soft tissues were not necessary. However, a copper filter was used during image acquisition to simulate soft tissue attenuation and to prevent overexposure.

On a 2D lateral cephalogram, the midline landmarks are located using the image-indicated midline. In 3D analysis, one dimension is added, thus to use the same landmarks as in 2D, a midsagittal plane must be created. In the present study, Maxilim® software was used to develop the 3D landmark reference system. The reference system developed in our study comprised 5 operator-indicated landmarks (MF-R, MF-L, M-R, M-L, and II), and 4 mandibular cephalometric landmarks (Pog, Gn, Me, and B), which were located on the mandibular midsagittal plane created by the reference system. The selection of the landmarks used in the reference frame was based on a previous pilot experiment that indicated that these are easily identified mandibular landmarks. MF-R, MF-L, M-R, M-L, and II are located on the mandible to develop a mandibular specific midsagittal reference plane. This mandibular specific midsagittal plane may deviate from the upper and mid-face midsagittal plane where sella turcica (S) is usually used as one of the elements in connecting this plane (10); however, the mandibular specific midsagittal plane represents the real mandibular midline. Using this mandibular midsagittal plane, the mandible can be analyzed in three dimensions instead of using a lateral virtual view created from the CBCT image dataset for 3D cephalometry. This plane will be different based on each individual.

A review of the literature did not reveal any studies on developing a 3D reference system that is specific for the mandibular region. The results of our study showed good intra-observer precision and reproducibility in locating the landmarks and generally moderate to good inter-observer precision and reproducibility in locating the landmarks except for Pog and B. The data was analyzed using the median because the data were not normally distributed.

The intra-observer precision results indicated that the mandibular foramina were the most precisely located landmarks. All landmarks were located with a median precision < 1 mm. Locating Point B had the poorest intra-observer precision and reproducibility among the landmarks. This can be explained by a previous study that found that when a landmark is situated on a curved surface the accuracy of its identification could be affected (20). Thus, Point B, which is normally defined as the point of maximum concavity in the midline of the alveolar process of the mandible, may be located less accurately compared to a landmark situated on a small specific area e.g. MF-R and MF-L (The points at the superior margin of the mandibular foramina). In this study, Point B was less reliable and more difficult to define or prone to subjectivity even though the mid-sagittal mandibular plane could help limit the error. Our results are also supported by other studies that demonstrated landmarks on a curved surface were usually less reliably located (14,18).

The difficulty in locating landmarks on a curved surface can also account for the inter-observer precision and reproducibility results. The most precisely located landmarks were the mandibular foramina (MF-R, MF-L). The mandibular cephalometric landmarks (Me, Pog, Gn, and B) were located with a median precision > 1 mm and the reproducibility in locating these landmarks ranged from poor to moderate. These results might be influenced by several factors. One factor is that these landmarks are located on a curved surface (20). Another factor is the observer, because observer performance can be affected by background experience, the familiarity of the observers with the software, and their ability to identify landmarks according to the definitions. Therefore, inter-observer performance can be expected to be poorer than intra-observer performance. In addition, landmark definition can also affect precision and reproducibility. In 3D, the definitions of the cephalometric landmarks should be different from the traditional 2D definitions. A previous study indicated that good landmark definitions improved observer performance (17). Therefore, the definitions of landmarks in the present study were slightly modified to fit with the developed 3D reference system. A calibration session was conducted prior to the first observation to minimize the effect of these factors as much as possible. Lastly, the measurements can also be influenced by the subjects or samples, i.e. anatomical variation at the chin area, and the quality of the CBCT scan (artifacts and noise). The outlying measurements of Pog and Me may have been influenced by the subject's individual anatomy.

A number of studies have investigated general cephalometric landmark identification precision and reproducibility (14,18,21,22). Ludlow *et al*. (21) compared the precision of landmark identification using displays of multiplanar CBCT volumes and conventional lateral cephalograms. The multiplanar reconstructed images (MPR) resulted in generally more precise landmark identification than on lateral cephalograms. Ludlow *et al*. found that 3D Pogonion received higher observer variation, similar to the results of the present study (21). Schlicher *et al.* (18) evaluated the precision and consistency in locating cephalometric landmarks. Their results showed the same trend as in the present study where landmarks situated on broad curved surfaces without clear anatomical boundaries had a tendency to have errors in identification. Schlicher *et al.* determined that Gn was the most consistent landmark among landmarks at the chin area (Pog, Gn, Me) (18). In contrast, in the present study, Me was the most precisely located landmark among the three. Due to differences between the methods of Ludlow *et al*., Schlicher *et al.,* and the present study, the results may not be directly compared. In their studies, 3D landmarks were identified on the MPR images; however, in our study the landmarks were solely identified on 3D surface models. These differences might affect how the observers viewed the landmarks and where the cursor was placed to identify the indicated landmarks.

In 2010, Olszewski *et al*. (14) compared the reproducibility of osseous landmark identification from two 3D cephalometric analyses: 3D-ACRO and 3D-Swennen analyses. Their results were in agreement with the present study, finding that intra-observer reproducibility was better than inter-observer reproducibility and that Pogonion was located with poor observer reproducibility (14).

A more recent study by Hassan *et al.* (22) evaluated the precision of landmark identification on MPR, 3D models, and MPR with 3D models. Their study found that the precision of measurements ranged between 0.29 ± 0.17 mm and 2.82 ± 7.53 mm (22). The authors suggested that utilizing both 3D models and MPR images could improve the precision of landmark identification (22).

Clinical implications and further studies

The reference system presented in this study allows clinicians to generate a patient specific mandibular midsagittal plane without the need to generate 2D images from 3D data. This system can be used with a limited FOV 3D dataset which is a significant advantage for 3D cephalometry. It requires only a mandible to create the mandibular specific midsagittal plane. It can be utilized when other reference areas, such as the base of skull (10), are not available. In a situation where only a limited size of FOV can be obtained, this new reference system can be used as an alternative.

Although in this study, the reference system was not tested and validated in asymmetric mandibles, based on its principle, this reference system shall be used in asymmetric faces. This system is constructed by using only landmarks in the mandible; therefore, it is in fact a 3D representative of the mandible both for symmetric and asymmetric ones. The locations of the mandibular midline cephalometric landmarks (Pog, Point B, Gn, Me) are dependent only on the shape and morphology of the mandible and are independent of the overall skull midsagittal plane. This must be further evaluated in future studies.

Another improvement can be added to the present system by using both MPR images and 3D models as suggested by Hassan *et al.* (22). At the study design process of this study, it was aimed to use only 3D surface models but was later found that some errors could occur during the 3D segmentation process. Therefore, using 3D surface models with the confirmation from MPR images may help decrease the error in landmark identification.

When the system is improved and validated in patients' data, the related angular and linear measurements after the incorporation of this system into the analyses should be tested. This step must be performed before it is used clinically.

7.6 Conclusions

A newly developed reference system was developed and its reproducibility was tested. This reference system offered moderate to good overall precision and reproducibility for mandibular cephalometric midline landmark identification in three dimensions.

7.7 References

1. Hofrath H. Bedeutung der Röntgenfern und Abstands Aufnahme für die Diagnostik der Kieferanomalien. *Fortschr Orthod.* 1931;1:231-258.
2. Broadbent BH. A new x-ray technique and its application to orthodontia. *Angle Orthod.* 1931;1:45-66.
3. Jacobson A, Jacobson RL (2006) Radiographic Cephalometry: From Basics to 3-D Imaging. 2nd ed., USA, Quintessence Publishing; 2006
4. Stuart CW, Michael JP. Oral Radiology. Principles and Interpretation. 7th ed., St.Lois, Elsevier Mosby; 2014.
5. Proffit WR, Fields HW, Jr., Sarver DM. *Contemporary Orthodontics.* 4th ed. St.Lois, MO: Elsevier Mosby; 2007.
6. Pauwels R, Beinsberger J, Collaert B, Theodorakou C, Rogers J, Walker A, *et al*. Effective dose range for dental cone beam computed tomography scanners. *Eur J Radiol.* 2012;81:267-271.
7. Kau CH, Richmond S, Palomo JM, Hans MG. Three-dimensional cone beam computerized tomography in orthodontics. *J Orthod.* 2005;32:282-293.
8. Mah JK, Huang JC, Choo H. Practical applications of cone-beam computed tomography in orthodontics. *J Am Dent Assoc.* 2010;141:7S-13S.
9. van Vlijmen OJ, Kuijpers MA, Bergé SJ, Schols JG, Maal TJ, Breuning H, *et al*. Evidence supporting the use of cone-beam computed tomography in orthodontics. *J Am Dent Assoc.* 2012;143:241-252.

10. Swennen GR, Schutyser F, Barth EL, De Groeve P, De Mey A. A new method of 3-D cephalometry Part I: the anatomic Cartesian 3-D reference system. *J Craniofac Surg.* 2006;17:314-325.
11. Olszewski R, Cosnard G, Macq B, Mahy P, Reychler H. 3D CT-based cephalometric analysis: 3D cephalometric theoretical concept and software. *Neuroradiology.* 2006;48:853-862.
12. Periago DR, Scarfe WC, Moshiri M, Scheetz JP, Silveira AM, Farman AG. Linear accuracy and reliability of cone beam CT derived 3-dimensional images constructed using an orthodontic volumetric rendering program. *Angle Orthod.* 2008;78:387-395.
13. Brown AA, Scarfe WC, Scheetz JP, Silveira AM, Farman AG. Linear accuracy of cone beam CT derived 3D images. *Angle Orthod.* 2009;79:150-157.
14. Olszewski R, Tanesy O, Cosnard G, Zech F, Reychler H. Reproducibility of osseous landmarks used for computed tomography based three-dimensional cephalometric analyses. *J Craniomaxillofac Surg.* 2010;38:214-221.
15. Olszewski R, Frison L, Wisniewski M, *et al*. Reproducibility of three-dimensional cephalometric landmarks in cone-beam and low-dose computed tomography. *Clin Oral Investig.* 2013;17:285-292.
16. Chien PC, Parks ET, Eraso F, Hartsfield JK, Roberts WE, Ofner S. Comparison of reliability in anatomical landmark identification using two-dimensional digital cephalometrics and three-dimensional cone beam computed tomography in vivo. *Dentomaxillofac Radiol.* 2009;38:262-273.
17. de Oliveira AE, Cevidanes LH, Phillips C, Motta A, Burke B, Tyndall D. Observer reliability of three-dimensional cephalometric landmark identification on cone-beam computerized tomography. *Oral Surg Oral Med Oral Pathol Oral Radiol Endod.* 2009;107:256-265.
18. Schlicher W, Nielsen I, Huang JC, Maki K, Hatcher DC, Miller AJ. Consistency and precision of landmark identification in three-dimensional cone beam computed tomography scans. *Eur J Orthod.* 2012;34:263-275.

19. Pittayapat P, Limchaichana-Bolstad N, Willems G, Jacobs R. Three-dimensional cephalometric analysis in orthodontics: a systematic review. *Orthod Craniofac Res.* 2014;17:69-91.
20. Baumrind S, Frantz RC. The reliability of head film measurements. 1. Landmark identification. *Am J Orthod.* 1971;60:111-127.
21. Ludlow JB, Gubler M, Cevidanes L, Mol A. Precision of cephalometric landmark identification: cone-beam computed tomography vs conventional cephalometric views. *Am J Orthod Dentofacial Orthop.* 2009;136:312.e311-310; discussion 312-313.
22. Hassan B, Nijkamp P, Verheij H, Tairie J, Vink C, Stelt PV, *et al*. Precision of identifying cephalometric landmarks with cone beam computed tomography in vivo. *Eur J Orthod.* 2013;35:38-44.

Chapter 8

Three-dimensional Frankfort horizontal plane revisited and evaluation of new horizontal planes

This chapter is based on:

Pittayapat P, Jacobs R, Odri G, Zogheib T, Lambrichts I, Willems G, Politis C, Olszewski R. Three-dimensional Frankfort horizontal plane revisited and evaluation of new horizontal planes. *Submitted.*

8.1 Abstract

Objectives: To assess in 3D the precision and reproducibility of existing landmarks used for the Frankfort horizontal plane (FH) as well as 2 new landmarks, and to evaluate the angular differences of newly introduced planes to the FH.

Materials and methods: 3D models from CBCT data of 26 dry human skulls were created in Maxilim® software. Porion (Po) and Orbitale (Or) were indicated for two possible FHs (FH 1 and FH 2). Two new landmarks, the internal acoustic foramen (IAF) and zygomatico-maxillary suture (ZyMS) were used to create new planes (Plane 1-6), closely parallel to the FH. Three observers completed the observation twice with 4 weeks interval. Angles between FH 1 and FH 2 and between FHs and Plane 1-6 were measured. Coordinates (x, y, z) were exported. Statistical analysis was performed.

Results: IAF showed significantly better both intra- and inter-observer precision than other landmarks ($p<0.0018$) and yielded the best intra-observer reproducibility (>90% of precision <1 mm) and the best inter-observer reproducibility (59-95% of precision <1 mm). Po showed poorest intra- and inter-observer precision and reproducibility. Mean angular difference between FH 1 and FH 2 was 0.7°. Two new planes approximated the FHs rather accurately (mean angle < 1°).

Conclusions: The findings showed that new landmarks (IAF and ZyMS) offered good precision and reproducibility. This study evaluated 3D FHs and demonstrated the possibility of using new planes when traditional FHs were not constructable. Future studies should focus on the validation of these findings on clinical data and their implementation in clinical practice.

8.2 Introduction

A cephalometric analysis is an essential part of orthodontic treatment planning. The technique has been used for several decades after its introduction by Hofrath (1) in Germany and Broadbent (2) in the United States. It is traditionally performed on a lateral and a frontal cephalogram. One analysis is comprised of several cephalometric landmarks.

One of the important elements in performing a cephalometric analysis is the horizontal reference plane. The Frankfort horizontal plane (FH) (also called the auriculo-orbital plane) was established at the World Congress of Anthropology, in Frankfort, Germany in 1882. First introduced by Von Ihering, in 1872, this plane used to pass through the center of the external auditory meatus to the lowest point of the inferior margin of each orbit. The Frankfort agreement then modified this definition, so that the plane would pass through the upper borders of each ear canal or external auditory meatus (Porion), and through the inferior border of the orbital rim (Orbitale). The Frankfort plane was employed for orientation of the patient and was chosen as the best anatomic indicator of the true horizontal line. It is also closely related to the natural head position (NHP) (3, 4). Although the reliability and validity of the FH for cephalometric analysis was questioned by several authors (5-9), it is still widely accepted in contemporary cephalometric use (4).

Recently, 3D imaging modalities, especially cone-beam computed tomography (CBCT), have become essential for diagnosis and treatment planning in the oral and maxillofacial region. In orthodontics, CBCT images allow 3D visualization of the craniofacial structures without any superimposition (10-12). With its relatively lower radiation doses than the multi-slice CT (MSCT) (13), this modality proves to be useful in several orthodontic aspects requiring advanced imaging such as canine impaction, root resorption, sleep disorders and orthognathic surgery. Cephalometric analysis, traditionally done on 2D radiographs, is also moving towards 3D direction.

In three-dimensional cephalometry, cephalometric landmarks are identified in 3 orthogonal planes or on 3D models with the aid of a 3D image viewing software (14, 15). The original 2D planes or lines were transformed and used in 3D cephalometry integrating within the analyses. Several publications have shown the advantages of this technique over the traditional 2D cephalometric analysis (16-18). Some publications have shown the reliability and accuracy of cephalometric landmark identification in 3D, including Po and Or which are used to form the Frankfort plane (19-24). In a few studies, it was found that precision and reliability of these two landmarks in 3D was not optimal (21-23) with only one study conducted on the 3D surface model (23). Only one publication evaluated the effect of these landmarks to the Frankfort horizontal plane in 3D magnetic resonance imaging (MRI) (25).

Therefore, the aim of this study was twofold: 1) to assess, in 3D CBCT, the precision and reproducibility of landmarks used in Frankfort horizontal plane (FH) and 2 new landmarks and 2) to evaluate the angular differences of newly introduced planes to the FH.

8.3 Materials and methods

Sample

Twenty-six dry human skulls with upper and lower first incisors and first molars present were selected from the Department of Anatomy, Hasselt University. Mandibles were fixed to the skulls using surgical tapes. The tape was wrapped around the skull, starting from the temporal area of one side, crossing the lower border of the mandible to the temporal area of the other side. The occlusion was fixed at maximum intercuspation. The study protocol was approved by the Medical Ethics Committee, University Hospitals Leuven, KU Leuven (reference number: ML6960, BE322201010078). The authors have read the Helsinki Declaration and have followed the guidelines in this investigation.

Imaging modalities

CBCT scans of the samples were taken using the largest field of view (FOV) (diameter 170 x height 120 mm) of 3D Accuitomo® 170 (J. Morita, Kyoto, Japan), using High-Fidelity (Hi-Fi) mode: 90 kVp, 154 mAs, voxel size 0.25 mm. A 1.7-mm-thick copper filter was attached in front of the X-ray source of the CBCT device during image acquisition to simulate soft tissue attenuation. CBCT data were exported to DICOM and then imported to Maxilim® software version 2.3.0.3

(Medicim NV, Sint-Niklaas, Belgium). Three-dimensional surface models were created for all samples using the full CBCT volume with 0.5 mm sub-sampling of voxels. The threshold was set at 276 to segment the hard tissues for the 3D models.

Frankfort horizontal plane analysis

A preset for Frankfort horizontal plane (FH) evaluation was created in Maxilim® software. The analysis was composed of 4 operator-indicated landmarks (8 landmarks when counting both sides) and 4 landmarks calculated by the software (Table 8.1). In 3D, a plane can be made from 3 landmarks/points, thus two possibilities of FH were created: FH 1 and FH 2 (Fig. 8.1) (Table 8.1). FH 1 was drawn using Orbitale left and right and a landmark in the middle of two Porions (mid-Po). On the other hand, FH 2 was created using left and right Porion and a landmark in the middle of the two Orbitales (mid-Or).

Based on a pilot study, two new landmarks were chosen: internal acoustic foramen (IAF) and zygomatico-maxillary suture (ZyMS). Four planes were drawn by connecting these new landmarks in combination with the traditional FH landmarks (Or and Po), thus creating Plane 1-4. In addition, these two landmarks were used to create 2 planes closely parallel to the FH (Plane 5 and Plane 6) (Table 8.1). In this study, the absolute angle differences of the 6 new planes (Plane 1-6) from the FH 1 and FH 2 were recorded.

Three observers (two dentomaxillofacial radiologists with more than 5 years of experience, one being the main operator, and one oral and maxillofacial surgeon with more than 10 years of experience) underwent an initial calibration session. Detailed instructions about landmark definition and software manipulation were given. The observers were given a few cases for training and calibration with the main operator prior to the observation. Thereafter, each observer completed the set of observations twice with a 4 week-interval.

Table 8.1 Landmarks and planes definition

Name	Definition
Landmark	
Orbitale right and left (Or-R, Or-L)	The lowest point on the inferior margin of the orbit
Porion right and left (Po-R, Po-L)	The most superior midpoint of the external auditory meatus. (anatomic Po)
Internal acoustic foramen right and left (IAF-R, IAF-L)	The most lateral point of the internal auditory meatus at the skull base
Zygomatico-maxillary suture right and left (ZyMS-R, ZyMS-L)	The zygomatico-maxillary suture line crossing at the lower orbital rim. The point is located on the inferior margin of the orbit.
mid-Po	A point in the middle between right and left Po indicated by the software
mid-Or	A point in the middle between right and left Or indicated by the software
mid-IAF	A point in the middle between right and left IAF indicated by the software
mid-ZyMS	A point in the middle between right and left ZyMS indicated by the software
Plane	
Frankfort horizontal plane 1 (FH 1)	FH by connecting mid-Po, Or-R and Or-L
Frankfort horizontal plane 2 (FH 2)	FH by connecting mid-Or, Po-R and Po-L
Plane 1	A plane connecting mid-Or, IAF-R and IAF-L
Plane 2	A plane connecting mid-Po, ZyMS-R and ZyMS-L
Plane 3	A plane connecting Or-R, Or-L and mid-IAF
Plane 4	A plane connecting Po-R, Po-L and mid-ZyMS
Plane 5	A plane connecting ZyMS-R, ZyMS-L and mid-IAF
Plane 6	A plane connecting IAF-R, IAF-L and mid-ZyMS

Statistical analysis

Coordinates (x, y, z) of all landmarks and the angular values were exported to Excel files.

The Euclidean distances (d) between coordinates for point 1 and point 2 were calculated by the formula:

$$d = \sqrt{\{(x_1-x_2)^2+(y_1-y_2)^2+(z_1-z_2)^2\}}$$

Point 1 coordinate: (x_1, y_1, z_1) = coordinate at time point 1or coordinate from observer 1

Point 2 coordinate: (x_2, y_2, z_2) = coordinate at time point 2 or coordinate from observer 2

(These are also applied for coordinates from observer 3.)

In this study, *the precision* was defined as “the mean Euclidean distance of all subjects for a specific landmark”. A distinction was made between intra- and inter-observer precision

Intra-observer precision

Intra-observer precision was defined as “the mean Euclidean distance of all subjects for a specific landmark for each observer between 2 time points”. The distances between point 1 and point 2 of each observer for all samples and all landmarks were calculated. All distances presented a log-normal distribution; therefore, parametric statistics were performed.

All data were tabulated in JMP® 10.0.0 (SAS Institute Inc., Cary, NC). Comparisons of the intra-observer precision between observers for each landmark, between landmarks for each observer and the overall precision between observers were done by a multiple paired *t*-test with Bonferroni correction. Comparison of the intra-observer precision between samples was done using ANOVA.

Inter-observer precision

Inter-observer precision was defined as “the mean distance of all subjects of a specific landmark for each pair of observers”. The Euclidean distances between each time point of each observer for each anatomical landmark and each sample was calculated. All distances were positive and normally distributed. Four distances between each pair of observers were measured for each combination of time points. The comparison of these 4 distances was performed using a multiple paired *t*-test with Bonferroni correction. As no significant difference was observed, the data were pooled together.

Comparisons of inter-observer precision between landmarks regardless of observers, between observers regardless of landmarks, between observers for each landmark and lastly between landmarks for each pair of observers were done using a multiple paired *t*-test with Bonferroni correction.

Reproducibility

The reproducibility was presented as a percentage and categorized into 3 levels, determined as the percentage of the precision < 0.5 mm, < 1 mm, and ≥ 1 mm. In this study, a good reproducibility referred to >50% of precisions being < 1 mm. A moderate reproducibility was determined when 51-75% of precisions were > 1 mm and a poor reproducibility was determined when >75% of precisions were >1.

Angular measurements between planes

All angular values showed a normal distribution (Shapiro-Wilk test). A statistical analysis was performed.

8.4 Results

Intra-observer precision and reproducibility

Table 8.2 presents the mean precision at a 95% confidence interval (CI). Comparison of the intra-observer precision between 3 observers for each landmark showed significant differences (multiple paired *t*-test with Bonferroni correction, $p<0.0167$). A significant difference between the intra-observer precision for the three observers was observed for Po-R and Po-L, showing that the precision of Observer 1 and 3 was better than the precision of Observer 2.
The precision of the IAF-R and IAF-L landmarks was significantly better than the other landmarks ($p<0.0018$) after comparing the intra-observer precision between 8 landmarks for each observer. No statistically significant difference between the precisions for each sample was observed.

Table 8.2 Intra-observer precision (mm) according to landmarks and observers. The overall precision of all landmarks of each observer is presented at the bottom row.

	Observer 1		Observer 2		Observer 3	
Landmark	Mean	CI 95%	Mean	CI 95%	Mean	CI 95%
Or-R	1.26	0.92-1.7	1.06	0.68-1.64	0.74	0.52-1.06
Or-L	0.83	0.54-1.26	1.14	0.79-1.65	0.64	0.41-1.00
Po-R	1.22	0.88-1.67	2.21	1.55-3.15	0.94	0.68-1.31
Po-L	0.76	0.57-1.03	2.58	2.00-3.33	0.77	0.54-1.10
IAF-R	0.40	0.30-0.53	0.37	0.28-0.48	0.23	0.16-0.34
IAF-L	0.39	0.29-0.52	0.37	0.26-0.52	0.33	0.23-0.47
ZyMS-R	0.90	0.59-1.36	1.16	0.80-1.67	0.59	0.38-0.91
ZyMS-L	0.83	0.52-1.34	1.12	0.73-1.72	0.61	0.42-0.90
Overall precision	0.76	0.67-0.87	1.02	0.88-1.19	0.56	0.48-0.64

The overall precision of the 3 observers was compared and it was found that Observer 3 showed significantly better overall precision than the precision of

Observer 1 and Observer 1 also showed significantly better overall precision than Observer 2 (p<0.0167).

Table 8.3 shows the intra-observer reproducibility expressed as a percentage (%). The landmark reproducibility was moderate to poor for Po and Or in 2 observers. The best reproducibility was observed for IAF-R and IAF-L (> 90% of precision below 1 mm).

Table 8.3 Intra-observer reproducibility for each observer. Percentage of the precision in locating landmarks < 0.5 mm, 0.5-1 mm and > 1 mm

Landmark	Observer 1			Observer 2			Observer 3		
	0-0.5	0.5-1	>1	0-0.5	0.5-1	>1	0-0.5	0.5-1	>1
Or-R	12	24	64*	20	24	56*	36	32	32
Or-L	20	28	52*	20	24	56*	44	24	32
Po-R	12	20	68*	12	8	80*	24	28	48
Po-L	20	48	32	0	4	96*	36	28	36
IAF-R	56	40	4	68	24	4	88	12	4
IAF-L	56	40	4	60	32	8	80	12	8
ZyMS-R	32	32	36	16	36	48	44	28	28
ZyMS-L	28	28	44	20	32	48	48	28	24

* >50%

Inter-observer precision and reproducibility

The inter-observer precision according to landmarks is shown in Table 8.4. The results revealed that IAF-R (mean inter-observer precision = 0.61 mm) and IAF-L (mean inter-observer precision = 0.57 mm) had a significantly better precision than all the other landmarks (p<0.0018). Po-R (2.28 mm) and Po-L (2.63 mm) showed poorest mean inter-observer precision.

Table 8.4 Inter-observer precision (mm) for individual according to landmarks

Landmark	Mean	CI 95%
Or-R	1.19	1.09-1.29
Or-L	1.40	1.29-1.53
Po-R	2.28	2.09-2.49
Po-L	2.63	2.41-2.87
IAF-R	0.61	0.56-0.67
IAF-L	0.57	0.52-0.62
ZyMS-R	1.57	1.44-1.71
ZyMS-L	2.08	1.91-2.27

When comparing the overall inter-observer precision between each pair of observers, a significant difference ($p<0.001$) was found. The inter-observer precision between Observer 2 and 3 (mean = 0.98 mm) was significantly better than that of the other pairs of observers (Observer 1 – Observer 2 mean = 1.57 mm, Observer 1 – Observer 3 mean = 1.61 mm).

Table 8.5 lists inter-observer precision in mm, taking both landmarks and observer pairs into account. It could be observed that the inter-observer precision of Po-L for 2 pairs of observers was > 3 mm. The best inter-observer precision was observed for IAF-R and IAF-L (mean < 1 mm for all pairs of observer). *For each landmark*, the inter-observer precisions between each pair of observers were compared. A significant difference ($p<0.001$) was found for all landmarks except Or-R and Or-L. Another comparison was done *for each pair of observers* between landmarks. IAF-R and IAF-L showed a significantly better precision ($p<0.001$) for all observers.

Table 8.5 Inter-observer precision (mm) according to observers and landmarks

Landmark	O1 vs O2		O1 vs O3		O2 vs O3	
	Mean	CI 95%	Mean	CI 95%	Mean	CI 95%
Or-R	1.24	1.04-1.47	1.32	1.13-1.54	1.02	0.87-1.21
Or-L	1.70	1.45-1.99	1.25	1.09-1.44	1.29	1.11-1.51
Po-R	2.38	2.11-2.68	2.98	2.64-3.35	1.67	1.42-1.97
Po-L	3.05*	2.71-3.43	3.49*	3.14-3.88	1.71	1.46-2.01
IAF-R	0.81	0.73-0.89	0.66	0.61-0.73	0.43	0.38-0.48
IAF-L	0.63	0.56-0.71	0.67	0.61-0.75	0.43	0.38-0.49
ZyMS-R	1.82	1.51-2.19	2.07	1.77-2.42	1.03	0.86-1.24
ZyMS-L	2.63	2.23-3.10	2.91	2.55-3.32	1.18	0.99-1.41

* The inter-observer precision > 3 mm

Table 8.6 presents the inter-observer reproducibility as a percentage. Po-R and Po-L showed the poorest reproducibility among landmarks with 74 to 97% of precision values > 1 mm. The best reproducibility was observed for IAF-R and IAF-L, showing 59-95% of precision values < 1 mm.

Table 8.6 Inter-observer reproducibility for each observer. Percentage of the precision in locating landmarks < 0.5 mm, 0.5-1 mm and > 1 mm

Landmark	O1 vs O2			O1 vs O3			O2 vs O3		
	0-0.5	0.5-1	>1	0-0.5	0.5-1	>1	0-0.5	0.5-1	>1
Or-R	15	24	61	8	28	64	17	34	49
Or-L	8	15	77*	9	26	65	9	28	63
Po-R	2	7	91*	1	5	94*	8	18	74*
Po-L	0	6	94*	1	2	97*	5	16	79*
IAF-R	16	43	41	19	66	15	58	37	5
IAF-L	30	49	21	19	57	24	62	28	10
ZyMS-R	8	17	75	3	12	85*	20	25	55
ZyMS-L	3	15	82*	2	3	95*	16	28	56

* > 75%

Angular measurements

A summary of angular measurements of each pair of planes is shown in Table 8.7. FH 1 and FH 2 exhibited 0.7° overall angular difference. The planes that were closest to FH 1 and FH 2 were Plane 3 (composed of Or-R, Or-L and mid-IAF) and Plane 4 (composed of Po-R, Po-L and mid-ZyMS) as the average angular difference was < 1° (Fig. 8.2).

Table 8.7 Summary angular measurements between planes (degree)

Plane	Observer 1		Observer 2		Observer 3		Overall	
	M	SD	M	SD	M	SD	M	SD
FH 1 - FH 2	0.72	0.65	0.74	0.58	0.64	0.52	0.70*	0.58
FH 1 - Plane 1	1.97	1.15	1.78	1.16	1.87	1.14	1.87	1.15
FH 1 - Plane 2	2.58	1.11	2.44	1.15	2.48	1.14	2.50	1.13
FH 1 - Plane 3	0.51	0.25	0.64	0.45	0.44	0.35	0.53*	0.37
FH 1 - Plane 4	0.84	0.60	0.86	0.56	0.77	0.47	0.82*	0.54
FH 1 - Plane 5	2.76	1.13	2.30	1.19	2.32	1.18	2.46	1.18
FH 1 - Plane 6	2.26	1.11	1.80	1.09	1.79	1.07	1.95	1.10
FH 2 - Plane 1	2.24	1.06	2.07	1.05	2.09	1.07	2.13	1.05
FH 2 - Plane 2	2.27	1.11	2.16	1.14	2.21	1.11	2.21	1.11
FH 2 - Plane 3	0.90	0.60	0.95	0.55	0.89	0.53	0.91*	0.56
FH 2 - Plane 4	0.31	0.18	0.28	0.33	0.25	0.26	0.28*	0.27
FH 2 - Plane 5	2.47	1.12	2.01	1.18	2.04	1.15	2.17	1.16
FH 2 - Plane 6	2.48	1.03	1.99	1.04	2.01	1.04	2.16	1.06

* The overall absolute angular difference < 1°

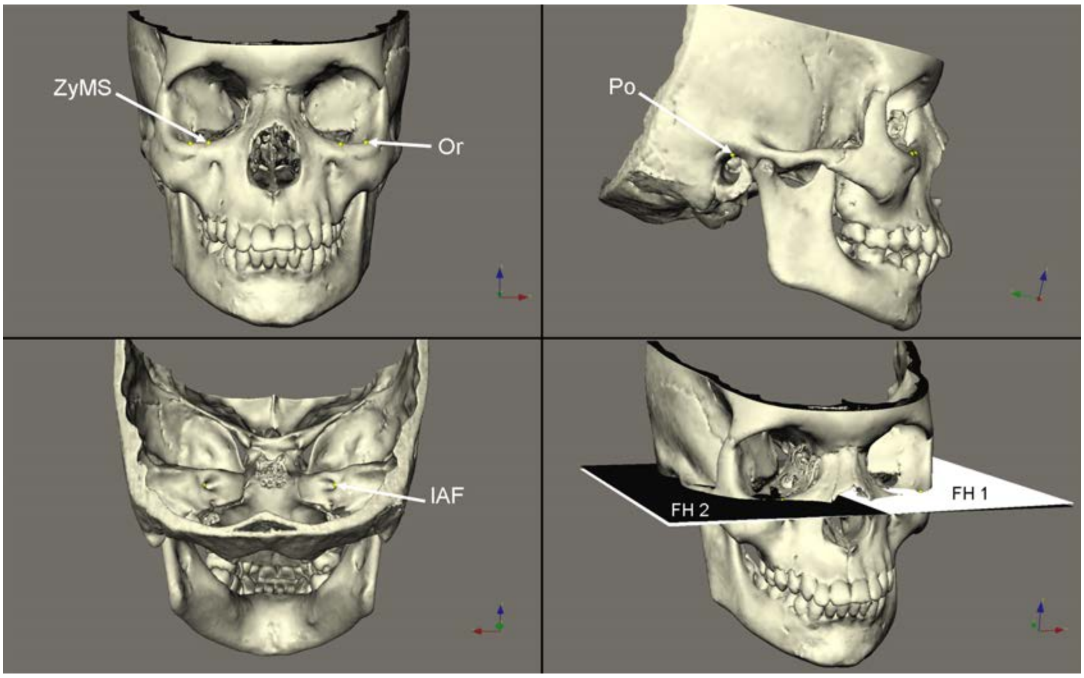

Figure 8.1 Landmarks indicated in this study. The frontal view shows Orbitale (Or-R and Or-L) and zygomatico-maxillary suture (ZyMS-R and ZyMS-L) located on the inferior orbital rim. The lateral view shows the right Porion (Po-R) and the posterior view shows the internal acoustic foramen (IAF-R and IAF-L) located at the latero-posterior point of the opening of the auditory canal inside the cranial cavity.

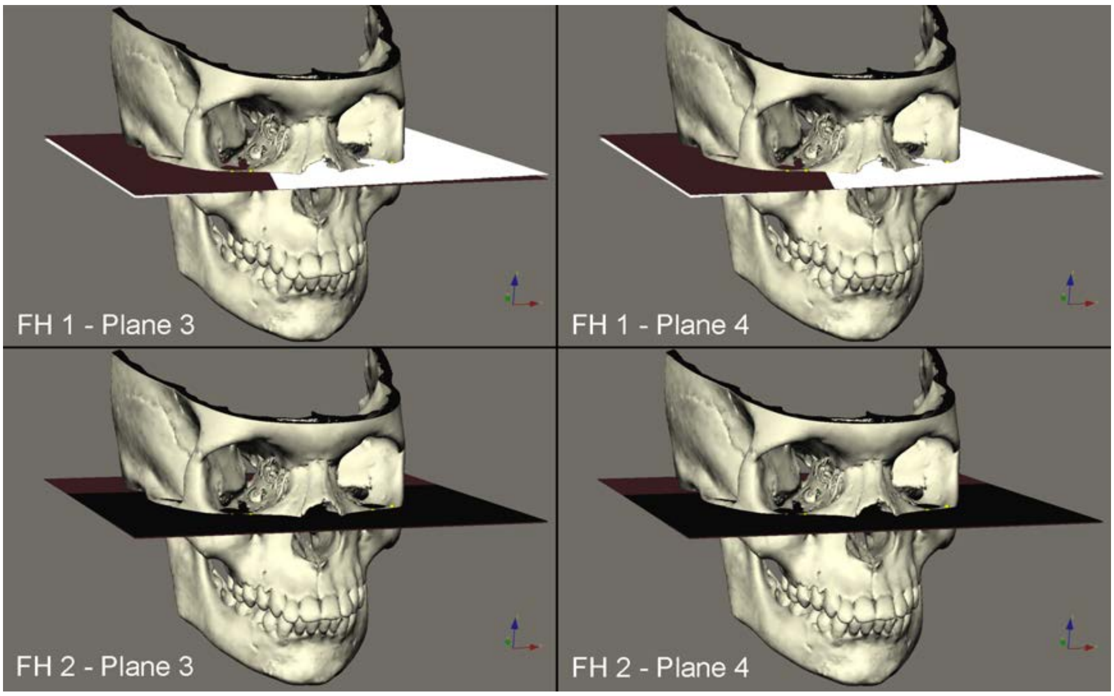

Figure 8.2 shows an example of the relationship between FH 1 (white) and FH 2 (black) to Plane 3 and Plane 4 (red). The mean differences between FH 1 and Plane 3 and 4 were 0.53° and 0.82°, respectively. The mean differences between FH 2 and Plane 3 and 4 were 0.91° and 0.23°, respectively. Both planes were closely parallel to the Frankfort horizontal plane.

8.5 Discussion

The present study investigated the precision and reproducibility of landmarks incorporated in a Frankfort horizontal plane in 3 dimensions. Frankfort horizontal plane has been used as a reference plane that closely links to the natural head position for decades. Although it has been widely used for anthropological and orthodontic purposes, as 3D imaging modalities have been emerging, still no research has been done to test its precision and reproducibility in 3 dimensions.

One study has been performed on the reproducibility of the FH plane on MRI images (25). This study revealed excellent intra- and inter-observer reproducibility and reliability of the FH plane through 3D landmark identification (25). This finding was interesting but in clinical practice, MRI images are still not widely used for orthodontic treatment. Further research is warranted on the application of MRI in orthodontics.

In the present study, new 3D landmarks that form planes closely parallel to the original FH were introduced and tested. An analysis of FH was made in order to precisely evaluate the angular differences between all pairs of planes. The results showed poorer intra- and inter-observer precision and reproducibility of the traditional FH landmarks (Po, Or) and showed good intra- and inter-observer precision and reproducibility of the new landmarks especially for IAF. From the newly proposed planes, the ones closest to the original FH are the plane formed by connecting Or-R, Or-L and mid-IAF (Plane 3) and the plane formed by connecting Po-R, Po-Land mid-ZyMS (Plane 4).

In this study, dry human skulls were used because there were too few patients in the hospital's CBCT database that fit the criteria (biggest FOV, no prominent pathology or no prominent asymmetry, and normal occlusion). Although this might pose some limitations as the dry skulls could not represent real human anatomy including soft tissues, due to ethical concerns it was not justified to take CBCT images on new patients in order to collect enough samples for this study. During image acquisition, a 1.7 mm thick copper filter was attached to the CBCT device to mimic soft tissue attenuation and to prevent any overexposure. In addition, the number of the samples was limited, because dry skulls in good condition and meeting all inclusion criteria were rare. In future studies, it would be useful to collect enough patient data in order to validate the findings in a clinical situation.

Traditionally, a Frankfort horizontal plane is indicated on a 2D lateral skull or a lateral cephalometric radiograph by placing the Porion and Orbitale landmark. There are two types of Po in 2D. One is the “machine Po” when the landmark is defined by a radiopaque marker in the ear rod as part of the cephalometric head positioning device. The other is called the “anatomic Po” which refers to the upper edge of the shadow of the auditory canal that can be seen on cephalometric films, (usually located slightly above and posterior to the machine Po) (4). The Orbitale is defined as the inferior border of the orbital rim. In this study, the anatomic Po was used because no positioning device was place in the external auditory meatus. In 3D, the real anatomical structures were used instead of the 2D shadows. As seen in a few studies and confirmed in the current pilot experiments, the reproducibility or reliability of both landmarks was found to be limited (21-23). After the pilot experiment, it was therefore opted to select other 2 new landmarks (IAF and ZyMS).

The internal acoustic meatus (IAF) was chosen because of its good visualization and because it relates with a traditional landmark, Porion, as it refers to the other end of the auditory canal. The upper edge of the oval shape was not selected because it was not well-defined; instead, the lateral end was chosen and defined as a landmark because of its corner-like area which is more well-defined. In clinical CBCTs of patients, this landmark is well visible but it must be noted that this landmark will only be included when the diameter of the CBCT FOV is big enough to cover the cranial cavity. A big FOV diameter (17 cm) was used in the present study.

The zygomatico-maxillary suture (ZyMS) was selected as it is close to the traditional Orbitale but might be more visible. A thin line or a notch on the inferior orbital rim is usually seen on the 3D model and could be identified as ZyMS. It must be noted that during the making of 3D models, this landmark could be made invisible by the software processing of the surface model. When the surface was smoothened, the ZyMS, which only appears as a notch, may not be visible for identification.

The results showed that the intra-observer mean precision and reproducibility of IAF-R and IAF-L (<0.5 mm) were statistically significantly better than other landmarks (Table 8.2). The reproducibility of Po and Or was moderate to poor for some observers. The same trend was found with the inter-observer precision and reproducibility. IAF-R and IAF-L had a significantly better precision than all the other landmarks (p<0.0018) and Po-R and Po-L were the poorest. These findings were in agreement with previous publications (21-23).

Ludlow *et al.* (21) compared the precision of cephalometric landmarks on lateral cephalograms and multi-planar reformatting images (MPR) of CBCT. It was reported that Po showed poorer precision on MPR images than other landmarks (21). Later in 2012, Schlicher *et al*. (22) reported that the Po was the most inconsistent landmark and the Or was the most imprecise landmark from the study conducted on MPR images (22). The same findings were also observed in the study by Hassan *et al*. (23), in which the precision of cephalometric landmark identification from CBCT data on both MPR and 3D models of 10 patients was evaluated. It was reported that the poorest precision was that of the Po. The precision of Or was moderate (23).

One issue that must be discussed and improved in 3D is the definitions of landmarks, especially of the Po. 2D definitions are normally based on shadows on conventional radiographs but when transforming to 3D, another dimension must be accounted for. The Po is located on the curvature at the opening of the external auditory canal (EAC) and it is usually difficult to define the "most superior midpoint" of that opening. In 3D cephalometry, it may be recommended to modify this definition for a more robust location of this landmark. It was shown in a study by de Oliviera *et al.* (20) that good definitions of landmarks could help improve observer performance.

It was also shown in both intra- and inter-observer precision that the observer is one of the key factors affecting the results. For the intra-observer precision, some observers were significantly better than others and for the inter-observer precision, some pairs of observers had a better inter-observer precision than other pairs. In this study, the main operator who had the most experience using the CBCT software showed the best precision. The other 2 observers (1 dentomaxillofacial radiologist with more than 5 years of experience and 1 oral and maxillofacial surgeon with more than 10 years of experience), unlike the main operator, had only little experience in using 3D image viewing software prior to the observations, an their results showed poorer in precision. Normally, observer performance could be biased by several factors such as background experience, familiarity of the observers to the software, landmark definitions and ability of the observer to identify landmarks according to these definitions. A training and calibration session was essential to reduce bias and inter-observer variability, enabling more robust conclusions to be drawn.

It was found from the results that FH 1 and FH 2 exhibited a clinically negligible average of 0.7° overall angular difference. The question was raised which FH should be used for 3D cephalometric analysis. There are several factors contributing in the selection. It should be noted that this study was done on *in-vitro* samples and all landmarks were clearly visible without the noise created from soft tissue. In clinical circumstances, CBCT scans may not offer well-defined 3D models and it is possible that noise and artifacts may affect the image quality (26). First of all, if both Po and Or are clearly visible, it might be wiser to use FH 1. FH 1 utilizes an average of Po-R and Po-L (mid-Porion) so the Po, which scored lower in terms of precision, may give less impact to the plane. Secondly, as it was shown in the results that Plane 3 and Plane 4 were very close to both FHs, they could be used as an alternative when Po or Or are not clearly visible, keeping in mind that the angulation difference of these planes to normal FH is approximately 0.3-0.9°. Plane 3 (composed of Or-R, Or-L and mid-IAF) may improve precision and reproducibility as compared to Plane 4 (composed of Po-R, Po-L and mid-ZyMS), because precision and reproducibility of Or was better than Po, while IAF yielded better scores than ZyMS.

In this study, a 3D evaluation of the Frankfort horizontal plane was conducted. Further studies should be performed in continuation of this study in order to verify and validate the proposed reference planes on clinical CBCT data meanwhile also increasing the sample size. Once a landmark system is validated on larger clinical datasets, it can be integrated into 3D cephalometric analyse software.

8.6 Conclusions

The present study investigated the precision and reproducibility of landmarks incorporated in a Frankfort horizontal plane in 3 dimensions. The results revealed poorer intra- and inter-observer precision and reproducibility of the traditional FH landmarks (Po, Or) and showed good intra- and inter-observer precision and reproducibility of the new landmarks, especially for IAF. This study also demonstrated the possibility of using new planes when traditional FHs were not feasible. Future studies should focus on the validation of these findings on clinical data and their implementation in clinical practice.

8.7 References

1. Hofrath H. Bedeutung der Röntgenfern und Abstands Aufnahme für die Diagnostik der Kieferanomalien. *Fortschr Orthod*. 1931;1:231-58.
2. Broadbent BH. A new x-ray technique and its application to orthodontia. *Angle Orthod*. 1931;1:45-66.
3. Ricketts RM, Schulhof RJ, Bagha L. Orientation-sella-nasion or Frankfort horizontal. *Am J Orthod*. 1976;69:648-54.
4. Proffit WR, Fields HW, Jr., Sarver DM. Contemporary Orthodontics. 4th ed. St.Lois, MO: Elsevier Mosby; 2007.
5. Bjerin R. A comparison between the Frankfort Horizontal and the sella turcica-nasion as reference planes in cephalometric analysis. *Acta Odontol Scand*. 1957;15:1-13.
6. Lundstrom A. Orientation of profile radiographs and photos intended for publication of case reports. *Proc Finn Dent Soc*. 1981;77:105-11.
7. Lundstrom A, Lundstrom F, Lebret LM, Moorrees CF. Natural head position and natural head orientation: basic considerations in cephalometric analysis and research. *Eur J Orthod*. 1995;17:111-20.
8. Lundstrom A, Lundstrom F. The Frankfort horizontal as a basis for cephalometric analysis. *Am J Orthod Dentofacial Orthop*. 1995;107:537-40.
9. Madsen DP, Sampson WJ, Townsend GC. Craniofacial reference plane variation and natural head position. *Eur J Orthod*. 2008;30:532-40.

10. Kau CH, Richmond S, Palomo JM, Hans MG. Three-dimensional cone beam computerized tomography in orthodontics. *J Orthod*. 2005;32:282-93.
11. Mah JK, Huang JC, Choo H. Practical applications of cone-beam computed tomography in orthodontics. *J Am Dent Assoc*. 2010;141:7S-13S.
12. van Vlijmen OJ, Kuijpers MA, Berge SJ, Schols JG, Maal TJ, Breuning H*, et al.* Evidence supporting the use of cone-beam computed tomography in orthodontics. *J Am Dent Assoc*. 2012;143:241-52.
13. Pauwels R, Beinsberger J, Collaert B, Theodorakou C, Rogers J, Walker A*, et al.* Effective dose range for dental cone beam computed tomography scanners. *Eur J Radiol*. 2012;81:267-71.
14. Swennen GR, Schutyser F, Barth EL, De Groeve P, De Mey A. A new method of 3-D cephalometry Part I: the anatomic Cartesian 3-D reference system. *J Craniofac Surg*. 2006;17:314-25.
15. Olszewski R, Cosnard G, Macq B, Mahy P, Reychler H. 3D CT-based cephalometric analysis: 3D cephalometric theoretical concept and software. *Neuroradiology*. 2006;48:853-62.
16. Periago DR, Scarfe WC, Moshiri M, Scheetz JP, Silveira AM, Farman AG. Linear accuracy and reliability of cone beam CT derived 3-dimensional images constructed using an orthodontic volumetric rendering program. *Angle Orthod*. 2008;78:387-95
17. Brown AA, Scarfe WC, Scheetz JP, Silveira AM, Farman AG. Linear accuracy of cone beam CT derived 3D images. *Angle Orthod*. 2009;79:150-7.
18. Olszewski R, Tanesy O, Cosnard G, Zech F, Reychler H. Reproducibility of osseous landmarks used for computed tomography based three-dimensional cephalometric analyses. *J Craniomaxillofac Surg*. 2010;38:214-21..
19. Chien PC, Parks ET, Eraso F, Hartsfield JK, Roberts WE, Ofner S. Comparison of reliability in anatomical landmark identification using two-dimensional digital cephalometrics and three-dimensional cone beam computed tomography in vivo. *Dentomaxillofac Radiol*. 2009;38:262-73.
20. de Oliveira AE, Cevidanes LH, Phillips C, Motta A, Burke B, Tyndall D. Observer reliability of three-dimensional cephalometric landmark

identification on cone-beam computerized tomography. *Oral Surg Oral Med Oral Pathol Oral Radiol Endod*. 2009;107:256-65.

21. Ludlow JB, Gubler M, Cevidanes L, Mol A. Precision of cephalometric landmark identification: cone-beam computed tomography vs conventional cephalometric views. *Am J Orthod Dentofacial Orthop*. 2009;136:312 e1-10; discussion -3.
22. Schlicher W, Nielsen I, Huang JC, Maki K, Hatcher DC, Miller AJ. Consistency and precision of landmark identification in three-dimensional cone beam computed tomography scans. *Eur J Orthod*. 2012;34:263-75.
23. Hassan B, Nijkamp P, Verheij H, Tairie J, Vink C, Stelt PV*, et al.* Precision of identifying cephalometric landmarks with cone beam computed tomography in vivo. *Eur J Orthod*. 2013;35:38-44.
24. Pittayapat P, Limchaichana-Bolstad N, Willems G, Jacobs R. Three-dimensional cephalometric analysis in orthodontics: a systematic review. *Orthod Craniofac Res*. 2014;17:69-91.
25. Daboul A, Schwahn C, Schaffner G, Soehnel S, Samietz S, Aljaghsi A*, et al.* Reproducibility of Frankfort horizontal plane on 3D multi-planar reconstructed MR images. *PLoS One*. 2012;7:e48281.
26. Bamba J, Araki K, Endo A, Okano T. Image quality assessment of three cone beam CT machines using the SEDENTEXCT CT phantom. *Dentomaxillofac Radiol*. 2013;42:20120445.

Chapter 9

General discussion and conclusions

9.1 Overview of thesis contributions

After several decades that conventional 2D radiographs have maintained its use for orthodontic treatment planning, 3D imaging especially acquired from the cone-beam computed radiograph has been gradually gaining ground. It has proven itself that it can overcome the 2D limitations and downsides but many aspects still need to be proven.

This present thesis addresses the use of 2D and 3D imaging in orthodontic treatment planning. The primary goal of this doctoral thesis was to investigate the use of 3D images in orthodontics compared to the conventional 2D modalities: the panoramic radiography and lateral cephalogram. All detailed hypotheses were explained in **Chapter 1.**

In this general discussion, summary findings of each chapter are discussed. Then some important issues are elaborated and future prospects of this topic are critically addressed. Finally, the general conclusion of this doctoral thesis is stated.

9.2 Part I Literature review

In **Chapter 2,** a systematic review on 3D cephalometry was conducted. The study focused mainly on the scientific evidence of diagnostic efficacy of 3D cephalometry. Although there have been numerous publications related to 3D cephalometry, there was no proper systematic review reported on this topic.

For 2D cephalometry, a systematic review was published (1). Yet, the latter surprisingly revealed that there was still lack of scientific evidence on the usefulness of the 2D technique. More rigorous research on a larger study population should be performed to achieve full evidence on this topic (1).

In the current review, most of the publications were about the measurement accuracy and landmark identification. This review was conducted based on the Cochrane guideline on the systematic review on diagnostic accuracy (2, 3). The radiographic guideline on the efficacy of diagnostic imaging was adapted from the published criteria (4). Quality of the publications was scored based on QUADAS tools (5-7) and PRISMA statement (8, 9) was opted for the publication.

During the process of forming the study design and creating inclusion criteria and protocols (Protocols 1 and 2), it was clear that cephalometric analysis is a unique diagnostic method unlike other diagnostic radiographs or tests. When a cephalometric analysis is performed, the results will help clinicians to determine the treatment planning but it does not necessary mean that the patients are diagnosed with a disease or no disease. Therefore, when developing the study design, the protocols have to be adapted to suit the nature of the cephalometry.

The results of the review showed that the scientific evidence on diagnostic efficacy of 3D cephalometry was limited and no study on diagnostic thinking and therapeutic efficacy was found. These findings suggest that the topic is still fairly new although it has been used already in some clinical practices around the world. Thus, more concrete studies need to be done on this topic.

The findings also demonstrate that methods of conducting research in this area are crucial. Radiation exposure to young patients is one of the main concerns. 3D cephalometry requires low-dose MSCT or CBCT scan with a big FOV (10, 11). Although the technology of CBCT has been continuously developed and improved to gain good image quality with lesser radiation but FOV size is still one of the factors affecting the radiation dose (12). Not many patients will be justified to have big FOV CBCT images taken without a significant pathology of the craniofacial region. Consequently, the 3D cephalometric studies usually had too small number of subjects. This limitation is also quite similar to the 2D cephalometric studies (1).

From the currently limited scientific evidence, it is doubtful to conclude that 3D cephalometry can generally improve the treatment planning and treatment outcome of orthodontic patients. More rigorous researches with well-designed methodology are necessary on this topic to ensure its usefulness in clinical orthodontic treatment.

9.3 Part II Panoramic imaging

Panoramic radiography is an important diagnostic tool in daily dental practice. It has been used widely for an overview look on patient's oral health and condition since its introduction in 1950s (13) although bearing in mind its limitation and geometric distortion (14-17). For orthodontic treatment, orthodontists use it for initial gathering patient's information of which later will be used to develop a treatment plan for each individual.

In this 2nd part of the thesis, panoramic images from the conventional 2D method and from the 3D derived view were investigated and compared.

First, in **Chapter 3,** we compared *in vitro* subjective image quality and diagnostic validity of reformatted panoramic views from CBCT with digital panoramic radiographs, regarding orthodontic treatment planning.

In this study, one digital panoramic machine was used as a clinical standard. Nine CBCT devices and 1 MSCT were included as 3D imaging modalities. The number of samples was quite limited due to the travel limitation and the lack of skulls.

During the panoramic view reformation, curves were manually drawn in the OnDemand® software, marking several points to create optimal panoramic curves for both upper and lower jaw (Fig. 3.1). Then, persepctively from the curve, a panoramic image was created with different selection of slice thicknesses. The panoramic curves from each scan with the same sample were compared on an axial view to achieve comparable panoramic reformatted images. This process might produce an error or a slight difference between each panoramic view. With new technology and software provided on the market, registration of 2 CBCT volumes can be done to achieve an accurate image slice which may result in a better comparison (18-20).

The study concentrated on a subjective image quality and a visualization of anatomical landmarks that are commonly assessed in panoramic radiographs. Image quality assessment of cone-beam CT has been published in many studies (21-23) but this study design did not aim to quantify the image quality in terms of noise or artifacts, but rather more in terms of clinical usage.

The results revealed that although the digital panoramic radiograph showed better image quality, some reformatted panoramic view from particular CBCT devices could achieve comparable image quality and visualization of anatomical structures. This finding offers scientific evidence that a reformatted panoramic view can be used and can give basic information normally obtained from a panoramic radiograph.

It has been known that CBCT images can assist and provide necessary information for specific orthodontic cases such as canine impaction, root resorption and an air-way evaluation (24-30). However, so far there is little evidence that CBCT helps in general orthodontic treatment planning (31). Therefore, another study was completed on panoramic imaging but this time more concentrated on the real use of CBCT data for orthodontic treatment planning considering the information usually gathered from panoramic radiograph. The study was presented in **Chapter 4**.

The study was designed to compare the agreement between observers for CBCT and digital panoramic radiographs related to initial orthodontic evaluation in the situation where CBCT images were a priori requested. It was stated clearly that the study was not meant to test differences or indicate superiority of 3D imaging in general or CBCT imaging more specifically. It was aimed to evaluate the suitability of CBCT for initial orthodontic evaluation, when a CBCT scan was indicated and a priori taken for some specific indication. This point must be discussed as currently radiation doses of CBCT to children and young patients must be taken into account. This research was performed retrospectively; therefore, no patient was exposed deliberately in order to fit the inclusion criteria. Data were collected from the hospital database and patients with both panoramic radiograph and CBCT images were carefully selected. It must be admitted that there might be some inherent biases because the patients were referred for an additional CBCT on top of a panoramic radiograph with some present indications that might have affected the results.

This was a questionnaire-based study. Fourteen questions about initial orthodontic evaluation were asked to the observers while viewing each image, either panoramic image or CBCT. The observers' reply was not compared to the real case findings (clinical standard); therefore, only agreement between the answers from 2 types of imaging groups could be evaluated.

The results showed that the agreement between the CBCT and panoramic radiograph is good and CBCT showed its ability to give all necessary information for initial orthodontic evaluation. Although the results only showed moderate agreement between panoramic and CBCT images but when looking in details, it was revealed that CBCT offered a greater depth of information about the patient' s conditions, e.g. the exact location of the impacted maxillary canine, leading to some disagreement in the observers' replies.

This part of the doctoral thesis addresses the ability of cone-beam CT to gain the amount of information that traditionally achieved by panoramic radiography. Some CBCT devices have proven their capacity to provide optimal reformatted panoramic views, mimicking a digital panoramic radiograph. Further, the whole CBCT volume also proved that it could offer necessary information for an initial orthodontic evaluation. It must be noted that this is applied only when big FOV CBCT images were taken prior to the panoramic radiograph. Radiation dose is undoubtedly one of the important issues when considering of the use of CBCT in orthodontic treatment. Lowering its dose to the level of panoramic imaging might reinforce its justification. The CBCT ability may finally help reduce the radiation burden to patients and that the clinician may be able to skip panoramic radiograph and maximally utilize the already existing CBCT images.

9.4 Part III Cephalometric imaging

After focusing on the 1st imaging modality, panoramic radiography, this part of the doctoral thesis investigated the 2nd imaging modality used in orthodontic treatment, the cephalometric imaging. The cephalometric technique was introduced several decades ago (32, 33) and has been used continuously since then. Traditionally, a cephalometric analysis or cephalometry is usually performed on 2 radiographic views. The first view is a lateral cephalography which is used for a cephalometric tracing in order to assess patients' craniofacial relationship and to form an individual's treatment plan. The 2nd view is or a frontal cephalography or it can be called a postero-anterior skull radiography (34). This imaging view and analysis are used specifically in patients with asymmetric craniofacial structures. In the past, using these 2 views together was called "a 3D cephalometry" although only the image projections were used and not the realistic 3 dimensions. In this doctoral project, only a lateral cephalogram is focused because this modality is more for general orthodonctic use, irrespective of any patients' condition.

Beginning with **Chapter 5.** In this chapter, the linear measurement accuracy of 3 imaging modalities: two lateral cephalograms and one 3D model from CBCT data, was evaluated. The two lateral cephalometric devices had a difference in source-to-mid-sagittal-plane distance (SMD). One machine is equipped with 1.5-meter SMD distance, and the other has 3-meter SMD.

Several studies have investigated the linear measurement accuracy of 3D CT or CBCT (35-38) and sometimes also compared with the 2D measurements (39-41) but no English publication covered the investigation using a 3-meter SMD cephalmetric device.

For the 3D modality, CBCT data of dry human skulls were used thus posed as a limitation as no soft tissue was present. Although a 1.7 mm thick copper filter was used to mimic soft tissue attenuation, still the images cannot be compared to images of patients obtained from real clinical settings. No fiducial marker was placed prior to image acquisition in order to mimic the clinical situation as much as possible as landmark identification factor is one of the variables causing the measurement errors (42).

3D surface models of CBCT data created from Maxilim® software showed good quality model but it must be kept in mind that these models were created from *in-vitro* subjects without soft tissues; therefore, less noise and artifacts were expected in the scans. As a result, there were fewer problems in removing noises or unwanted artefact from the images.

The results showed the accuracy of the measurements based on CBCT surface model and 1.5-meter SMD cephalogram was better than a 3-meter SMD cephalogram and a better observer agreement for 3D measurements. These findings have confirmed the knowledge about 3D measurements accuracy and reliability and also again proved its potential benefits in 3D cephalometric analysis.

During the first half of the thesis, 2D and 3D comparisons were completed and subsequently the doctoral project was later concentrated on the 3D modality. In **Chapter 6, 7** and **8**, 3D cephalometry was meticulously investigated. The research on 3D cephalometry was divided into different studies to be able to evaluate each element in detail.

Observations of these 3 studies were performed on 3D models and coordinates of each landmark in 3D (x, y, z) were used. Unlike measurements in 2D, it was much more difficult to obtain a gold standard in 3 dimensions. Euclidean distances between coordinates were calculated and presented in precision (mm). The results of landmark reproducibility were presented in percentage by categorizing into 3 levels: < 0.5 mm, < 1 mm, and > 1 mm.

At the study design process of these 3 studies, the aim was to use only 3D surface models but it was later found that some errors could occur during the 3D segmentation process (43). The threshold selection for CBCT data is very variable and not as constant as the threshold for MSCT data. The intensity values in CBCT images are influenced by device, imaging parameters and positioning (44,45). Many authors have attempted to compare CBCT bone density to Hounsfield values and to apply CBCT bone density value for clinical use (44-48). As many factors can influence the CBCT density value, more studies are needed (44-48). Therefore, using 3D surface models with the confirmation from MPR images may help decrease the error and also aid the clinicians in landmark identification.

In **Chapter 6**, the sella turcica landmark (S), which was one of the most commonly used cephalometric and craniometric landmarks (34), was studied in order to develop a new reference system to improve its reproducibility in 3D. The system was developed in a way that this landmark could be localized on a 3D surface model without using a 2D cephalometric image derived from 3D CBCT as commonly used in 3D software (49).

Many publications have described about its morphology and variation in shape and size (50-56); therefore, patient's CBCT scans without any significant pathology, anatomical variation or asymmetry were retrospectively selected out of the database.

The results showed that the new landmarks-based reference system offered high precision and reproducibility for sella turcica identification in 3 dimensions without based on 2D images generated from 3D data.

In **Chapter 7** and **Chapter 8,** the study designs were slightly different from **Chapter 6**, as CBCT scans of dry human skulls were used instead of CBCT scans from patients. This was intentionally planned because big FOV CBCT data from patients that passed the inclusion criteria was rare. In these 2 chapters, the number of samples was limited at 26 skulls as the dentate skulls that met the inclusion criteria were also scarce.

In **Chapter 7**, the focus moved on to another element of 3D cephalometry, mandibular cephalometric landmarks (Pog, Gn, Me and point B). These landmarks form a part of several important angular measurements (34). The study was aimed to develop a new reference system to systematically improve the reproducibility of mandibular cephalometric landmarks in 3D, without having to 2D lateral cephalometric views from 3D data.

The results revealed moderate to good overall precision and reproducibility for mandibular cephalometric midline landmark identification although it was observed that Pog and B posed some difficulties. The location of the landmark situated on a curved surface could affect the accuracy of its identification (57).

It might be of interest to continue on this path of research and try to utilize the MPR view of the scans as a study was published suggesting that utilizing both 3D models and MPR images could improve the precision of landmark identification (58).

Chapter 8 is the last study on 3D cephalometry of this doctoral thesis**.** In this chapter the Frankfort horizontal plane (FH) was revisited but this time in three dimensions. The Frankfort plane has been used as a horizontal reference plane for anthropologic and cephalometric measurements since the late 19th century (34, 59). Its reliability and validity for cephalometric analysis was questioned by some authors (60-64) but it is still widely used today, even in 3D cephalometry.

This last study aimed to evaluate the Frankfort horizontal plane in 3D; focusing on the precision and reproducibility of landmarks that form Frankfort horizontal plane (Po, Or) and two newly chosen landmarks (IAF and ZyMS). Secondly, it aimed to assess angular differences of the new planes compared to the Frankfort plane in 3D.

The findings demonstrated that the precision and reproducibility of Po and Or was moderate, which were similarly shown in a few published studies (58,65,66). IAM and ZyMS showed good precision and reproducibility. New reference planes that yielded results closest to the FHP were 1) the plane that was composed of Or-R, Or-L and mid-IAF and 2) the plane that was composed of Po-R, Po-L and mid-ZyMS with less than 1° different from the tested FHs. This study offers the possibility of using new planes when traditional FHs are not constructible.

This part of the doctoral thesis both confirmed the knowledge on 2D and 3D cephalometry and developed a more robust system for a future 3D cephalometric analysis.

9.5 General discussion

In this section of the discussion, important aspects related to research within the field were discussed point-by-point. Some issues were evident while conducting the systematic review and some were found during the experiments.

Experimental set-up

It was apparent while conducting the systematic review that the cephalometry was a distinct diagnostic method that could not be included in general diagnostic imaging. The design of all protocols must be adapted to fit well with its uniqueness (4).

With this uniqueness, it became clear that it had also an effect on the experimental design of research on this topic which caused the studies to be categorized in a low-level of evidence due to its questionable quality assessed by QUADAS (6). These factors were listed below:

1) *Sample*

The type of samples represents the population which, in this case, refers to orthodontic patients. As the study design mostly required radiographic images, the ethic must be concerned.

In two-dimensional cephalography, the patients were usually exposed and lateral cephalograms were collected. This imaging modality is used widely for patients' treatment planning. On the contrary, when the study involved three-dimensional modality, usually the 3D images were defined as and 'extra' or 'additional' radiographic images which are used to gain more information to assist with the patient's treatment planning process. In some specific cases such as canine impaction, supernumerary teeth, root resorption and orthognathic surgery, 3D images are necessary.

To retrospectively collect a big FOV CBCT data may not be feasible as there are not enough cases with such big FOV for 3D cephalometric analysis and also patients these scans usually had some specific indications and pathology that must be ruled out from the study. To acquire big FOV CBCT images from a healthy patient with no indication cannot be achieved because the radiation dose the patient will receive from these CBCT is still generally higher than a panoramic radiograph and a lateral cephalogram (12,67,68).

With this limitation, many studies decided to use *in-vitro* samples such as dry skulls, formalin-fixed human heads or a fabricated phantom. These samples are useful in conducting a research that the samples need to be exposed by X-ray. However, these samples cannot represent real human condition. Dry skulls lack soft tissue which may cause overexposure of the images if the parameter is not correctly adjusted or a radiation filter is not used. Formalin-fixed heads, although having soft tissue, the density of the formalin-embalmed soft tissues is usually different from living soft tissues (69). A fabricated phantom may be useful to test and investigate and help quantify some fixed variables but it frequently does not represent a real human head. Some phantoms are in a shape of human head with embedded human skulls but these phantoms are expensive. Many researches have encountered not only the type of samples but also the number of samples to reach an optimal level of statistical outcome, as the number of these *in-vitro* samples is also quite limited.

2) *Reference standard*

Another variable is a reference standard or a gold standard. To be able to evaluate the accuracy of measurements, a reference standard is needed. When the studies deal with images from patients and evaluate hard tissue measurements accuracy, it is impossible to obtain direct measurements to be used as a reference standard as the landmarks are located inside the skulls or on the surface of the bone.

Although most direct physical measurements can be obtained from a digital calliper or a 3D coordinate measuring device on *in-vitro* samples, it must embrace that the samples then will not represent a human condition.

A few studies attempted to use calculated reference standard (11,70) but it is not preferable according to QUADAS (6).

Radiation dose to patients

Not only this affects the research but also it is one of the most concerned topics in using 3D imaging in orthodontic treatment. Mostly orthodontic patients are children or adolescents who are clearly more sensitive to radiation exposure than adults (71-73), thus acquiring CBCT images on these patients must receive a full attention. Many publications have reported on CBCT doses (12,72,74-76).

At this moment, it is still not justified to replace conventional radiographic method, namely panoramic radiography and lateral cephalography, with the CBCT as the effective dose that patients will receive from CBCT is generally higher than a conventional digital modality (68). When used, dental CBCT examinations should be fully justified over conventional X-ray imaging and dose optimisation by using FOV collimation and low dose settings should be achieved (12). Large FOV CBCTs should be used only with specific indications and only for the benefit of the patient because scientific evidence showed that the radiation dose received from the CBCTs is strongly related to FOV size and also dependent on the specific CBCT machine (12).

Recent guidelines on the use of CBCT imaging were published and some orthodontic application and recommendation were applied (77-81). These guidelines offer some guidance for clinicians in using CBCT while keeping the ALARA principle: *as low as reasonably achievable*.

In clinical situation, the selection of radiographic imaging should be based on patient's history, clinical examination, present radiographic imaging, and the presence of clinical symptoms for which the benefits of the diagnosis outweigh the potential risks of exposure to radiation. Therefore, the application of 3D cephalometric analysis and 3D orthodontic treatment planning performed and developed in this doctoral thesis should only be performed clinically when their benefits to the patients in specific cases can overcome the radiation risk. This thesis can be used as scientific evidence that priori available big FOV CBCT images could be maximally utilized for a benefit of the patients.

9.6 Clinical implications and future prospects

This doctoral thesis has helped creating a good basis for future studies by investigating both 2D and 3D imaging modality and its use in orthodontic treatment. Although the influence of the 2D and 3D imaging modality on the treatment planning and treatment outcome of orthodontic patients could not be evaluated within this doctoral thesis, the findings of this PhD project has opened a way for new studies to further improve and evaluate the use of 3D images for orthodontics.

The 3D cephalometry is one of the many elements incorporated in 3D treatment planning. In this thesis, the hard tissue part of the analysis was investigated. 3D reference systems were developed in order to improve the 3D cephalometric analysis and to build a solid base for further research.

As discussed in **the general discussion,** the experimental set-up is a crucial factor in obtaining good scientific results. The research methods of new studies must be carefully standardized in order to obtain good scientific evidence and to build a strong basis for future generation.

Continuing researches from this thesis should be conducted so that the effect of these systems on the performance of 3D cephalometry can be evaluated. How these new methods can be implemented into existing cephalometric analyses must be addressed. Subsequently, the systems should be validated and tested on patients' 3D data. Finally, an evaluation of the effect of 3D cephalometry on orthodontic treatment planning and orthodontic treatment outcome should be performed, as this is an area with the lack of available scientific knowledge (31).

With continuously developing of imaging technology, automated landmark identification may be a new approach. A few studies have been done on automated 3D landmark identification (82-84). More research and development must be employed to integrate and apply this procedure for clinical orthodontic treatment.

Another important element of the 3D treatment planning is the soft tissue (85). This is becoming more and more important especially for esthetics. To achieve a complete evaluation of the patient condition, soft tissues must be accounted for. The technology that helps clinicians evaluate soft tissue condition and change in 3D is expanding. Several publications reported that 3D facial scanning systems could be used to analyse soft tissue landmarks and soft tissue change, comparing pre- and post-operative results (86-92). Recently, an experiment was performed on a facial scanning system incorporated in a CBCT device, using a phantom head

(93). The study tested the soft tissue landmark reproducibility and the linear measurement accuracy. The results showed a promising performance of the system but a clinical study should be followed (93). When well studied, the soft tissue part should be integrated to the hard tissue analysis to give a full 3D evaluation of patient's craniofacial structures.

In addition to a static soft tissue analysis, the dynamics of the soft tissue, for example the dynamic of a smile, has become a hot topic. Smiling is very important not only for esthetics, but also important for speech and functional evaluation e.g. in patients with cleft lip and cleft palate. A few studies have been published over this topic and they have found some interesting findings about the muscle function, factors influencing the attractiveness of a smile and the dynamic movement of a smile. More studies are essential and with the help of 3D imaging technology, new findings may help lead to the more understanding of a dynamic orthodontic treatment (94-99).

9.7 Conclusions

This present doctoral thesis elaborated the use of 2D and 3D imaging modality for orthodontic treatment and showed the possibility and a new developing path to improve 3D cephalometry. Although the scientific evidence on clinical use of 3D cephalometry is limited, this project helps provide a solid basis for future studies. New studies should focus on standardized research methodology, the validation and the implementation of 3D cephalometry in clinical practice. The effect of this new development on the orthodontic treatment outcome must be investigated.

In the near future, one CBCT scan may be able to yield all necessary information and replace a cascade of 2D radiographic images while keeping the ALARA principle. Whether or not those strategies are equally valid remains to be proven.

9.8 References

1. Durao AR, Pittayapat P, Rockenbach MI, Olszewski R, Ng S, Ferreira AP*, et al.* Validity of 2D lateral cephalometry in orthodontics: a systematic review. *Prog Orthod*. 2013;14:31.
2. Higgins JPT, Green S. Cochrane Handbook for Systematic Reviews of Interventions: The Cochrane Collaboration; 2011. Available from: http://www.cochrane-handbook.org/.
3. Deeks JJ, Bossuyt PM, Gatsonis C. Cochrane Handbook for Systematic Reviews of Diagnostic Test Accuracy. : The Cochrane Collaboration; 2010. Available from: http://srdta.cochrane.org/handbook-dta-reviews.
4. Fryback DG, Thornbury JR. The efficacy of diagnostic imaging. *Med Decis Making*. 1991;11:88-94.
5. Whiting P, Rutjes AW, Reitsma JB, Bossuyt PM, Kleijnen J. The development of QUADAS: a tool for the quality assessment of studies of diagnostic accuracy included in systematic reviews. *BMC Med Res Methodol*. 2003;3:25.
6. Whiting PF, Weswood ME, Rutjes AW, Reitsma JB, Bossuyt PN, Kleijnen J. Evaluation of QUADAS, a tool for the quality assessment of diagnostic accuracy studies. *BMC Med Res Methodol*. 2006;6:9.
7. Whiting PF, Rutjes AW, Westwood ME, Mallett S, Deeks JJ, Reitsma JB*, et al.* QUADAS-2: a revised tool for the quality assessment of diagnostic accuracy studies. *Ann Intern Med*. 2011;155:529-36.
8. Liberati A, Altman DG, Tetzlaff J, Mulrow C, Gotzsche PC, Ioannidis JP*, et al.* The PRISMA statement for reporting systematic reviews and meta-analyses of studies that evaluate health care interventions: explanation and elaboration. *J Clin Epidemiol*. 2009;62:e1-34.
9. Moher D, Liberati A, Tetzlaff J, Altman DG, Group P. Preferred reporting items for systematic reviews and meta-analyses: the PRISMA statement. *BMJ*. 2009;339:b2535.
10. Olszewski R, Cosnard G, Macq B, Mahy P, Reychler H. 3D CT-based cephalometric analysis: 3D cephalometric theoretical concept and software. *Neuroradiology*. 2006;48:853-62.

11. Olszewski R, Reychler H, Cosnard G, Denis JM, Vynckier S, Zech F. Accuracy of three-dimensional (3D) craniofacial cephalometric landmarks on a low-dose 3D computed tomograph. *Dentomaxillofac Radiol*. 2008;37:261-7.
12. Pauwels R, Beinsberger J, Collaert B, Theodorakou C, Rogers J, Walker A, *et al.* Effective dose range for dental cone beam computed tomography scanners. *Eur J Radiol*. 2012;81:267-71.
13. Paatero Y. A new tomographic method for radiographing curved outer surfaces. *Acta Radiol*. 1949;32:177.
14. Tronje G, Welander U, McDavid WD, Morris CR. Image distortion in rotational panoramic radiography. I. General considerations. *Acta Radiol Diagn (Stockh)*. 1981;22:295-9.
15. Tronje G, Eliasson S, Julin P, Welander U. Image distortion in rotational panoramic radiography. II. Vertical distances. *Acta Radiol Diagn (Stockh)*. 1981;22:449-55.
16. Tronje G, Welander U, McDavid WD, Morris CR. Image distortion in rotational panoramic radiography. III. Inclined objects. *Acta Radiol Diagn (Stockh)*. 1981;22:585-92.
17. Wyatt DL, Farman AG, Orbell GM, Silveira AM, Scarfe WC. Accuracy of dimensional and angular measurements from panoramic and lateral oblique radiographs. *Dentomaxillofac Radiol*. 1995;24:225-31.
18. Nada RM, Maal TJ, Breuning KH, Berge SJ, Mostafa YA, Kuijpers-Jagtman AM. Accuracy and reproducibility of voxel based superimposition of cone beam computed tomography models on the anterior cranial base and the zygomatic arches. *PLoS One*. 2011;6:e16520.
19. Fourie Z, Damstra J, Schepers RH, Gerrits PO, Ren Y. Segmentation process significantly influences the accuracy of 3D surface models derived from cone beam computed tomography. *Eur J Radiol*. 2012;81:e524-30.
20. Almukhtar A, Ju X, Khambay B, McDonald J, Ayoub A. Comparison of the accuracy of voxel based registration and surface based registration for 3D assessment of surgical change following orthognathic surgery. *PLoS One*. 2014;9:e93402.

21. Schulze R, Heil U, Gross D, Bruellmann DD, Dranischnikow E, Schwanecke U*, et al.* Artefacts in CBCT: a review. *Dentomaxillofac Radiol*. 2011;40:265-73.
22. Bamba J, Araki K, Endo A, Okano T. Image quality assessment of three cone beam CT machines using the SEDENTEXCT CT phantom. *Dentomaxillofac Radiol*. 2013;42:20120445.
23. Pauwels R, Stamatakis H, Bosmans H, Bogaerts R, Jacobs R, Horner K*, et al.* Quantification of metal artifacts on cone beam computed tomography images. *Clin Oral Implants Res*. 2013;24 Suppl A100:94-9.
24. Kau CH, Richmond S, Palomo JM, Hans MG. Three-dimensional cone beam computerized tomography in orthodontics. *J Orthod*. 2005;32:282-93.
25. Liu DG, Zhang WL, Zhang ZY, Wu YT, Ma XC. Localization of impacted maxillary canines and observation of adjacent incisor resorption with cone-beam computed tomography. *Oral Surg Oral Med Oral Pathol Oral Radiol Endod*. 2008;105:91-8.
26. Alqerban A, Jacobs R, Souza PC, Willems G. In-vitro comparison of 2 cone-beam computed tomography systems and panoramic imaging for detecting simulated canine impaction-induced external root resorption in maxillary lateral incisors. *Am J Orthod Dentofacial Orthop*. 2009;136:764 e1-11; discussion -5.
27. Dudic A, Giannopoulou C, Leuzinger M, Kiliaridis S. Detection of apical root resorption after orthodontic treatment by using panoramic radiography and cone-beam computed tomography of super-high resolution. *Am J Orthod Dentofacial Orthop*. 2009;135:434-7.
28. Mah JK, Huang JC, Choo H. Practical applications of cone-beam computed tomography in orthodontics. *J Am Dent Assoc*. 2010;141:7S-13S.
29. Alqerban A, Jacobs R, Fieuws S, Willems G. Comparison of two cone beam computed tomographic systems versus panoramic imaging for localization of impacted maxillary canines and detection of root resorption. *Eur J Orthod*. 2011;33:93-102.
30. Bouwens DG, Cevidanes L, Ludlow JB, Phillips C. Comparison of mesiodistal root angulation with posttreatment panoramic radiographs

and cone-beam computed tomography. *Am J Orthod Dentofacial Orthop*. 2011;139:126-32.

31. van Vlijmen OJ, Kuijpers MA, Berge SJ, Schols JG, Maal TJ, Breuning H, *et al.* Evidence supporting the use of cone-beam computed tomography in orthodontics. *J Am Dent Assoc*. 2012;143:241-52.
32. Hofrath H. Bedeutung der Röntgenfern und Abstands Aufnahme für die Diagnostik der Kieferanomalien. *Fortschr Orthod*. 1931;1:231-58.
33. Broadbent BH. A new x-ray technique and its application to orthodontia. *Angle Orthod*. 1931;1:45-66.
34. Proffit WR, Fields HW, Jr., Sarver DM. Contemporary Orthodontics. 4th ed. St.Lois, MO: Elsevier Mosby; 2007.
35. Cavalcanti MG, Rocha SS, Vannier MW. Craniofacial measurements based on 3D-CT volume rendering: implications for clinical applications. *Dentomaxillofac Radiol*. 2004;33:170-6.
36. Periago DR, Scarfe WC, Moshiri M, Scheetz JP, Silveira AM, Farman AG. Linear accuracy and reliability of cone beam CT derived 3-dimensional images constructed using an orthodontic volumetric rendering program. *Angle Orthod*. 2008;78:387-95.
37. Brown AA, Scarfe WC, Scheetz JP, Silveira AM, Farman AG. Linear accuracy of cone beam CT derived 3D images. *Angle Orthod*. 2009;79:150-7.
38. Pittayapat P, Limchaichana-Bolstad N, Willems G, Jacobs R. Three-dimensional cephalometric analysis in orthodontics: a systematic review. *Orthod Craniofac Res*. 2014;17:69-91.
39. Varghese S, Kailasam V, Padmanabhan S, Vikraman B, Chithranjan A. Evaluation of the accuracy of linear measurements on spiral computed tomography-derived three-dimensional images and its comparison with digital cephalometric radiography. *Dentomaxillofac Radiol*. 2010;39:216-23.
40. Olmez H, Gorgulu S, Akin E, Bengi AO, Tekdemir I, Ors F. Measurement accuracy of a computer-assisted three-dimensional analysis and a conventional two-dimensional method. *Angle Orthod*. 2011;81:375-82.

41. Gribel BF, Gribel MN, Frazao DC, McNamara JA, Jr., Manzi FR. Accuracy and reliability of craniometric measurements on lateral cephalometry and 3D measurements on CBCT scans. *Angle Orthod*. 2011;81:26-35.
42. Perillo M, Beideman R, Shofer F, Jacobsson-Hunt U, Higgins-Barber K, Laster L, *et al.* Effect of landmark identification on cephalometric measurements: guidelines for cephalometric analyses. *Clin Orthod Res*. 2000;3:29-36.
43. Engelbrecht WP, Fourie Z, Damstra J, Gerrits PO, Ren Y. The influence of the segmentation process on 3D measurements from cone beam computed tomography-derived surface models. *Clin Oral Investig*. 2013;17:1919-27.
44. Nackaerts O, Maes F, Yan H, Couto Souza P, Pauwels R, Jacobs R. Analysis of intensity variability in multislice and cone beam computed tomography. *Clin Oral Implants Res.* 2011;22:873-9.
45. Pauwels R, Nackaerts O, Bellaiche N, Stamatakis H, Tsiklakis K, Walker A et al. Variability of dental cone beam CT grey values for density estimations. *Br J Radiol*. 2013;86:20120135.
46. Mah P, Reeves TE, McDavid WD. Deriving Hounsfield units using grey levels in cone beam computed tomography. *Dentomaxillofac Radiol*. 2010;39:323-35.
47. Reeves TE, Mah P, McDavid WD. Deriving Hounsfield units using grey levels in cone beam CT: a clinical application. *Dentomaxillofac Radiol*. 2012;41:500-8.
48. Molteni R. Prospects and challenges of rendering tissue density in Hounsfield units for cone beam computed tomography. *Oral Surg Oral Med Oral Pathol Oral Radiol*. 2013;116:105-19.
49. Swennen GR, Schutyser F, Barth EL, De Groeve P, De Mey A. A new method of 3-D cephalometry Part I: the anatomic Cartesian 3-D reference system. *J Craniofac Surg*. 2006;17:314-25.
50. Teal JS. Radiology of the adult sella turcica. *Bull Los Angeles Neurol Soc*. 1977;42:111-74.

51. Axelsson S, Storhaug K, Kjaer I. Post-natal size and morphology of the sella turcica. Longitudinal cephalometric standards for Norwegians between 6 and 21 years of age. *Eur J Orthod*. 2004;26:597-604.
52. Alkofide EA. The shape and size of the sella turcica in skeletal Class I, Class II, and Class III Saudi subjects. *Eur J Orthod*. 2007;29:457-63.
53. Andredaki M, Koumantanou A, Dorotheou D, Halazonetis DJ. A cephalometric morphometric study of the sella turcica. *Eur J Orthod*. 2007;29:449-56.
54. Alkofide EA. Sella turcica morphology and dimensions in cleft subjects. *Cleft Palate Craniofac J*. 2008;45:647-53.
55. Brock-Jacobsen MT, Pallisgaard C, Kjaer I. The morphology of the sella turcica in monozygotic twins. *Twin Res Hum Genet*. 2009;12:598-604.
56. Kjaer I. Sella turcica morphology and the pituitary gland--a new contribution to craniofacial diagnostics based on histology and neuroradiology. *Eur J Orthod*. 2012. in press.
57. Baumrind S, Frantz RC. The reliability of head film measurements. 1. Landmark identification. *Am J Orthod*. 1971;60:111-27.
58. Hassan B, Nijkamp P, Verheij H, Tairie J, Vink C, Stelt PV*, et al.* Precision of identifying cephalometric landmarks with cone beam computed tomography in vivo. *Eur J Orthod*. 2013;35:38-44.
59. Ricketts RM, Schulhof RJ, Bagha L. Orientation-sella-nasion or Frankfort horizontal. *Am J Orthod*. 1976;69:648-54.
60. Bjerin R. A comparison between the Frankfort Horizontal and the sella turcica-nasion as reference planes in cephalometric analysis. *Acta Odontol Scand*. 1957;15:1-13.
61. Lundstrom A. Orientation of profile radiographs and photos intended for publication of case reports. *Proc Finn Dent Soc*. 1981;77:105-11.
62. Lundstrom A, Lundstrom F. The Frankfort horizontal as a basis for cephalometric analysis. *Am J Orthod Dentofacial Orthop*. 1995;107:537-40.
63. Lundstrom A, Lundstrom F, Lebret LM, Moorrees CF. Natural head position and natural head orientation: basic considerations in cephalometric analysis and research. *Eur J Orthod*. 1995;17:111-20.

64. Madsen DP, Sampson WJ, Townsend GC. Craniofacial reference plane variation and natural head position. *Eur J Orthod*. 2008;30:532-40.
65. Ludlow JB, Gubler M, Cevidanes L, Mol A. Precision of cephalometric landmark identification: cone-beam computed tomography vs conventional cephalometric views. *Am J Orthod Dentofacial Orthop*. 2009;136:312 e1-10; discussion -3.
66. Schlicher W, Nielsen I, Huang JC, Maki K, Hatcher DC, Miller AJ. Consistency and precision of landmark identification in three-dimensional cone beam computed tomography scans. *Eur J Orthod*. 2012;34:263-75.
67. Gijbels F, Sanderink G, Bou Serhal C, Pauwels H, Jacobs R. Organ doses and subjective image quality of indirect digital panoramic radiography. *Dentomaxillofac Radiol*. 2001;30:308-13.
68. Grunheid T, Kolbeck Schieck JR, Pliska BT, Ahmad M, Larson BE. Dosimetry of a cone-beam computed tomography machine compared with a digital x-ray machine in orthodontic imaging. *Am J Orthod Dentofacial Orthop*. 2012;141:436-43.
69. Fonseca AA, Cherubini K, Veeck EB, Ladeira RS, Carapeto LP. Effect of 10% formalin on radiographic optical density of bone specimens. *Dentomaxillofac Radiol*. 2008;37:137-41.
70. Olszewski R, Frison L, Wisniewski M, Denis JM, Vynckier S, Cosnard G*, et al.* Reproducibility of three-dimensional cephalometric landmarks in cone-beam and low-dose computed tomography. *Clin Oral Investig*. 2013;17:285-92.
71. International Commission on Radiological Protection. Recommendations of the International Commission on Radiological Protection. ICRP Publication 103. Ann ICRP 37. Oxford, UK: Pergamon Press; 2007.
72. Ludlow JB, Davies-Ludlow LE, White SC. Patient risk related to common dental radiographic examinations: the impact of 2007 International Commission on Radiological Protection recommendations regarding dose calculation. *J Am Dent Assoc*. 2008;139:1237-43.

73. Theodorakou C, Walker A, Horner K, Pauwels R, Bogaerts R, Jacobs R*, et al.* Estimation of paediatric organ and effective doses from dental cone beam CT using anthropomorphic phantoms. *Br J Radiol*. 2012;85:153-60.
74. Ludlow JB, Davies-Ludlow LE, Brooks SL. Dosimetry of two extraoral direct digital imaging devices: NewTom cone beam CT and Orthophos Plus DS panoramic unit. *Dentomaxillofac Radiol*. 2003;32:229-34.
75. Ludlow JB, Davies-Ludlow LE, Brooks SL, Howerton WB. Dosimetry of 3 CBCT devices for oral and maxillofacial radiology: CB Mercuray, NewTom 3G and i-CAT. *Dentomaxillofac Radiol*. 2006;35:219-26.
76. Grunheid T, Kolbeck Schieck JR, Pliska BT, Ahmad M, Larson BE. Dosimetry of a cone-beam computed tomography machine compared with a digital x-ray machine in orthodontic imaging. *Am J Orthod Dentofacial Orthop*. 2012;141:436-43.
77. European Commission. Radiation Protection 136. European guidelines on radiation protection in dental radiology. The safe use of radiographs in dental practice. 2004. Available from: http://ec.europa.eu/energy/nuclear/radiation_protection/doc/publication/136.pdf.
78. Carter L, Farman AG, Geist J, Scarfe WC, Angelopoulos C, Nair MK*, et al.* American Academy of Oral and Maxillofacial Radiology executive opinion statement on performing and interpreting diagnostic cone beam computed tomography. *Oral Surg Oral Med Oral Pathol Oral Radiol Endod*. 2008;106:561-2.
79. American Dental Association Council on Scientific Affairs. The use of cone-beam computed tomography in dentistry: an advisory statement from the American Dental Association Council on Scientific Affairs. *J Am Dent Assoc*. 2012;143:899-902.
80. European Commission. Guidelines on CBCT for Dental and Maxillofacial Radiology: Evidence Based Guidelines: Radiation Protection Publication 2012. Available from: http://www.sedentexct.eu/content/guidelines-cbct-dental-and-maxillofacial-radiology.
81. American Academy of Oral Maxillofacial Radiology. Clinical recommendations regarding use of cone beam computed tomography in

orthodontic treatment. Position statement by the American Academy of Oral and Maxillofacial Radiology. *Oral Surg Oral Med Oral Pathol Oral Radiol*. 2013;116:238-57.

82. Leonardi R, Giordano D, Maiorana F, Spampinato C. Automatic cephalometric analysis. *Angle Orthod*. 2008;78:145-51.
83. Keustermans J, Mollemans W, Vandermeulen D, Suetens P. Automated cephalometric landmark identification using a local shape and appearance model. ICPR; 2010; Istanbul: IEEE.
84. Keustermans J, Smeets D, Vandermeulen D, Suetens P. Automated cephalometric landmark identification using shape and local appearance models. *Lect Notes Comput Sci*. 2011;7009:249-56.
85. Farkas LG. Anthropometry of the Head and Face. 2 ed. New York, USA: Raven Press; 1994.
86. Hajeer MY, Ayoub AF, Millett DT, Bock M, Siebert JP. Three-dimensional imaging in orthognathic surgery: the clinical application of a new method. *Int J Adult Orthodon Orthognath Surg*. 2002;17:318-30.
87. Kusnoto B, Evans CA. Reliability of a 3D surface laser scanner for orthodontic applications. *Am J Orthod Dentofacial Orthop*. 2002;122:342-8.
88. Plooij JM, Swennen GR, Rangel FA, Maal TJ, Schutyser FA, Bronkhorst EM, *et al.* Evaluation of reproducibility and reliability of 3D soft tissue analysis using 3D stereophotogrammetry. *Int J Oral Maxillofac Surg*. 2009;38:267-73.
89. Toma AM, Zhurov A, Playle R, Ong E, Richmond S. Reproducibility of facial soft tissue landmarks on 3D laser-scanned facial images. *Orthod Craniofac Res*. 2009;12:33-42.
90. de Menezes M, Rosati R, Ferrario VF, Sforza C. Accuracy and reproducibility of a 3-dimensional stereophotogrammetric imaging system. *J Oral Maxillofac Surg*. 2010;68:2129-35.
91. Fourie Z, Damstra J, Gerrits PO, Ren Y. Evaluation of anthropometric accuracy and reliability using different three-dimensional scanning systems. *Forensic Sci Int*. 2011;207:127-34.

92. Brons S, van Beusichem ME, Bronkhorst EM, Draaisma J, Berge SJ, Maal TJ, *et al.* Methods to quantify soft-tissue based facial growth and treatment outcomes in children: a systematic review. *PLoS One*. 2012;7:e41898.
93. Pittayapat P, Kwon MS, Olszewski R, Coucke W, Politis C, Jacob R. Validation of a 3D facial scanning system. *manuscript in preparation*.
94. Sarver DM, Ackerman MB. Dynamic smile visualization and quantification: part 1. Evolution of the concept and dynamic records for smile capture. *Am J Orthod Dentofacial Orthop*. 2003;124:4-12.
95. Sarver DM, Ackerman MB. Dynamic smile visualization and quantification: Part 2. Smile analysis and treatment strategies. *Am J Orthod Dentofacial Orthop.* 2003;124:116-27.
96. Trotman CA, Faraway JJ, Phillips C. Visual and statistical modeling of facial movement in patients with cleft lip and palate. *Cleft Palate Craniofac J*. 2005;42:245-54.
97. Tarantili VV, Halazonetis DJ, Spyropoulos MN. The spontaneous smile in dynamic motion. *Am J Orthod Dentofacial Orthop*. 2005;128:8-15.
98. Maulik C, Nanda R. Dynamic smile analysis in young adults. *Am J Orthod Dentofacial Orthop*. 2007;132:307-15.
99. Lin AI, Braun T, McNamara JA, Jr., Gerstner GE. Esthetic evaluation of dynamic smiles with attention to facial muscle activity. *Am J Orthod Dentofacial Orthop*. 2013;143:819-27.

Summary / Samenvatting

Summary

In orthodontic treatment, for many decades, panoramic radiographs and lateral cephalograms are considered the standard two-dimensional radiographic techniques required for treatment planning and follow up. Nevertheless, both imaging techniques present with several limitations such as geometric distortion and superimposition of anatomical structures. During recent years, there has been an upward trend in utilizing 3D images, especially from CBCT, as an aid in orthodontic diagnosis and treatment planning but the scientific evidence is still lacking in many aspects. Therefore, the primary goal of this doctoral thesis was to investigate the use of 3D images in orthodontics compared to conventional 2D modalities including panoramic radiography and lateral cephalography. Subsequently, an attempt was made to develop 3D reference systems to increase the reproducibility of several crucial cephalometric landmarks in 3 dimensions. Finally, the Frankfort horizontal plane was revisited, focusing more on its 3D version.

This thesis begins with **Chapter 1**, explaining the general principles of orthodontic treatment planning and imaging modalities traditionally used to achieve the information needed to perform an orthodontic treatment. At the end of the chapter, the overall aims and hypotheses of this doctoral project were presented in detail.

In **Part I: Chapter 2**, a systematic review on 3D cephalometry was presented. This systematic review focused on the scientific evidence for the diagnostic efficacy of 3D cephalometry, especially for landmark identification and measurement accuracy. It was clearly observed that this topic is fairly new and the scientific evidence of the diagnostic efficacy of 3D cephalometry is still limited and more concrete studies need to be performed. Methods of conducting research in this area are very crucial as radiation exposure to young patients is one of the main factors for ethical concern.

In **Part II**, it was aimed to investigate and compare the use of panoramic radiography and the 3D data. In the first chapter of part II, **Chapter 3,** an attempt was made to compare *in vitro* subjective image quality and diagnostic validity of

reformatted panoramic views from CBCT with digital panoramic radiographs, regarding orthodontic treatment planning. Results revealed that although digital panoramic radiograph still showed better image quality, some reformatted panoramic view from particular CBCT devices could achieve comparable image quality and visualization of anatomical structures.

Next in this panoramic imaging part, the agreement between CBCT and panoramic radiographs for initial orthodontic evaluation was assessed. **Chapter 4** showed that the agreement between CBCT and panoramic radiograph was good and CBCT could offer the same amount of information necessary for initial orthodontic evaluation.

Subsequently, cephalometric imaging modalities were investigated in **Part III** of this doctoral thesis, beginning with **Chapter 5.** In this chapter, the linear measurement accuracy of three imaging modalities: two lateral cephalograms and one 3D model from CBCT data, was evaluated. The results showed better observer agreement for 3D measurements. The accuracy of the measurements based on CBCT and 1.5-meter SMD cephalogram was better than a 3-meter SMD cephalogram. These findings have confirmed that the linear measurements accuracy and reliability of 3D measurements based on CBCT data was good when compared to 2D techniques.

Chapters 6, 7 and **8** concentrated on the reproducibility of cephalometric landmarks in 3 dimensions and attempted to develop a more robust system for 3D cephalometry. In **Chapter 6**, a new reference system was designed in Maxilim® software to improve the reproducibility of the sella turcica landmark in 3D. The results showed that the new reference system offered high precision and reproducibility for sella turcica identification in 3 dimensions.

In **Chapter 7**, this time**,** a new reference system was developed in order to systematically improve the reproducibility of mandibular cephalometric landmarks (Pog, Gn, Me and point B) in 3D. It offered moderate to good overall precision and reproducibility for mandibular cephalometric midline landmark identification.

Chapter 8 was the last study on 3D cephalometry in this doctoral thesis**.** The aim was to evaluate the Frankfort horizontal plane (FH), which is widely used in 3D cephalometric analysis. In this chapter, the precision and reproducibility of landmarks that form the Frankfort horizontal plane (Po, Or) and newly chosen landmarks (IAF, ZyMS) was investigated. The angular differences of optional planes compared to the Frankfort plane in 3D were measured. It was demonstrated that the precision and reproducibility of Po and Or was moderate. IAM and ZyMS showed good precision and reproducibility. From the newly proposed planes, the ones closest to the original FH are the plane formed by connecting Or-R, Or-L and mid-IAF (Plane 3) and the plane formed by connecting Po-R, Po-Land mid-ZyMS (Plane 4). This study demonstrated the possibility of using new planes when traditional FHs were not feasible.

Lastly, in **Chapter 9**, the general discussion and conclusions were thoroughly discussed and presented. The findings of the present doctoral thesis elaborated the use of 2D and 3D images for orthodontic treatment and showed the possibility and new development to improve the use of 3D cephalometry. Although the scientific evidence on clinical use of 3D cephalometry is still limited, this project helps to provide a solid base for future studies. New studies should focus on the implementation of 3D cephalometry in clinical practice and evaluate how this new technology may improve the treatment outcome of orthodontic patients. In the near future, one ultra-low dose CBCT scan may be able to yield all necessary information and replace a cascade of 2D radiographic images while still keeping the ALARA principle. Whether those strategies are equally valid, remains to be proven.

Samenvatting

Panoramische radiografie en laterale cefalograms werden tientallen jaren lang beschouwd als de standaard twee-dimensionale radiografische technieken voor de planning en opvolging van orthodontische behandelingen. Desondanks hebben beide beeldvormingstechnieken verschillende beperkingen zoals geometrische distortie en superimpositie van anatomische structuren. Er is een recente, stijgende trend inzake het gebruik van 3D beelden, voornamelijk CBCT, als een hulpmiddel in orthodontische diagnose en planning, maar het wetenschappelijk bewijs ontbreekt nog voor veel aspecten. De primaire doelstelling van deze doctoraatsthesis was daarom om het gebruik van 3D beelden in orthodontie te onderzoeken en vergelijken met conventionele 2D modaliteiten zoals panoramische radiografie en laterale cefalografie. Vervolgens werd een poging gedaan om 3D referentiesystemen te ontwikkelen om de reproduceerbaarheid van verschillende cruciale cefalometrische referentiepunten te verbeteren. Tenslotte werd het Frankfort horizontale vlak herbekeken met een focus op 3D.

De thesis begint met **Hoofdstuk 1** waarin de algemene principes van orthodontische behandeling, en de beeldvormingsmodaliteiten die traditioneel gebruikt werden om de informatie te verkrijgen die nodig is voor orthodontische behandeling, uitgelegd worden. Op het einde van het hoofdstuk worden de algemene doelstellingen en hypotheses van dit doctoraatsproject in detail gepresenteerd.

In **Deel I: Hoofdstuk 2** wordt een systematische review over 3D cefalometrie gepresenteerd. Deze systematische review focust op het wetenschappelijk bewijs voor de diagnostische doeltreffendheid van 3D cefalometrie, voornamelijk voor de identificatie van herkenningspunten en accuraatheid van metingen. Een duidelijke observatie werd gemaakt dat dit een nieuw onderwerp is met beperkt wetenschappelijk bewijs over de diagnostische doeltreffendheid, en dat meer concreet onderzoek nodig is. De methodes gebruikt voor het uitvoeren van onderzoek in dit gebied is uitermate cruciaal, aangezien de stralingsdosis voor jonge patiënten één van de voornaamste ethische factoren is.

De doelstelling in **Deel II** was om het gebruik van panoramische radiografie en 3D data te onderzoeken en vergelijken. In het eerste hoofdstuk van dit deel, **Hoofdstuk 3**, werd gepoogd om een vergelijking te maken tussen *in vitro* subjectieve beeldkwaliteit en diagnostische validiteit van gereformatteerde panoramische beelden van CBCT en digitale panoramische radiografieën, inzake orthodontische planning. De resultaten toonden dat, hoewel de beeldkwaliteit van panoramische radiografieën beter was, sommige gereformatteerde panoramische beelden van bepaalde CBCT toestellen vergelijkbare beeldkwaliteit en visualizatie van anatomische structuren toonden.

Vervolgens werd in dit deel de overeenkomst tussen CBCT en panoramische radiografieën voor initiële orthodontische evaluatie nagegaan. **Hoofdstuk 4** toonde dat er een goede overeenkomst tussen CBCT en panoramische radiografie was en dat CBCT dezelfde informatie voor initiële orthodontische evaluatie zou kunnen bieden.

Vervolgens werden cefalometrische beeldvormingsmodaliteiten onderzocht in **Deel III** van deze doctoraatsthesis, beginnend met **Hoofdstuk 5**. In dit hoofdstuk werd de lineaire meetnauwkeurigheid van drie beeldvormingsmodaliteiten geëvalueerd: twee laterale cefalograms en een 3D model van CBCT data. De resultaten toonden een betere overeenkomst voor observatoren voor 3D metingen. De nauwkeurigheid van de metingen gebaseerd op CBCT en 1.5-meter SMD cefalogram was beter dan een 3-meter SMD cefalogram. Dit bevestigt dat de lineaire meetnauwkeurigheid en betrouwbaarheid van 3D metingen gebaseerd op CBCT data goed is vergeleken met 2D technieken.

Hoofdstukken 6, 7, en **8** concentreerden op de reproduceerbaarheid van cefalometrische herkenningspunten in 3 dimensies en probeerde om een meer robuust systeem voor 3D cefalometrie te ontwikkelen. In **Hoofdstuk 6** werd een nieuw referentiesysteem ontwikkeld in de Maxilim® software om de reproduceerbaarheid van het sella turcica herkenningspunt in 3D te verbeteren. De resultaten toonden dat het nieuwe referentiesysteem een hoge precisie en reproduceerbaarheid heeft voor sella turcica identificatie in 3 dimensies.

In **Hoofdstuk 7** werd een nieuw referentiesysteem ontwikkeld om de reproduceerbaarheid van mandibulaire cefalometrische herkenningspunten (Pog, Gn, Me en punt B) systematisch te verbeteren in 3D. Het systeem toonde matig tot goede algemene precisie en reproduceerbaarheid voor mandibulaire cefalometrische identifcatie van herkenningspunten.

Hoofdstuk 8 was de laatste studie over 3D cefalometrie in deze doctoraatsthesis. Het doel was om het frequent gebruikte Frankfort horizontale vlak (FH) te evalueren in 3D cefalometrische analyse. In dit hoofdstuk werd de precisie en reproduceerbaarheid van herkenningspunten die het Frankfort horizontale vlak vormen (Po, Or) en nieuw gekozen herkenningspunten (IAF, ZyMS) onderzocht. De angulaire verschillen tussen optionele vlakken vergeleken met het Frankfort vlak in 3D werd nagegaan. De precisie en reproduceerbaarheid van Po en Or was matig. IAM en ZyMS toonden een goede precisie en reproduceerbaarheid. Nieuw vlakken dichter bij het FH waren: een vlak dat bestond uit Or-R, Or-L en mid-IAF en een ander vlak dat bestond uit Po-R, Po-L en mid-ZyMS. Deze studie toonde de mogelijkheid om nieuwe vlakken te gebruiken wanneer traditionele FH's niet bruikbaar zijn.

Hoofdstuk 9 bevat de algemene discussie en conclusies. De bevindingen van deze doctoraatsthesis omvatten het gebruik van 2D en 3D beelden voor orthodontische behandelingen en toonden de mogelijkheden en nieuwe ontwikkelingen om het gebruik van 3D cefalometrie te verbeteren. Hoewel het wetenschappelijk bewijs inzake het klinisch gebruik van 3D cefalometrie nog steeds beperkt is, geeft dit project een grondige basis voor toekomstige studies. Nieuwe studies kunnen dieper ingaan op de implementatie van 3D cefalometrie in de klinische praktijk en kunnen evalueren hoe deze nieuwe technologie de behandeling van orthodontische patiënten kan verbeteren. In de nabije toekomst zou een ultra lage-dosis CBCT scan alle nodige informatie kunnen bezorgen en een cascade van 2D radiografische beelden kunnen vervangen, met behoud van dosisoptimisatie en het ALARA principe. Of deze diagnostische strategieën equivalent zijn met betrekking tot het behandelingsplan valt nog te bekijken.

Curriculum vitae

Curriculum vitae

Name	Pisha Pittayapat
Date of Birth	January 2, 1981.
Birth place	Bangkok, Thailand
Nationality	Thai
Work address	Oral Imaging Center, OMFS-IMPATH Research Group, Department of Imaging and Pathology, Katholieke Universiteit Leuven, University Hospitals Leuven Kapucijnenvoer 33, B-3000 Leuven, Belgium Tel. +32 16 33 2951
Email address	p.pittayapat@gmail.com pisha.pittayapat@med.kuleuven.be

Education Background

2008-2014	PhD candidate in Biomedical Sciences, KU Leuven, Belgium
2007-2008	Master of Forensic Odontology, KU Leuven, Belgium (cum laude)
2006	Graduate Diploma of Clinical Sciences in Maxillofacial Radiology, Chulalongkorn University, Bangkok, Thailand
2004	Doctor of Dental Surgery (first class of honour), Chulalongkorn University, Bangkok, Thailand

Grant/Award

2012	Travel grant from the 13th Congress of European Academy of Dento-Maxillo-Facial Radiology, Leipzig, Germany
2010-2013	Doctoral scholarship in the framework of the Interfaculty Council for Development Co-operation (IRO)

2009	Travel grant from the 17th International Congress of Dento-Maxillo-Facial Radiology, Amsterdam, The Netherlands
2007-2008	Master scholarship from Nenbutsushu Buddhist Sect of Japan
2003	Award for first rank in class of 101 dental students, Faculty of Dentistry, Chulalongkorn University, Bangkok, Thailand
1999	Award for top scores in Anatomy courses, Faculty of Dentistry, Chulalongkorn University, Bangkok, Thailand

Publications

Peer-reviewed journals

Pittayapat P, Bornstein MM, Imada T, Coucke W, Lambrichts I, Jacobs R. Accuracy of linear measurements using 3 imaging modalities: two lateral cephalograms and one 3D model from CBCT data. *Eur J Orthod.* 2014. (in press)

Kosalagood P, Silkosessak OC, **Pittayapat P**, Pisarnturakit P, Pauwels R, Jacobs R. Linear Measurement Accuracy of Eight Cone Beam Computed Tomography Scanners. *Clin Implant Dent Relat Res*. 2014. (in press)

Pittayapat P, Limchaichana Bolstad N, Willems G, Jacobs R. 3D Cephalometric analysis in orthodontics: a systematic review. *Orthod Craniofac Res.* 2014;17:69-91.

Pittayapat P, Willems G, Alqerban A, Coucke W, Ribeiro-Rotta RF, Couto Souza P, Westphalen FH, Jacobs R. Agreement between cone beam computed tomography images and panoramic radiographs for initial orthodontic evaluation. *Oral Surg Oral Med Oral Pathol Oral Radiol.* 2014;117:111-9.

Durão AR, **Pittayapat P**, Rockenbach IV, Olszewski R, Ng S, Ferreira AP, Jacobs R. Validity of 2D lateral cephalometry in orthodontics: a systematic review. *Prog in Orthod.* 2013;14:31.

Pauwels R, Jacobs R, Bosmans H, **Pittayapat P**, Kosalagood P, Silkosessak O, Panmekiate S. Automated implant Segmentation IN cone-beam CT using edge detection and particle counting. *Int J Comput Assist Radiol Surg*. 2014;9:733-43.

Pittayapat P, Jacobs R, De Valck E, Vandermeulen D, Willems G. Forensic Odontology in the Disaster Victim Identification Process. *J Forensic Odontostomatol.* 2012;30:1-12.

Pittayapat P, Galiti D, Huang Y, Dreesen K, Schreurs M, Souza PC, Rubira-Bullen IR, Westphalen FH, Pauwels R, Kalema G, Willems G, Jacobs R. An in vitro comparison of subjective image quality of panoramic views acquired via 2D or 3D imaging. *Clin Oral Investig*. 2013;17:293-300.

Van Assche N, **Pittayapat P**, Jacobs R, Pauwels M, Teughels W, Quirynen M. Microbiological outcome of two screw-shaped titanium implant systems placed following a split-mouth randomised protocol, at the 12th year of follow-up after loading. *Eur J Oral Implantol*. 2011;4:103-16.

Jacobs R, **Pittayapat P**, van Steenberghe D, De Mars G, Gijbels F, Van Der Donck A, Li L, Liang X, Van Assche N, Quirynen M, Naert I. A split-mouth comparative study up to 16 years of two screw-shaped titanium implant systems. *J Clin Periodontol*. 2010;37:1119-27.

Pittayapat P, Oliveira-Santos C, Thevissen P, Michielsen K, Bergans N, Willems G, Debruyckere D, Jacobs R. Image quality assessment and medical physics evaluation of different portable dental X-ray units. *Forensic Sci Int.* 2010;201:112-7.

Thevissen PW, Alqerban A, Asaumi J, Kahveci F, Kaur J, Kim YK, **Pittayapat P**, Van Vlierberghe M, Zhang Y, Fieuws S, Willems G. Human dental age estimation using third molar developmental stages: Accuracy of age predictions not using country specific information. *Forensic Sci Int*. 2010;201:106-11.

Pittayapat P, Thevissen P, Fieuws S, Jacobs R, Willems G. Forensic oral imaging quality of hand-held dental X-ray devices: Comparison of two image receptors and two devices. *Forensic Sci Int*. 2010;194:20-7.

Thevissen PW, **Pittayapat P**, Fieuws S, Willems G. Estimating age of majority on third molars developmental stages in young adults from Thailand using a modified scoring technique. *J Forensic Sci*. 2009;54:428-32.

Book chapters

Pittayapat P. Forensic Odontology. In: Sribanditmongkol P, Vichairat K, editors. Mass fatality management. [หลักการบริหารจัดการศพจำนวนมาก: ทันตนิติวิทยา] Department of Forensic Medicine, Faculty of Medicine, Chiang Mai University, Thailand; 2011.

Presentations at international conferences

Oral presentation

Pittayapat P, Olszewski R. Willems G, Jacobs R. Reliability of Sella Turcica Landmark in 3-dimensions .In: the 2nd Meeting of International Association for Dental Research, Bangkok, Thailand on August 21-23, 2013.

Pittayapat P, Schreuers M, Willems G, Jacobs R. In-vivo comparison of panoramic radiographs vs. CBCT for Orthodontics In: Research award session, 13th Congress of European Academy of Dento-Maxillo-Facial Radiology, Leipzig, Germany, June 13-16, 2012.

Pittayapat P, Galati D, Huang Y, Dreesen K, Schreurs M, Couto Souza P, Rubira IR, Westphalen FH, Jacobs R. An in-vitro comparison of panoramic views acquired via 2D or 3D imaging to aid diagnosis of oral health. In: the 24th Annual Meeting and Refresher Course of the European Society of Head and Neck Radiology in Brugge, Belgium, September 8-10, 2011.

Pittayapat P, Thevissen P, Oliveira-Santos C, Debruyckere D, Michielsen K, Jacobs R, Willems G. Image quality assessment and medical physics evaluation of different portable dental X-ray units. In: 12th Congress of European Academy of Dento-Maxillo-Facial Radiology, Istanbul, Turkey, June 2-5 2010.

Jacobs R, **Pittayapat P**, De Mars G, Gijbels F, Van Der Donck A, Liang X, Quirynen M, Van Steenberghe D, Naert I. An up to 14-years split-mouth comparative study of two screw-shaped titanium implant systems. In: 17th International Congress of Dento-Maxillo-Facial Radiology, Amsterdam, The Netherlands, June 28 - July 2, 2009.

Pittayapat P, Thevissen P, Jacobs R, Willems G. Image quality assessment of portable dental x-ray units for forensic odontologic applications. In: 11th Congress of European Academy of Dento-Maxillo-Facial Radiology, Budapest, Hungary, June 25-28, 2008.

Pittayapat P, Chuenchampoonut V, Thevissen P, Willems G. Third molars and estimating age of majority in young adults from Thailand. In: American Academy of Forensic Sciences 60th anniversary meeting, Washington DC, USA, February 18-23, 2008.

<u>Poster presentation</u>

Pittayapat P, Bornstein MM, Imada TSN, Rovaris K, Coucke W, Lambrichts I, Willems G, Jacobs R. Comparison of linear measurements from several lateral cephalometric techniques. In: 14th Congress of European Academy of Dento-Maxillo-Facial Radiology, Cluj-Napoca, Romania on June 25-28, 2014.

Pittayapat P, Limchaichana Bolstad N, Willems G, Jacobs R. 3D Cephalometric analysis in orthodontics: a systematic review. In: 19th International Congress of Dento-Maxillo-Facial Radiology, Bergen, Norway on June 22-27, 2013.

Pittayapat P. In: 20th International Association for Dental Research (South East Asian Division) Annual Scientific Meeting, Malacca, Malaysia, September 1-4, 2005.

Presentations at other conferences and symposia

Speaker on the topic of 'CBCT in Orthodontics' at the scientific day organized by the orthodontic society: Belgische Beroepsvereniging van Nederlandstalige Orthodontisten (BBNO) at the Waerboom, Belgium on Thursday 21, 2013.

Speaker at the mid-year meeting of Thai Society of Oral Diagnostic Science, Bangkok, Thailand on June 16-17, 2011.

Speaker at Vlaamse Vereniging Tandheelkundige Experten meeting: 30 jaar Forensische odontologie in België : Een retrospectieve, Grimbergen, Belgium, 2009.

Professional and Research Experiences

<u>Journal reviewer</u>

2014	Reviewer for Angle Orthodontist
2014	Reviewer for European Journal of Orthodontics (EJO)

2013-present	Reviewer for Journal of Oral Rehabilitation (JOR)
2013-present	Reviewer for Oral Radiology journal (ORRA)
2009-present	Reviewer for Clinical Oral Investigations journal

Teaching experiences

2013-2014	Supervisor for a master student in Biomedical Science, KU Leuven.
2011	Supervisor for a capita student project, KU Leuven.
2009	Supervisor in preclinical courses in radiology and radioprotection 3rd bachelor in dentistry, University Hospital Leuven
2004-2006	Research advisor for 3rd year dental students, Faculty of Dentistry, Chulalongkorn University, Bangkok, Thailand
2004-present	Lecturer at Department of Radiology, Faculty of Dentistry, Chulalongkorn University, Bangkok, Thailand.

Other experiences

2013	Chairman in an oral presentation session at the 2nd Meeting of International Association for Dental Research, Bangkok, Thailand on August 21-23, 2013.
2012	Participant in Belgian DVI team at the 21st Meeting of the Standing Committee on Disaster Victim Identification, Interpol Headquarter, Lyon, France, 18 - 20 May 2009.
2010-present	Attended and assisted in “CBCT workshop” and “CBCT diagnostic workshop” for dentists at the Oral Imaging Center, University Hospital Leuven, KU Leuven.
2010	Attended the 3rd International Symposium on “3D Diagnosis and Virtual Treatment Planning of Cranio-Maxillo-Facial Deformity”, Eindhoven, the Netherlands.
2009-2010, 2013	Editorial committee, Newsletters of the European Academy of Dento-Maxillo-Facial Radiology.
2004-2005	Participated in disaster victim identification operation of the victims from Thailand Tsunami in 2004 at the Information Management Center (IMC), Phuket, Thailand.